Alma Mater Studiorum – Università di Bologna

DOTTORATO DI RICERCA IN

CHIMICA

Ciclo XXX

Settore Concorsuale di afferenza: 03/A2

Settore Scientifico disciplinare: CHIM02

PRODUCTION AND CHARACTERIZATION OF NEW NANO-STRUCTURED COMPOSITES FOR AERONAUTICAL APPLICATION

Presentata da: NICOLA MIROTTA

Coordinatore Dottorato: ALDO RODA

Supervisore: FRANCESCO ZERBETTO

Co-Supervisori: VINCENZO PALERMO, EMANUELE TREOSSI

Esame finale anno 2018

Presented: 15 December 2017

nano-chemistry Laboratory of CNR - ISOF

University of Bologna ALMA MATER and National Research Council

PRODUCTION AND CHARACTERIZATION OF NEW NANO-STRUCTURED COMPOSITES FOR AERONAUTICAL APPLICATION

Supervisor:

Prof. Francesco Zerbetto

Prof. Vincenzo Palermo

Dr. Emanuele Treossi

PhD thesis in chemistry and chemicals science - Advanced materials for structural and multifunctional application

PhD candidate: Nicola Mirotta freshmen n. 0000739673

Summary

List of figures

Preface

This thesis has been written as a partial fulfillment of the requirements for obtaining the PhD at the University of Bologna "Alma Mater Studiorum". The work was carried out in the Bologna Research Area of the Consiglio Nazionale delle Ricerche (CNR – Italian National Research Council), at the Istituto di Sintesi Organica e Fotoreattività (ISOF – Institute of Organic Synthesis and Photoreactivity). The project, entitled "PRODUCTION AND CHARACTERIZATION OF 2D-BASED POLYMER NANO-COMPOSITES" started in November 2014 and ended in November 2017.

The work including two-dimensional material characterization and optimization/production of composite materials was carried out in the laboratories of ISOF-CNR.

CNR - ISOF
Istituto per la Sintesi Organica e la Foto reattività
Nano-chemistry Laboratory, Building 4
Via P. Gobetti 101 – 40129 Bologna
Italia

Acknowledgements

First, I would like to thank my research advisors Emanuele Treossi and Vincenzo Palermo who gave me the opportunity to complete my PhD thesis here in Bologna.
Secondly, I would like to thank my parents Anna and Antonino, for their blessing and support, and my brother and grandmother Maria, no longer with us, and all my family.
I also thank professor Francesco Zerbetto from Bologna University for his availability as my supervisor.
Sincere thanks go to my colleagues, for fruitful discussions and advice, Alessandra, Alessandro, Simone, Vanesa, Konstantinos, Maria, Zhen (Jeff) and Giulio, who have helped me with experimental work in the laboratory and especially Derek Jones for his strong support. Finally, I would like to thank Anna Maria for her patience with me.
Last but not least, I would like to thank all the other people in the nano-chemistry Group with all whom I met at ISOF, and who helped me directly and indirectly with many of the experiments presented in this thesis.
Many thanks to you all.
As Einstein said, "**Imagination is more important than knowledge**", so thank you to my will and imagination to brought me to do this experience.

1. Abstract

The main goal of this thesis is to create new composites to merge at the nanoscale the exceptional optical, electronic and structural properties of 2D materials with those of conventional materials.

We prepared a series of composites with 2D materials to be tested for applications in various fields including aeronautics and the automotive industry.

Some of these materials were then benchmarked and selected for scaled-up production.

Systems of increasing complexity were studied, from the modelling of simple, defectless sheets of graphene in vacuum to the modelling of highly defective graphene oxide sheets, featuring voids of different sizes.

The results obtained allowed the correlation of mechanical behavior of composites under mechanical (tensile, bending or compressive), thermal and electrical stress with the 2D graphene materials used.

Graphene is one of the most interesting 2D materials, with a two-dimensional monolayer of covalently bonded carbon atoms which is the basic building block of graphite and carbon nanotubes. Having caught the attention of the scientific community for its high rigidity (1 TPa, Tera-pascal) specific surface area (2600 m^2g^{-1}) and interesting electronic properties, it has now become a potential competitor to carbon nanotubes and carbon black in the field of composites.

Although commercially available graphene does not reach the theoretical values of “ideal graphene” in terms of its intrinsic properties, dispersing graphene and its derivatives in polymers yield nano-composites with better properties compared to other carbon- and 2D-filler-based polymer composites.

The work presented in this thesis demonstrates the properties of polymer composites reinforced with various types of 2D nano-fillers, prepared by dispersing the fillers in the polymer using a three-roll mill. The effect of filler type on the mechanical, electrical and thermal properties of the nano-composite was studied. Graphene-based nano-composites outperformed graphene/epoxy composites in terms of mechanical, electrical and thermal properties.

Studies on the fracture resistance of epoxy nanocomposites reinforced with graphene were investigated at Bologna University with Dr. Laura Sisti. The electrical properties of the nano-composites were measured using the four-point-probe method at ISOF-CNR; thermal characteristics were analyzed with the hot-probe method by Dr. Alberto Fina at Turin Polytechnic and humidity measurements carried out at the AIRBUS Getafe plant in a

climatic chamber. The piezo resistive tests were conducted at the Fiat Research Centre of Torino under the supervision of Dr. Antonino Veca.

2. Introduction

The production and study of 2D materials such as graphene, boron nitride (BN), or molybdenum disulfide (MoS_2) is rapidly expanding in the scientific community, the main production methods being based on exfoliation in liquids, CVD growth and top-down approaches.

In fact, various graphene nano-platelets (GnP), boron nitride and other types of two-dimensional materials are now being produced by small companies and even academic laboratories.

Moreover, the possibility of forming composites by stacking together various 2D materials in order to produce novel properties is now one of the most important developments in this field.

Great emphasis has recently been placed on the study of graphene-polymer nano-composites, as the use of nano-scale over micron-scale materials has the advantage of better physical and chemical properties due to their large surface area. Different types of nano-platelets can be prepared for specific purposes in the fields of:

Electrical conductivity, for anti-static or high electrical field gradient applications; thermal conductivity, for de-icing applications; gas barrier properties, to reduce moisture adsorption on polymer surfaces (an important problem, especially in aeronautics applications, because it degrades material properties)[1]; 2D nano-fillers as reinforcements, producing materials with better mechanical, electrical and thermal properties, offering great potential for novel materials and their applications in the field of polymer nano-composite[2].

Graphene/polymer nanocomposites shows their potential application in automotive, aerospace, electronics, and packaging. However, there are several challenges: the cost, the dispersion of the filler in polymer, the uniformity of the concentration in the epoxy resin, and the fabrication method in industrial scale. In this thesis composites were performed to observe the changes properties of the blank resin under electrical, thermal, mechanical and gas barrier aspects.

2.1. Aim of the work

In aeronautics, the use of epoxy resins is particularly important, and our aim was to produce nanoparticle composites with such thermosetting polymers, by loading the polymeric matrix with nano-fillers such as graphene nano-platelets or other 2D-material platelets as a means of enhancing the tensile strength without compromising other properties of the composite. Recent work in the scientific literature suggests that the use of graphene as a filler in epoxy matrices can yield nano-composites with improved multifunctional properties[10].

Here, various types of graphene fillers were dispersed in epoxy matrices using techniques such as three-roll milling and high shear-force mixing, to prepare 2D-material-based epoxy nano-composites which were then compared to standard epoxy materials. The object of the work was to study the effects of the fillers on storage modulus, glass transition temperature, fracture toughness and electrical conductivity of nano-composites through variations in filler concentrations. The effects of intermixing different fillers were also studied using bi-filler epoxy composites containing boron nitride and graphene through combined electro-thermal and mechanical measurements. The main object was thus to study the possibilities of producing epoxy nanocomposites exhibiting the multifunctional effects of graphene-based fillers.

2.2. Structure of the thesis

Chapter is an introduction of this thesis.

The second chapter describes the work carried out at ISOF-CNR.

Chapter 3 provides descriptions of graphene and other 2D materials, and Chapter 4 the literature description of the composites, and especially the production and properties of graphene- and 2D-material-based polymer composites.

Chapter 5 describes the benchmarking of the filler used, graphene powder, and boron nitride.

Chapter 6 outlines the design of the experiments, materials used, sample preparation and details of the experiments performed. The main results are presented and discussed in Chapter 7 together with the conclusions drawn.

3. Carbon materials, graphene and 2-dimensional materials

Carbon is one of the most abundant elements on Earth (after oxygen, silicon and hydrogen), and has the ability to bind with a wide variety of other elements, creating single, double or even triple bonds, greatly extending the possibilities of potential structures.

There are cases where carbon forms bonds with other carbon atoms leading to particular spatial arrangements giving rise to morphological forms called allotropes.

One of the most common is graphite, consisting of multiple layers of two-dimensional honeycomb lattices (graphene) which interact with one another through a weak Van der Waals interaction, Should the dimensionality change, then molecular species and nanostructures may emerge as in the case of fullerenes or nanotubes. The particular case of diamond finds the carbon atoms in tetrahedral sp3 hybridization forming a cubic crystal structure. Thus, fullerene can be considered as a zero-dimensional structure, carbon nanotubes as a one-dimensional structure, graphene as a two-dimensional structure and diamond and graphite as three-dimensional structures as schematized in Figure 3.1.

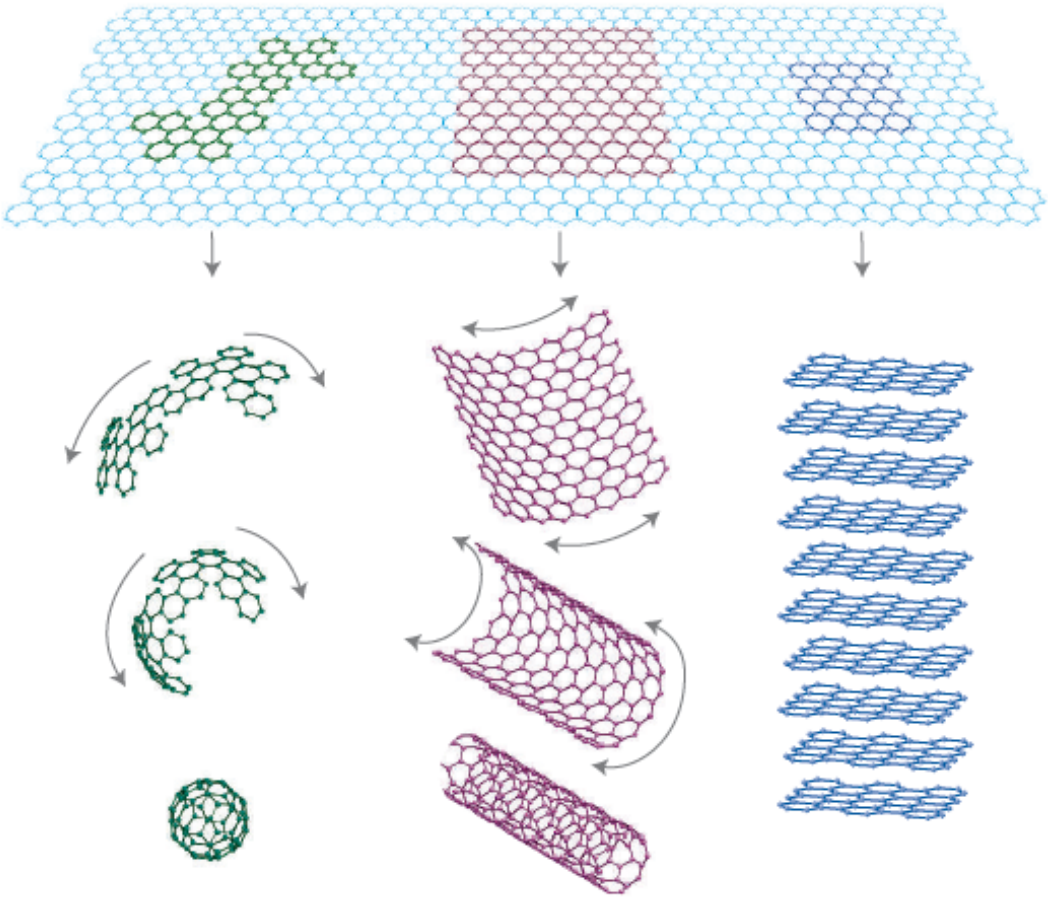

Figure 3.1: Basic building block of all graphitic forms. graphene is a 2D building material for carbon materials of all other dimensionalities. It can be wrapped up into 0D bucky-balls, rolled into 1D nanotubes or stacked into 3D graphite[14]

.

3.1. Graphene

Graphene is the most recently investigated of the carbon allotropes. It is a two-dimensional sheet of sp^2-hybridized carbon and is receiving growing interest from scientist's due to its extraordinary gas barrier capacity, as well as its thermal, mechanical and electrical properties. Due to these properties graphene promises to have many applications in various sectors.

It is a material composed of carbon atoms bonded to each other to form a planar structure. The atoms are arranged in a hexagonal honeycomb geometry (Figure 3.2) in which each atom bonds to three adjacent atoms, at angles of 120° within the plane, with interatomic distances d = 1.42 Å and centre to centre distances of 2.46 Å [15]. The bonds formed are covalent C-C σ bonds together with delocalized π bonding providing a particularly strong and rigid structure.

Andre K. Geim and Konstantin S. Novoselov at the University of Manchester, UK, used a simple but effective mechanical exfoliation with adhesive tape and then transferred these layers onto a silicon substrate, and were recently (2010) awarded the Nobel Prize in Physics for their work in this field.

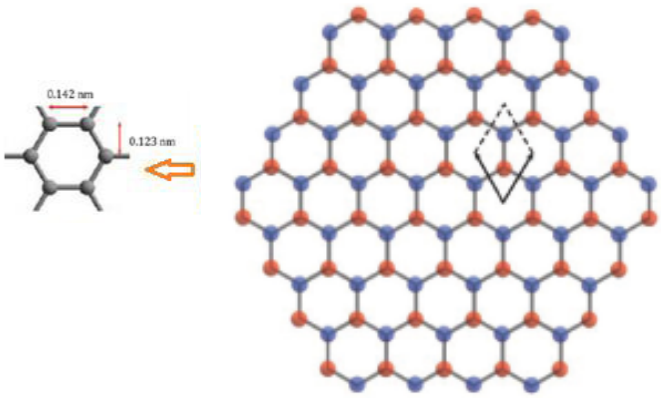

Figure 3.2: Unit cell of graphene and the two sub-lattices (red and blue)[16]

3.2. Graphene properties

Graphene is promising because it combines a range of interesting properties in a single material. Its transparency, conductivity, and elasticity allow its use in flexible electronics; its high charge mobility (μ), and its mono-atomic thickness in efficient transistors for RF applications; its transparency, impermeability to water and its conductivity can be exploited for transparent conductive coatings.

3.2.1. Electronic properties

Tests have shown that the electronic mobility in graphene is very high, with previously reported results of 2.5 x 10^5 cm^2/Vs [17] and 6 x 10^6 cm^2/Vs at 4 °K[15] (limited by the scattering of graphene's acoustic photons). In graphene, electrons have the behavior of a photon and, for this reason, charge carriers can move sub-micrometer distances without scattering, i.e., ballistic transport.
In real materials, the quality of the graphene and substrate can affect electron transport. For example, with silicon dioxide as the substrate, the mobility is around 40,000 $cm^2 \cdot V^{-1} \cdot s^{-1}$.

3.2.2. Mechanical strength

Graphene, as a monoatomic layer is actually the strongest material ever discovered, with an ultimate tensile strength of 130 GPa compared to 200 MPa for steel, or 375 MPa for Aramid (Kevlar). Together with such strength, graphene is very light at 0.77 mg per square meter, and graphene also has a Young modulus of 1 TPa[15] double that of steel.
In 2014, an experiment performed using atomic force microscopy (AFM) on graphene sheets suspended over silicon dioxide cavities showed a huge impact deformation[17].

3.2.3. Optical properties

Graphene can produce a high opacity for an atomic monolayer absorbing $\pi\alpha \approx 2.3\%$ of red light even if it is only 1 atom thick [15].

3.2.4. Thermal properties

Early measurements of the thermal conductivity of suspended graphene reported an exceptionally large thermal conductivity of approximately $\kappa \sim 2000$ to 5300 W/(m K) [15], order of magnitude greater than for example a copper that shows a conductivity of 390 W/(m K).

3.3. Graphene synthesis

There is an increasing number of publications and patents on graphene (see Figure 3.3), literature shows the possibility to use graphite nano-platelets (GNP) or graphene as cheap substitute for carbon nanotubes (CNT)[18] in nano-composites[3].

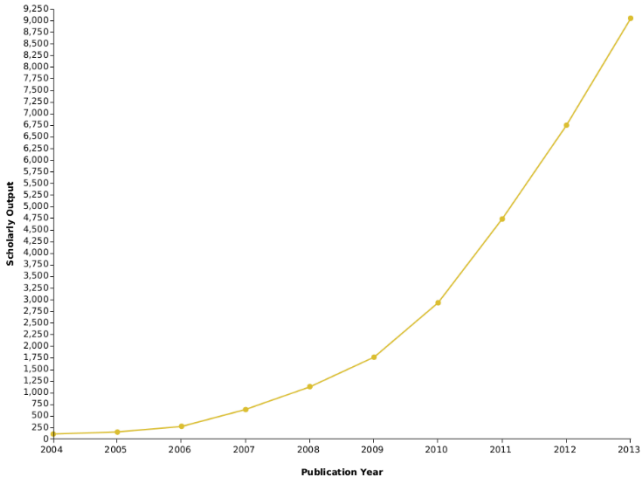

Figure 3.3: Numbers of paper published in the period 2004-13 from a search for "graphene" in the titles, abstracts or keyword[2]

In 2004 Geim and Novoselov using a low-budget technique based on scotch tape, were able to isolate the graphene monoatomic sheet growing up a lot of interest. With this method, it was possible to isolate monolayers with size of several - microns and irregular shape.
There are two different approaches to fabricate graphene materials, the top-down and the bottom-up:

1. **Top down approach[3]:**

With top-down approach the use of raw massive graphite is possible to synthetizes graphene related material producing a large amount of refuse waste, in particular is possible to obtain such as graphite oxide (GO), graphite intercalated compounds (GIC), highly oriented pyrolytic graphite (HOPG) and not pure graphene. In this thesis were used a graphene nano-platelets typically obtained from exfoliation techniques that separate the layers of graphite to obtain graphene.

2. **Bottom up approach[3]:**

With the bottom-up approach it is possible to synthesize a very pure quality of graphene, typically grown on a suitable substrate. Some examples are: chemical vapor deposition (CVD), epitaxial growth on SiC (silicon carbide), arc discharge. Then is possible to etch the substrate and isolate the graphene sheet

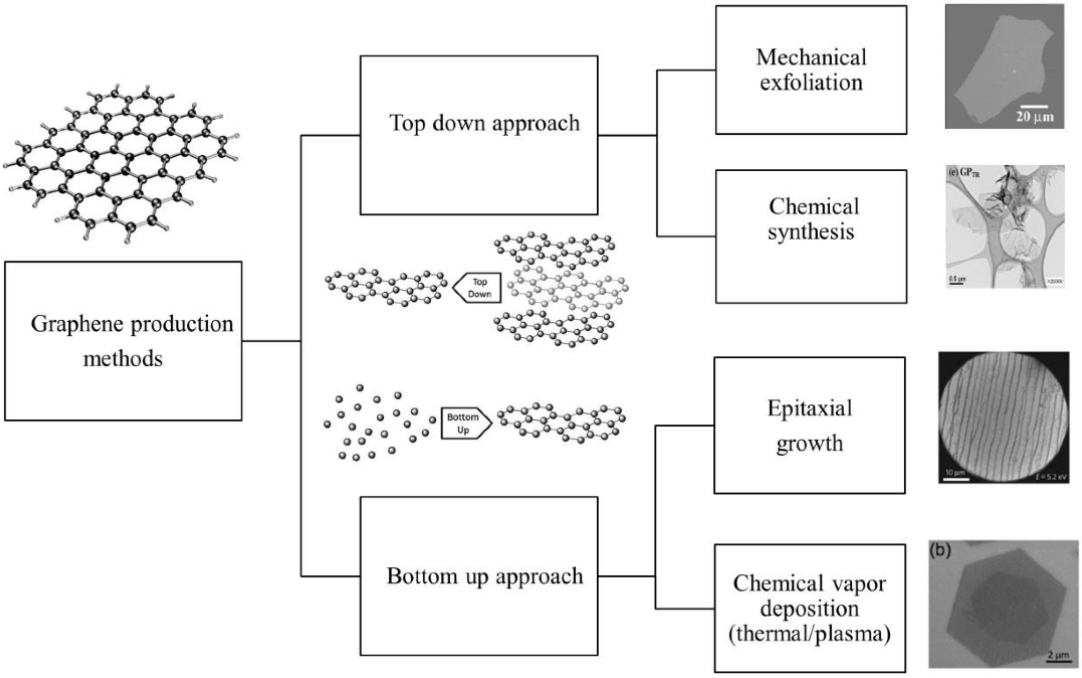

Figure 3.4: A flow chart on graphene production methods; mechanical exfoliation, epitaxial growth, CVD, thermally reduced graphene[3]

In this thesis, we used commercial graphene nano-platelets for mass-production of graphene, thus allowing ample choice in terms of size, quality and price for any application as shown in the figure below (see Figure 3.5)

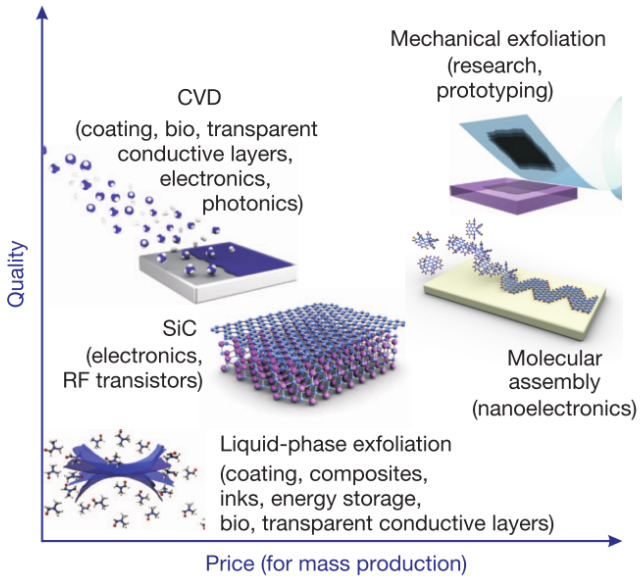

Figure 3.5: Price (for mass production) vs quantity of different graphene production techniques[1]

3.3.1. Liquid phase exfoliation

Liquid-phase exfoliation of graphite produces graphene by treatment with a solvent having a surface tension suitable to promote the splitting of the crystalline planes. A non-aqueous solvent is generally used, but aqueous solutions with surfactants can also be used.
Exfoliation is achieved by using disruptive techniques such as sonication or ball milling.
An alternative is the graphite oxide route in which graphite pellets are first oxidized and then ultrasonically exfoliated in an aqueous solution[15].

3.3.2. Thermal and mechanical exfoliation

Another scalable and very quick method is thermal and mechanical exfoliation from graphite intercalated compounds (GICs). The formation of GICs can be obtained through the insertion of an atomic or molecular (intercalant) layer between the graphene layers, followed by thermal/microwave shock which separates the graphite layers. Then ball milling or sonication can be used to obtain graphene nano-platelets (GnPs).

3.3.3. Chemical vapor deposition

Large-area, uniform polycrystalline graphene films can be grown by chemical vapor deposition (CVD) on copper foil leading to a product with promising properties for applications requiring an excellent quality of mono-atomic layers.
Despite the presence of defects, grain boundaries, inclusions of thicker layers, and so on, such films are virtually ready for use in transparent conductive coating applications.
Currently, CVD is expensive as it requires high energy consumption, an expensive chamber for conditioning during production, as well as high quality specification gases (methane, ethane). Also, removal of the metal substrate is also energy expensive, and process transfer to industrial levels might be as complicated as the growth of graphene itself.

3.4. Graphene nomenclature

Graphene is only one member of a very large class of materials. During the early years following the discovery of graphene, scientists and industrial concerns sell and use various qualities of graphene classified according to the fabrication method and the morphological properties of the graphene produced[13], so classification of the terms used for different types of graphene are important::

1. **Graphene** – a single-atom-thick sheet of hexagonally arranged, sp^2-bonded carbon atoms which is not an integral part of a carbon material, but freely suspended or layered onto a substrate [13];
2. **Bilayer graphene, tri-layer graphene** – 2D (sheet-like) materials consisting of 2 or 3 well-defined, countable, stacked graphene layers of extended lateral dimension [13];
3. **Multi-layer graphene (MLG)** – a 2D (sheet-like) material consisting of a number of layers (usually between 5 and 10) of well-defined, countable, stacked single graphene layers of extensive lateral dimensions [13];
4. **Few-layer graphene (FLG)** – a subset of multi-layer graphene (defined as above) with layer numbers from about 2 to 5 [13].
5. **Graphite nanoplates** – graphite nano-sheets; graphite nano-flakes, having a thickness and/or lateral dimensions below 100 nm. An acceptable alternative term is 'ultrathin graphite'', though ''ultra'' is less specific than ''nano'' in describing the maximum thickness [13].
6. **Exfoliated graphite** – MLG made by partial exfoliation (thermal, chemical, or mechanical) of graphite into thin multilayer packets that retain the 3D crystal stacking of graphite [13];
7. **Graphene nanosheet** – a single-atom-thick sheet of hexagonally arranged, sp^2-bonded carbon atoms which is not an integral part of a carbon material, but freely suspended or layered onto a substrate, with lateral dimensions below 100 nm [13];
8. **Graphene micro-sheet** – a single-atom-thick sheet of hexagonally arranged, sp^2-bonded carbon atoms which is not an integral part of a carbon material, but freely suspended or layered onto a substrate, with lateral dimensions between 100 nm and 100 μm[13].

Graphene-related materials and their definition as a function of the lateral size of the flake, the degree of oxidation and the surface area of the powder can be represented in a clear graphical diagram as reported in Figure 3.6,

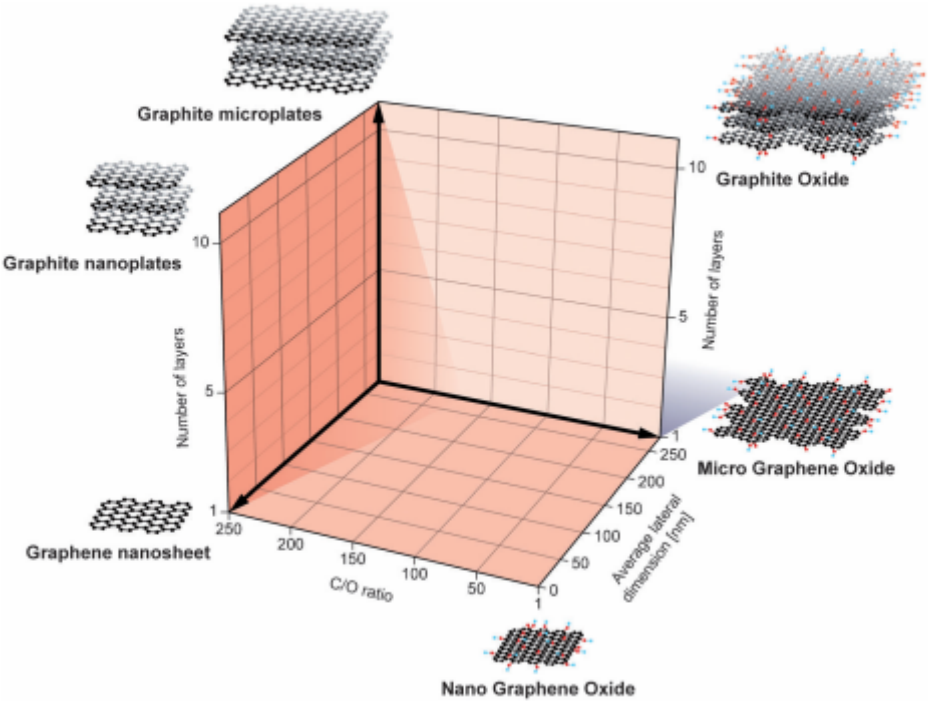

Figure 3.6: Classification grid for the categorization of various graphene-based materials (GBM) according to three fundamental properties: number of graphene layers, average lateral dimensions, and carbon/oxygen atomic ratio. The different materials drawn at the six corners [13]

3.5. Graphene market

Throughout Europe and worldwide the majority of graphene producers sell graphene powder and graphene master batches which are not always suitable for our use. Facing this jungle of products and producers, both universities and private companies, the work in this thesis included analysis and evaluation of products to find the most suitable producer providing graphene in the amounts required and with the necessary characteristics:

1. **Graphenea** – is a private European company (based in Spain) focused on the production of high quality graphene for industrial applications. The company produces single-layer graphene sheets, bi-layer graphene, multi-layer graphene, graphene oxide and other GBMs - on any substrate the customer requires and/or provides. In November 2012, the company launched an online store. In 2015, the company announced plans to build a new graphene pilot plant in a $2.5 million investment.
2. **Xg Science** – is a private company based in Michigan, US, which develops and produces graphene flakes using technology developed at Michigan State University. XgS uses its xGnP (graphene flakes) materials also to develop graphene applications. In August 2013, XgS launched a new graphene-based anode material for Li-Ion batteries. In August 2012, the company began production at their new 80-ton facility in Lansing, Michigan.
3. **Nanesa** – is an Italian-based start-up company which aims to produce and market conductive silver-based inks, pastes and GBMs. The company currently offers graphene flakes, graphene oxide and graphene-based thermal foils.
4. **Avanzare** – Avanzare Innovacion Tecnologica (based in Spain) provides high-performance nanomaterials and nanotechnology-based solutions for a wide range of applications. The company produces graphene flakes and graphene oxide and specializes in the development, production and commercialization of additives for a range of materials, mainly plastics and rubber, across many different industries.

3.6. Application

This section discusses some relevant applications developed both in scientific research and commercially for graphene and composite materials reinforced with graphene.

3.6.1. Biological engineering

Graphene possessing such an extremely large specific surface area, high electrical conductivity, and high strength, make it a good candidate for the development of bio-electric sensors, to monitor, for example, glucose levels, hemoglobin levels, hydrogen peroxide [19], cholesterol and even DNA sequencing[20].

3.6.2. Optical electronics

Due to its optical and electronic properties, graphene and graphene-related materials is used in optoelectronics, including touchscreens, liquid crystal displays (LCD) and organic light-emitting diodes (OLEDs)and, for example, to replace ITO (Indium tin oxide) [20].

3.6.3. Ultrafiltration

Due to its gas barrier capacity graphene is used in ultrafiltration acting as a barrier between two substances. It also has a future in the clean-up of oil leaks using graphene-related materials, and can be used in water filtration systems, and desalination systems in an efficient and economical manner [20].

3.6.4. Energy storage

Due to its high specific surface area (2600 m^2/g) graphene can enhance the storage capacity of lithium ion batteries (by incorporating graphene as an anode) as well as increasing longevity and reducing recharging times. Also, graphene is being studied and developed for use in the manufacture of supercapacitors which can be charged very quickly [20].

3.7. Boron nitride (BN)

Boron nitride shows important properties as a ceramic material, it is thermally stable at temperatures up to 2370 °C, chemically inert, and an electrical insulator with high thermal conductivity coupled with thermal-shock resistance [21] and high-temperature lubricity.

The world market for boron nitride is forecast to reach 3.1 thousand metric tons in 2017 [22]. The main growth of the overall market is due to these unique features. Turkey is the single largest boron producer, garnering a substantial proportion of global production, followed by Argentina, Chile, Russia and Peru.

Boron nitride is formed by atoms of boron (B) and nitrogen (N). In the periodic table these elements are located to the immediate left and right of carbon (C). There are two allotropic forms of boron nitride, a hexagonal form which corresponds to graphite, and a cubic form analogous to diamond.

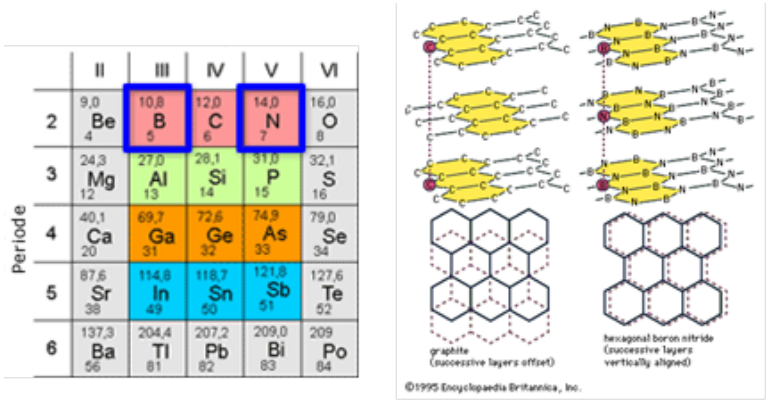

Figure 3.7: Hexagonal Boron Nitride (hBN) [4]

Due to its very high working temperatures, above 1800°C, it uses is possible in both inert and reducing atmospheres, its crystallographic structure also allowing its use as a dry lubricant and in low-friction applications. Boron nitride is a white powder.

An important difference between graphite and boron nitride lies in their electrical properties, and also in their performance as lubricants in the presence of water: graphite layers adsorb humidity.

The structure of boron nitride as a lamellar lattice is shown in Figure 3.7, boron and nitrogen atoms alternate around an atomic hexagon. At room temperature, the B-N separation in the sheets is 1.45 Å and the separation between the sheets is 3.33 Å[21].

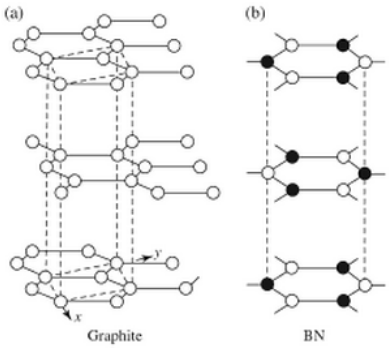

Figure 3.8: Comparison between graphite and Boron nitride atom structure[4]

Boron nitride is available in a variety of purities and particle sizes. The properties of these varieties influence the degree of lubrication provided by BN since particle size affects the degree of adhesion to a substrate, the burnishing ability of BN offers a unique combination of properties not to be found in any other material [4].

Table 3.1: Boron nitride properties

Property	value
Molecular weight	24.83
Density	2.27 g/cm3
Crystal structure	Hexagonal
Color	White
Dielectric strength	35 KV/mm
Dielectric Constant	4.2
Thermal conductivity	55 W/m K
Coefficient of friction	0.2-0-7
Service temperature	1200 °C (oxidizing atmosphere)
Practice size	1-10 microns grades

A comparison of melting points (°C) between boron nitride and other common ceramics is reported in following Figure 3.9

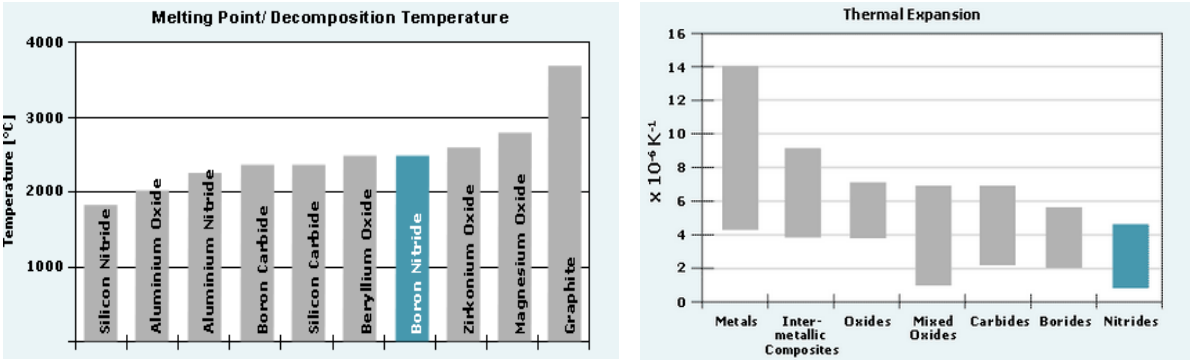

Figure 3.9: (A) In air, BN is useable to temperatures as high as 950 °C. In inert or vacuum conditions, to temperatures above 2500 °C; (B) thermal shock of BN is superior to that of other high temperature ceramic materials [4]

BN has relativity low density, as shown here below in Figure 3.10

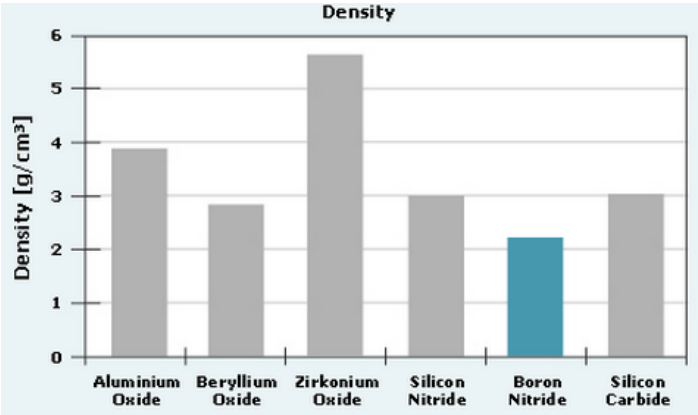

Figure 3.10: diagram of BN Density; BN has the lowest density of all ceramic materials[4]

And for this reason, together with its lubricant properties, BN in its hexagonal form (h-BN) is a good candidate for aerospace applications, providing solutions to a variety of technical problems, but also many other applications could be listed

- hBN powder as a lubricant additive can be dispersed in lubricating oil, water and solvents, and as an additive in paints.
- hBN powder is used in the extrusion of metals, because of its high working temperatures.
- hBN is used as an electrical insulator in electronics as a substrate for semiconductors, microwave transparent windows, seals, electrodes and as a catalyst in fuel cells and batteries.

- hBN is used in the manufacture of crucibles and other high-temperature containers, molten-metal carrier pipes, pumps, thermocouple protection sheaths and linings for reaction vessels.
- Its high lubricity allows its use as a mold release agent for plastic injection and metal injection molds.
- Due to its non-wetting properties, hBN is widely used in glass manufacturing processes.
- **hBN powder can be mixed with ceramics, alloys, resins, plastics, rubbers and other material to obtain self-lubricating composites**.
- hBN is also used in cosmetics, paints, dental cements, pencil leads, etc.
- Due to its high temperature stability, it is used in many aerospace applications.

3.8. Epoxy resin

For this study, a low-viscosity epoxy system (Huntsman, Switzerland) containing Araldite LY5052 (resin), with Aradur 5052 as hardener, was used as the polymeric matrix, as commonly used in high-performance aeronautics composite parts.

Advantages of these products include:

- Low viscosity
- easy impregnation of reinforcement materials.
- Long pot life (2 hours for 100 ml at ambient), ample processing time allows production of big objects.
- High temperature resistance (glass transition temperature) after ambient cure;
- Excellent mechanical and dynamic properties after ambient cure with potential for even higher properties after post-cure at elevated temperatures.

Laminates produced with this material show outstanding mechanical and dynamic properties.

We also used another high-performance resin, Hexcel Hexflow RTM 6, aeronautical grade, because it is a mono-component resin able to reach high curing temperature (± 200 °C).

Advantages of this resin include:

- Mono-component system
- Already degassed. Ready for use
- High glass transition temperature
- Excellent hot/wet properties
- Easy to process (low injection pressure)
- Long injection window ≥150 min at recommended injection temp.
- Low moisture absorption
- Short, simple cure cycles

3.9. Polydimethylsiloxane

In this thesis, another type of polymer used is silicone elastomer from DOW CORNING (USA) Sylgard® 184, the advantages are:

1. It is flowable
2. Room temperature and heat cure
3. Good dielectric properties
4. Rapid, versatile cure processing controlled by temperature
5. High transparency allows easy inspection of components

3.10. Composite materials into the market

As mentioned above, this thesis discusses the fabrication and the possibility of inserting 2-dimensional materials into composites and this paragraph reports some industrial applications already on the market.

Currently, aerospace and high-performance sports products companies are trying to incorporate nano-reinforcement in their macroscopic composites, following the use of carbon fiber composites, to improve the inter-laminar resistance, and the strength of the final product [20].

Obviously, these excellent properties are significant at the nano scale, but the challenge is to achieve complete and homogeneous dispersion of particular graphene-related materials in various polymers.

Many graphene-based composites are already on sale worldwide, and many important companies are betting on graphene-containing products, including:

- **HEAD**

  In early 2013, the YouTek Graphene Speed series tennis rackets incorporated graphene to make the shaft stronger and lighter. In 2014, , a line of skis called Joy were produced to be more lightweight and durable, including several different models, which are currently about 20% more expensive than traditional skis.

Figure 3.11: Head graphene products on the market

- **VITTORIA**

In October 2014, Vittoria released a new range of racing bicycle wheels (Qurano) built from graphene-enhanced composite materials.

http://www.graphene-info.com/graphene-products

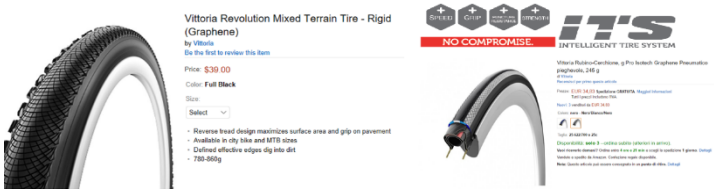

Figure 3.12: Vittoria graphene products

- **CATLIKE**

Catlike launched a line of cycling helmets called Mixino 2014, enhanced with graphene. These helmets are said to be light and strong, and offer major improvements in the field of safety and impact absorption.

http://www.graphene-info.com/graphene-products

Figure 3.13: Catlike graphene products on the market

- **GRAPHENSTONE**

Graphenstone produce an extensive range of graphene-based color paints, including emulsions and dispersion paints with graphene-based calcium hydroxide.

Figure 3.14: Graphenestone graphene products on the market

- **SHER-WOOD**

In 2016 Sher-wood presents a new line of graphene-infused composite hockey sticks, with graphene integrated into the key breakage areas of the REKKER EK60 to make the stick not only lighter, but more durable and more resistant to hacks and blows from other sticks.

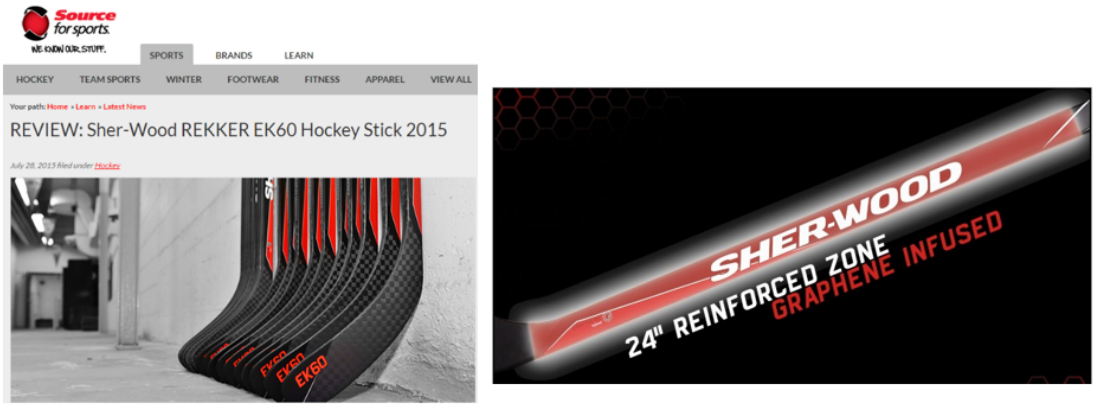

Figure 3.15: Sher-wood graphene products

4. Composite materials

Nowadays many applications in the aerospace and automotive fields involve thermosetting polymer (thermoset) systems used as matrices in composite materials [23].

Thermosets can be used in applications such as casting resins, adhesives, high-performance parts, structural and secondary parts.

The structure of the polymeric chains influences the mechanical properties of the composite matrix, for example, by increasing the crosslink density, the velocity of crosslinking with curing temperature, generating enormous differences in the final composites obtained.

This thesis investigates the possibility of making composite materials with multi-functional properties, for example, with greater toughness without sacrificing other important characteristics such as thermo-electrical properties, water barrier capacity and electro-mechanical properties which are required in many applications.

To achieve this, technical nano-composites were prepared with nanomaterials such as graphene, boron nitride and 2-dimensional materials being used to reinforce thermosetting polymers.

In the literature, one can find reports of many composites created with incorporation of low- and high-aspect ratio nano-fillers, which have already demonstrated improvements to toughness and other properties of polymers such as thermal resistance and electrical resistivity. However, such materials for industrial applications involve high costs, complex processes and limitations in production technology limiting production and the application of nano-composites on a large industrial scale.

High specific surfaces of reinforcement materials in polymer composites create a huge interface between polymer and filler, an extremely important aspect in the fabrication of composites.

The fraction of atoms localized at the surface in nano-materials is much higher than the corresponding microscale materials and, although this provides a better wettability of the filler to the polymer matrix, the physico-chemical properties at the nanoscale of the same material can be significantly different. The interactions between filler and matrix depend on the particle surface structure, geometry and functionalization, exerting great influence over formation of the interface.

In this thesis, in order to develop improvements in multiple properties, low- and high-aspect ratio fillers were incorporated into epoxy, using fillers with the following characteristics:

1. Higher rigidity to increase tensile strength and toughness,
2. High and low specific surface areas

3. Small and large lateral dimensions to ensure good levels of bonding between matrix and filler.

The aim of this study is to demonstrate the excellent properties of high performance epoxy/graphene systems and other two-dimensional-based nano-composites through the characterization of their electrical, thermal gas barrier and mechanical properties.

4.1. Mechanical reinforcement

Thanks to the impressive mechanical properties of graphene, graphene-based composites show unexpected improvements in the mechanical performance of the composites accompanied by modifications in functional properties such as electrical conductivity, thermal conductivity and water barrier behavior.

A large portion of this work was based on different forms of graphene, such as graphene nano-platelets (GnP), graphene bi-layer, graphite micro platelets and so on and, as discussed above, it is often difficult to confirm the nature and the form of the graphene supplied.

An important and crucial task is obtaining a good distribution and dispersion of the nano-filler in the fabrication of polymer-based nanocomposites since the properties of the nanocomposites can be compromised by a poor dispersion [8, 12].

There are many different processes for fabricating composites such as, for example, using graphene oxide to allow preparation of the composites in aqueous solution and, in particular, nanocomposites can readily be prepared with water-soluble polymers such as poly(vinyl-alcohol) and poly(ethylene-oxide).

Nanocomposites can also be prepared using solution-based methods with non-water-soluble polymers such as poly(methyl-methacrylate) and polyurethanes.

The *in-situ* polymerization of the polymer matrix is also possible and, although solvents are often employed to reduce the viscosity of the dispersions and increase the miscibility of the polymer with the filler, nanocomposites with *in-situ* polymerization of epoxy resins and graphene nano-platelets, for example, can be produced to enhance the properties of the final composites [24].

Graphene-based nanocomposites have, in fact, been prepared with a wide range of different matrix materials including silicone foams, epoxy resin, PMMA (poly methyl methacrylate) and poly(vinylidene-fluoride) PVDF, besides thermoplastic polymers [25].

An important technique used to study the mechanical properties of composites is the measurement of stress–strain curves. Figure 4.1 shows, for example, some stress-strain curves of poly(vinyl-alcohol) reinforced with reduced graphene oxide, with improvements in tensile strength depending on the reinforcement percentage in the polymer matrix.

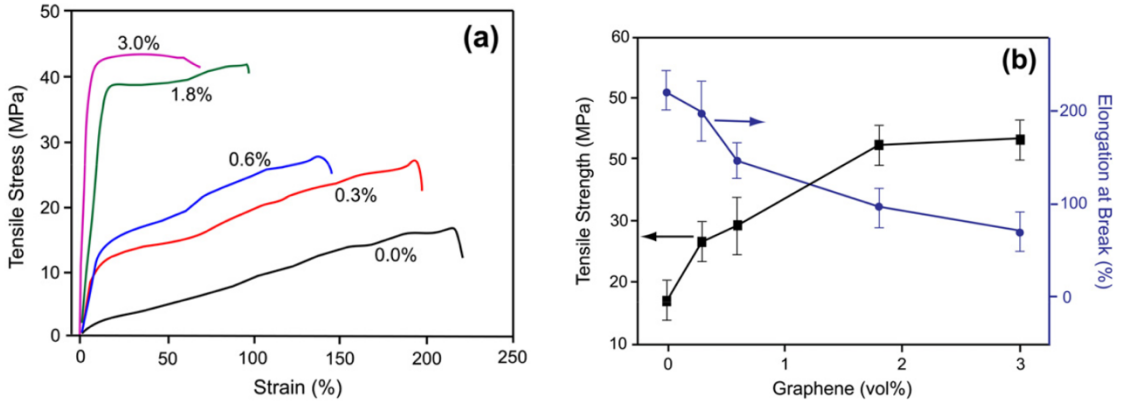

Figure 4.1: Mechanical properties of nanocomposites consisting of reduced graphene oxide in PVA at various loadings (vol. %). (a) Stress–strain curves, (b) tensile strength and elongation at break versus graphene loadings[12]

There is a large effect on the stress–strain curve with a loading of only 0.3% by volume of reduced graphene oxide. The addition of 10x more material (up to 3.0%) leads to only a minor effect on mechanical properties. Both the Young's modulus and tensile strength of the polymer are found to increase with the loading of reduced graphene oxide but the elongation at break decreases. This behavior is typical of many graphene/polymer systems of which have been reported in the literature [12].

Kinloch and coworkers investigated the reinforcement of a polyurethane using pristine graphene produced by solvent exfoliation instead of reduced graphene oxide, Figure 4.2 shows a series of stress–strain curves for different graphene loadings by weight [5].

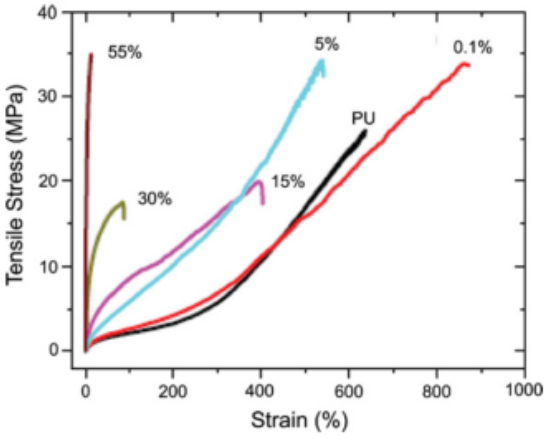

Figure 4.2: Stress–strain curves for nanocomposites consisting of solvent-exfoliated[5]

There is a large increase in the slope of the stress–strain curve (the Young's modulus increases by a factor of around 10^2 for their highest loadings) with the strain-to-failure decreasing with graphene loading.

Kinloch et al. studied the reinforcement of flexible polyurethane with a Young's modulus of only around 10 MPa. It was shown that much higher levels of reinforcement are generally found with low-modulus polymers than with more rigid matrix materials.

But the introduction of graphene-related materials in polymer matrices is not always advantageous for the final composites. For example, Kinloch et al. studied in detail the effects of the size of graphene flakes on the reinforcement of PMMA. Electrochemically exfoliated graphene of two different lateral dimensions (20 μm and 5 μm) and similar thicknesses was successfully incorporated by melt mixing using a twin-screw compounder in a PMMA matrix at loadings from 0.5 wt.% to 20 wt. %. In this case, the thermal stability of the polymer with the addition of graphene improved significantly, with higher T_d (thermal degradation temperature) values being observed for 5-FLG (few layer graphene) relative to 20-FLG. Shifts in the T_g (glass transition temperature) determined by DMTA (Dynamic mechanical thermal analysis) were found only for the 20-FLG/PMMA composites, which suggested the existence of attractive interactions between the 20 μm graphene flakes and the polymer. The DMTA data revealed substantial reinforcing effects for both fillers, up to the optimal loadings of 20 wt.% and 2 wt.% for 20-FLG and 5-FLG, respectively [25].

Tensile testing showed glassy polymeric behavior with increased elastic modulus for 5-FLG up to the optimal 2 wt.% loading and up to 20 wt.% for 20-FLG and increased tensile strengths for both fillers up to 5 wt.% loading. Increased brittleness with loading was found for both fillers due to the formation of agglomerates of graphene deteriorating the graphene–PMMA interface. The use of graphene with large lateral dimensions seems to provide better interfacial stress transfer with the polymer relative to smaller flakes, due to a more extensive contact area, improving the overall mechanical properties of the nanocomposites as showed in the following Figure 4.3

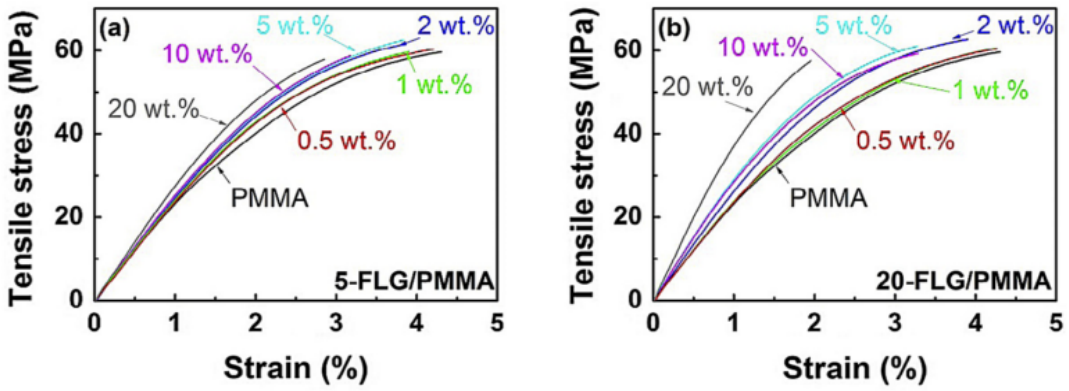

Figure 4.3: Stress–strain curves of 5-FLG/PMMA (a) and 20-FLG/PMMA (b) nanocomposites at the loadings studied[25]

A list of improvement in mechanical properties observed in different polymers is reported in Table 4.1

Table 4.1: Mechanical properties of graphene/polymer composites from the literature[26]

Filler type and % loading	Matrix	% increase in tensile or yield strength	% increase in elastic modulus	Fabrication method
0.7 wt% GO	PVA	76	62	Solution mixing
4 wt% GO	PVA	136		Solution mixing
0.5 wt% in situ CRGO	PVA	212		
2 wt% GO	PVA	92.2	167	Solution mixing
0.8 wt%GO	PVA	52	54	Solution mixing
0.8 wt% in situ CRGO	PVA	66.3	66.7	
0.5 wt% CNT+1 wt% GO	PVA	41	31	Solution mixing
2 wt% Graphene by directly sonicating and exfoliating graphite	PVC	130	58	Solution mixing
0.44 vol% GO	Hydrogenated carboxylated nitrile-butaduene rubber	50	100	Solution mixing
1 wt% in situ CRGO	PMMA	60.7		In situ polymerization
1 wt% TRGO	PMMA	20	80	Solution mixing
1 wt% TRGO	PMMA foam	13	20	Blending and foaming
0.5 wt% Graphene from XG Science	PA12	32.2		Melt blending
2 wt% CRGO	PBS	22		Solution mixing and then melt blending
1 wt% GO	PA/polyphenylene (PA/PPO, 90/10)	87		Solution mixing and then melt blending
0.5 wt% GO	PCL film	77	49	Solution casting
0.3 wt% GO	PCL nanofibrous membranes	95	66	Electrospin
3 wt% GO	PI	7	27	In situ polymerization
3 wt% ODA- GO	PI	893	1419	
0.5 wt% In situ CRGO	PS	27.8	28.4	Solution mixing
0.9 wt% PS grafted GO	PS	69.5	57.2	Solution mixing
0.05 wt% in situ TRGO	Polyester	72.2		Solution mixing
0.5 wt% TRGO	PLA	12.9		Melt blending
0.54 vol% GO	Epoxy	10	25	Solution mixing

4.2. Electrical conductivity in graphene based composites

Thermoset polymers are usually insulating, but it is possible to obtain electrical percolation in final composites using a graphene filler.

Stankovich et al. achieved electrical conductivity with ca. 0.1 vol.% loading (Figure 4.4). This percolation threshold is about three times lower than reported for any other two-dimensional filler percolation threshold for three-dimensional materials due to the extremely high aspect ratio of the graphene sheets [8].

At a loading of about 0.15 vol.%, the conductivity of those composites already satisfies the antistatic criterion (10^{-6} Sm^{-1}) for thin films and rapidly rises over a 0.4 vol.% range. An increase in graphene sheet loading above 0.5 vol.% yields a more gradual increase in electrical conductivity, with values of ≈0.1 Sm^{-1} at ≈1 vol.% and ≈1 Sm^{-1} at 2.5 vol.%.

Samples investigated in the study of Stankovich et al. were 0.24, 1.44 and 2.4 vol.%.

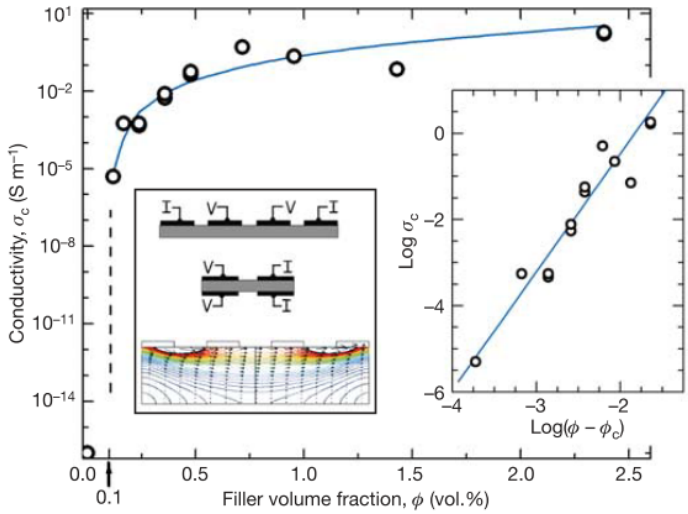

Figure 4.4: Electrical conductivity of the polystyrene–graphene composites[8]

Also, Debelak et al.tudied the electrical properties of macro-composites with graphene fillers, Figure 4.5 shows the electrical resistivity of the exfoliated graphite micro-platelets-based polymers versus the graphite filler concentration for three different sizes of the graphene micro-platelets,

- large (specific surface area 16.02 m^2/g),
- medium (specific surface area 15.61 m^2/g),
- small (specific surface area 15.35 m^2/g)

They reported that the electrical resistivity of the exfoliated-graphite-filled polymers decreases with increasing exfoliated graphite micro-platelet concentration. At 8 wt.% of exfoliated graphite micro-platelets, for all three sizes, the resistivity for the composites was already nearly four orders of magnitude lower than the baseline polymer. When the polymers were filled with 20 wt.% of exfoliated graphite micro-platelets, for the three sizes, the resistivity reached levels that were between six to eight orders of magnitude lower than baseline.

The large-graphite-flake-filled polymers showed the lowest resistivity at each graphite concentration, followed by medium- and small-flake-filled, respectively. The large flakes also produced the highest rate of decrease in resistivity with initial increase in concentration. The trends show that the electrical resistivity decreased with increasing particle size. Clearly, the electrical conductivity critically depends on how the graphite micro-platelets are processed, exfoliated, and dispersed in the polymer matrix.

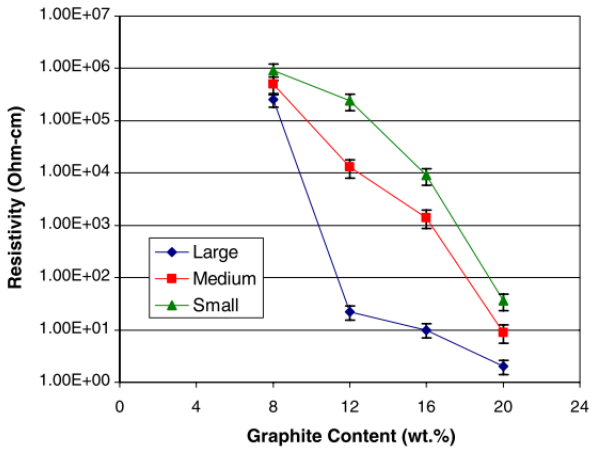

Figure 4.5: Electrical resistivity of exfoliated graphite filled polymers with different graphite sizes as a function of the graphite content[7]

Table 4.2 gives a quick overview of the electrical properties in different polymers reinforced with different graphene type

Table 4.2: Electrically Conductive Graphene/Polymer Nanocomposites [18]

polymer[a]	graphene type	processing	electrical percolation threshold (vol %)	ref
		chemically modified		
PS	iGO[b]	solvent blending + hydrazine	0.1	81
vinyl chloride/vinyl acetate copolymer	GO	solvent blending + hydrazine	0.15	142
PS	electrochemically exfoliated graphite	solvent blending + ionic liquid	0.13−0.37	51
epoxy	partially reduced GO	in situ polymerization at 250 °C	0.52	147
PMMA	GO (17 mol % O)	in situ polymerization	(1.3)[c]	116
PMMA	GO (12 mol % O)	in situ polymerization	(1.6)	144
		thermally exfoliated		
TPU	TRG, ~800 m^2/g, 4 mol % oxygen	solvent blending	0.3	112
		in situ polymerization	0.4	
		melt compounding	0.8	
PEN		melt compounding	0.5	125
PC		melt compounding	0.6	124
natural rubber	> 600 m^2/g, 5 mol % oxygen	melt or solvent blending + vulcanization	(0.8, solvent blend), (> 2.0, melt blend)	123
PS−PI−PS		melt or solvent blending	(0.6)	
PDMS		oligomer blending + polymerization	(0.6)	
TPU	apparent specific volume: 410 cm^3/g, 5 mol % oxygen	solvent blending	(1.0)	145
TPU		solvent blending	(1.0)	146
TPU		in situ polymerization	(1.6)	120
PVDF	–	solvent blending	(1.6)	143
SAN	600−950 m^2/g, up to 14 mol % oxygen	preblending using solvents, followed by melt compounding	(1.9)	91
PC			(1.3)	
PP			(2.0)	
PA6			(3.8)	

4.3. Thermal conductivity in graphene based composites

Debelak et all [7] showed that the thermal properties of the additive-filled polymers should be greatly improved following addition of exfoliated graphite micro-platelets.

After exfoliation, a lower concentration should be needed to reach high thermal conductivity expanding the area of applications where a quick thermal release is needed. Figure 4.6 shows the thermal conductivities of the exfoliated graphite-filled polymers versus the graphite micro-platelet filler content for the large, medium, and small flakes.

As with the electrical conductivity, thermal conductivity for the three particulate sizes increases with higher graphite concentration.

The large-graphite-flake polymers have a threshold at 3 wt.%, while medium and small have thresholds at 6 and 10 wt.%, respectively. This is because the larger graphite flakes have larger aspect ratios performing better in thermal conduction improvement.

With the addition of 4 wt.% of large graphite micro-platelets to polymers, the thermal conductivity was 0.868 W/m K, nearly a 300% increase over the baseline polymer (0.219 W/m K). The large flake systems increase almost linearly with increasing graphite content while both medium and small systems increased at an increasing rate.

At 20 wt.% all the series were about 4.3 W/m K [7].

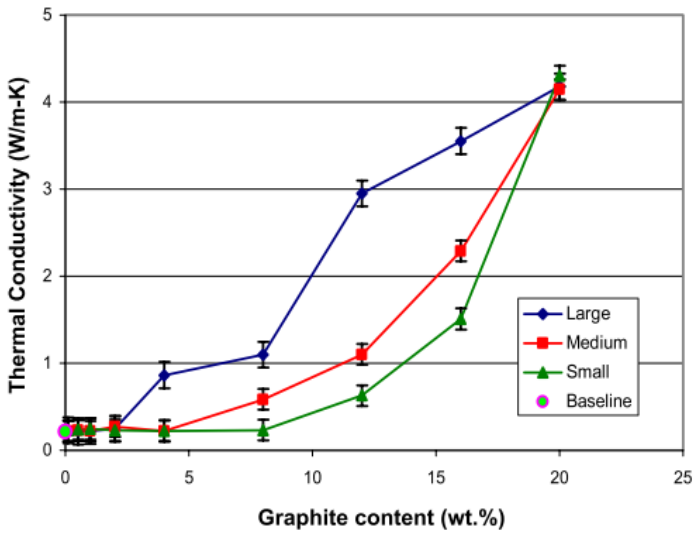

Figure 4.6: Thermal conductivity of exfoliated graphite filled polymers with different graphite flake sizes as a function of the graphite content[7]

Hyunwoo et al. [18] demonstrated superior thermal transport properties of graphene dispersions in thermal management. They reported that 2-D, platelet-like graphene nano-platelets (GNP) can improve thermal conductivity more effectively than 1-D, rod-like carbon nanotubes or carbon fullerenes.

However, unlike the exponential increase in electrical conductivity, thermal conductivity enhancement by the carbon nano-fillers is not as dramatic, and often even lower than expected from effective medium theory. This is partly due to the smaller contrast in thermal conductivity between polymers (0.1-1 W/m K) and graphitic carbons (MWCNT 3000 W/m K and graphene 5000 W/m K).

Improving thermal conductivity using GNP was demonstrated for epoxy, polypropylene (PP), polyethylene (PE), polyamide (PA), and paraffin wax, see Table 4.3.

For epoxy systems, up to a 30-fold increase in thermal conductivity was attained by incorporating 33 % vol. or 25 % vol. of few-nanometer-thick graphite micro-platelets.

Exfoliation, orientation, and interfacial functionalization of the flake can influence the thermal transport in composites, if the platelets are forced to be anisotropic by extrusion or solvent casting, conductivity was higher along the direction of the graphite.

Table 4.3: Thermal properties of graphene/polymer composite from the literature [26]

Filler type	Matrix	%increase in thermal conductivity	Increase in T_{on} [°C]	Reference
25 vol% TRGO	Epoxy	3000		[45]
0.3 wt% CRGO	Epoxy		5	[51]
0.5 vol% DDS-GO	Epoxy	800	16	[89]
2 wt% PS-g - CRGO	PS	260		[90]
0.19 vol% RGO	PS		60	[6c]
4 wt% TRGO	1-octadecanol (stearyl alcohol)	140		[91]
2 wt% CRGO	PBS		16	[58]
0.5 wt% PP-g-TRGO	PP		~90	[56]
0.7 wt%GO	PVA		3	[37a]
3 wt% Microwave-exfoliated GO	PC	21	Very little	[9b]
3 wt% TRGO	Polylactide		14	[55]

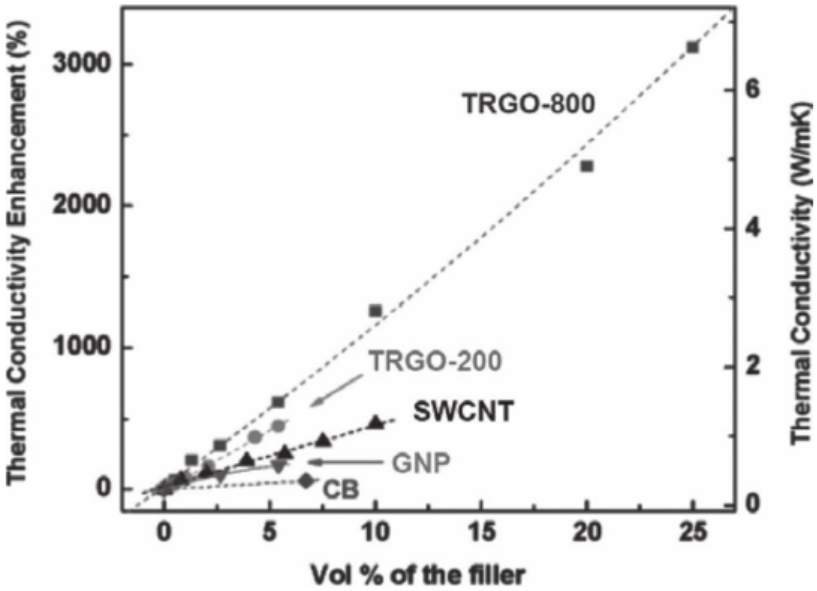

Figure 4.7: Thermal conductivity improvement of epoxy-based composites at 30 °C using GNP, TRGO (thermal reduced graphene oxide) reduced at 200 °C (TRGO-200) and 800 °C (TRGO-800), CB, and purified SWCNTs. Reproduced with permission [26]

4.4. Gas and water barrier properties in graphene based composites

Other important applications of graphene-based composites exploit its water/gas impermeability, as graphene, because of its monoatomic honeycomb lattice, is impermeable to all gases.

Cheng et al. [26] investigated the resistance of CRGO (chemically reduced graphene oxide)/PVA (polyvinyl-alcohol) composites to water permeability. Contact angle measurements showed that the composites became hydrophobic ($\theta > 90°$) in contrast to the highly hydrophilic ($\theta < 90°$) pure PVA. In PVA, water absorption ratios pass from 105.2% to 48.8% with 1 wt. % filler percentage, after testing in distilled water at 30 °C for 24 h, indicating a significant improvement in its water barrier properties.

It was also reported that some graphene/polymer composites have good gas barrier properties, which is very important in their use as physical barriers for gases such as O_2, N_2 and He in packaging materials [26], GNP addition induces an important increase in the hydrophobicity of composites.

Neat epoxy resin is a hydrophilic material having a contact angle around 70°, the addition of GNPs inducing hydrophobicity. The contact angle of water over GNP/epoxy composites is in the range of 92–104° [10].

The higher hydrophobic behavior of GNP/epoxy composites could give a higher chemical strength in humid environments [10].

The water uptake curves are shown in Figure 4.8 where the maximum water content absorbed decreases for GNP/ epoxy composites in comparison with white thermosetting resin.

At low GNP loadings, the maximum water percentage absorbed varies from 1.78% for neat resin to 1.42% for composite reinforced with 2 wt. % GNPs. This is with the presence of barriers of graphene since the diffusion coefficient, measured as the initial slope of the curve, also decreases [10].

But this effect is not as significant if homogenization of the graphene/matrix is not achieved limiting the water barrier effect.

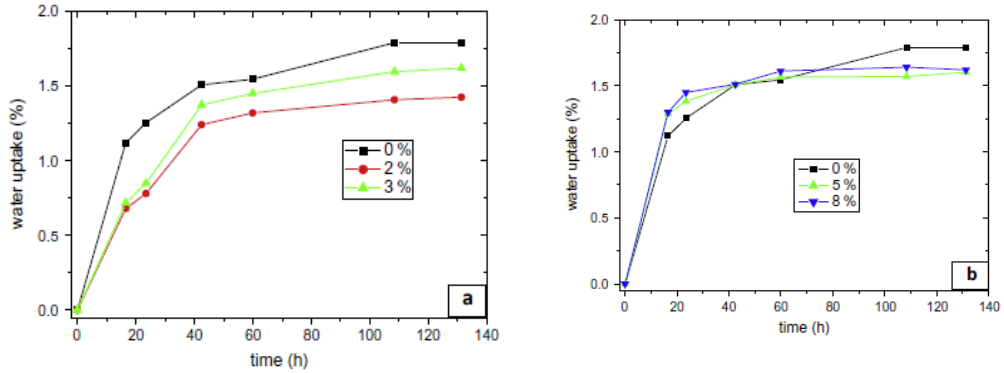

Figure 4.8: Curves of water uptake in water immersion at 80 °C for neat epoxy [10]

In the curves, it is possible to observe the decreasing water uptake, which increases the operational life of the composites.

4.5. Graphene based composite with novel electrical and dielectric properties

The globally increasing demand for energy is a technical challenge for electricity generation, transmission and distribution systems [9], It often requires contradictory features such as increasing voltage levels in combination with more compact designs in urban environments implying an increased electric stress on the insulation systems.

Another aspect that this thesis investigates is the possibility of using insulating materials (ceramics such as boron nitride) with tunable non-linear conductivity, as well as high dielectric constant and low loss, for electric field grading applications.

Electrical field grading or electrical stress control is important to evaluate in high voltage cables and devices accessories to mitigate and dissipate high electrical stresses which may cause a breakdown in the overall electrical system.

Current field grading materials consist of polymers, semi-conducting ceramic particles such as SiC, ZnO, etc., as well as lower amounts of carbon black, embedded in polymer matrices. The nonlinear electrical conductivity is created by the percolated structure of these particles inside the matrix with a volume loading of 30% to 40% [9], but such quantities of filler could affect the mechanical properties, higher weight and a tendency to overheat at elevated electric fields.

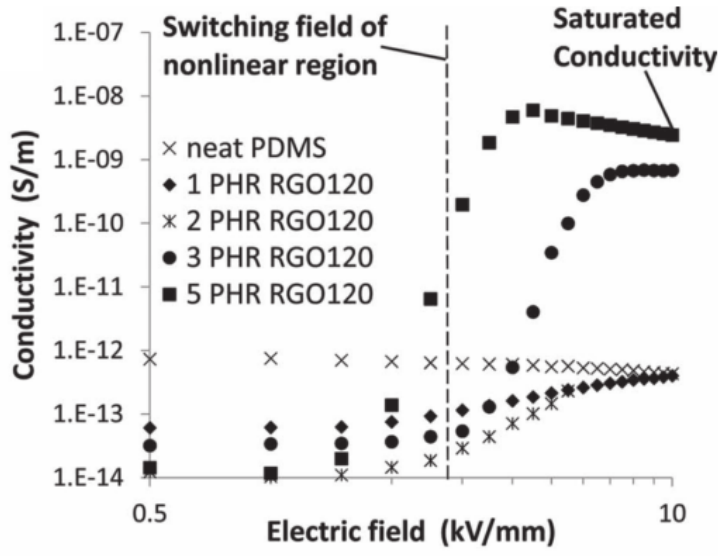

Figure 4.9: Plot of conductivity with respect to field strength, in composite with different loading of GO reduced at 110 °C [9]

Figure 4.9 shows the ability to tailor the properties of the composites by altering the GO (graphene oxide) oxidation state. For example, 3PHR-RGO120 (The samples are denoted with their GO loading and reduction temperature 3PHR-RGO120 means the loading was 3 PHR (parts per hundred parts of resin) and the GO was thermally reduced at 120 °C).

4.6. Commercial graphene related products

As mentioned in the previous chapter, nowadays there are a lot of products, especially in the field of composites, for structural applications and high-performance sport. However, most of these products do not contain standard, monoatomic graphene. For example, Young et al. [6] analyzed a tennis racquet from HEAD to understand the real presence of graphene in that product, using a combination of optical microscopy and Raman spectroscopy, discovering that the main structural components in the racquet frame are high-strength carbon fibers in an epoxy resin matrix.

This article reported that graphene-based nanoparticles are used to reinforce resin-rich regions in the shaft of the racquet at the discontinuity in the fiber rows, where the handle is joined to the racquet head.

From a detailed analysis of the relative positions and intensities of the Raman G and 2D bands, it is demonstrated that the nanoparticles employed in the racquet are most probably graphite nano-platelets which have been added to improve the mechanical properties of the resin-rich regions.

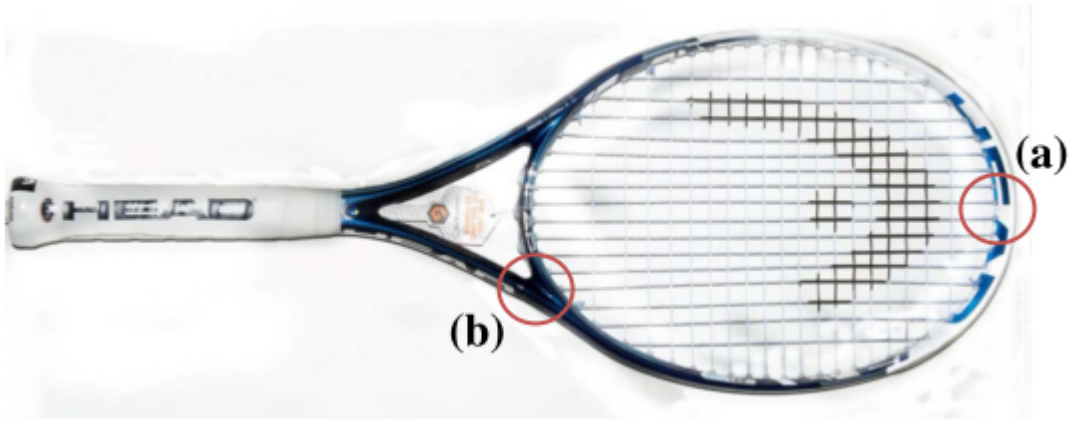

Figure 4.10: The HEAD graphene tennis racquet showing the two regions investigated (a) the tip and (b) the shaft [6]

The racquet structure was examined by optical microscopy and it was found that up to 18 plies of prepreg (pre-impregnated carbon fiber) were arranged such that the fibers were aligned mainly tangentially around the racquet head.

The combination of optical microscopy and Raman spectroscopy is a powerful method to characterize the microstructure of a graphene-based tennis racquets.

The main structural component in the racquet is high-strength carbon fibers in an epoxy resin matrix.

Resin-rich regions were observed in the area where the head of the racquet is joined to the handle. It appears that this area, which is a point of potential weakness in the racquet, was reinforced with graphene in the form of graphite nano-platelets.

Resin-rich regions were observed in the area where the head of the racquet is joined to the handle. It appears that this area, which is a point of potential of weakness in the racquet, has been reinforced with graphene in form of graphite nano-platelets.

4.7. Aeronautical composites

This thesis studies the possibility of improving polymers commonly used in aeronautics with nano-fillers, and in the aerospace industry there is a remarkable increase in the use of composites as shown in the following Figure 4.11,

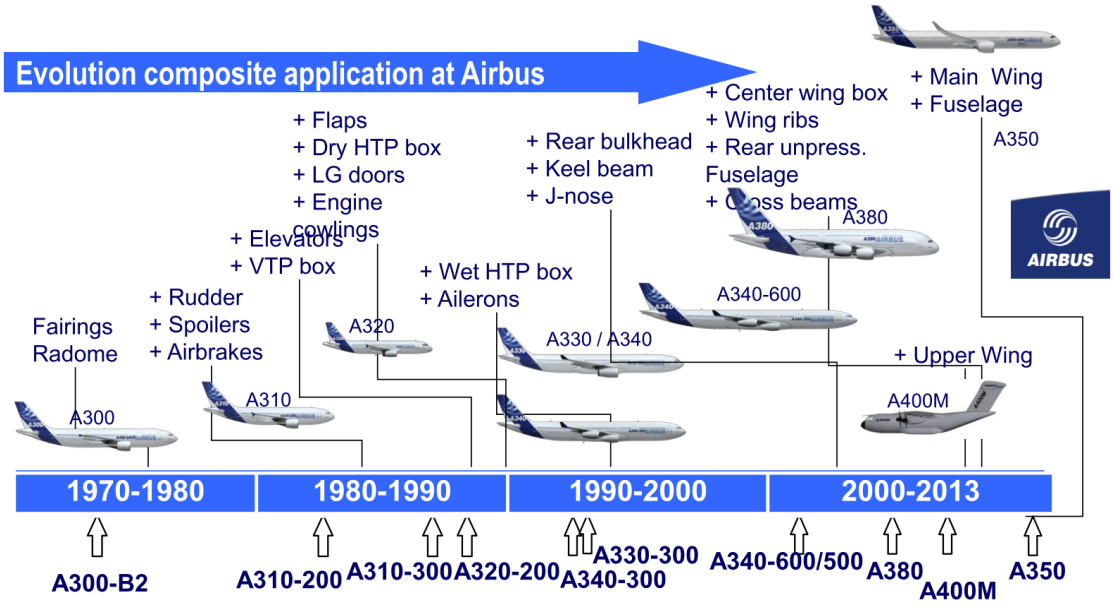

Figure 4.11: Evolution composite application at AIRBUS[27]

Over the past few years, polymer nano-composites (PNC) have received much attention from researchers, attempting to enhance the properties of engineering polymers whilst retaining their facile processing aspects.

Compared to traditional filler-polymer systems, nanocomposites require relatively low dispersant loadings to achieve significant property enhancements, as mentioned above.

This makes them key candidates for aerospace applications. Some of these enhancements include increased modulus, improved gas barrier properties and better thermal resistance and conduction. An example is shown in Table 4.4 [28] where it is possible to observe the mechanical properties of materials used in the aeronautics industry.

Table 4.4: Mechanical properties for various polymer nano-composite

	Tensile Strendth [MPa]	Tensile Modulus [GPa]	Elongation [%]	Nanomaterials
Poly(tetramethylene glycol)/Clay	6.09	0.0278	517.6	Clay
Poly(butylene adipate)diol/Clay	9.74	0.0401	419.9	Clay
VGCF/Epoxy composite	0.749	6.05	-	18.2% VGCF
Laser ablation SWNT/TOR-NC[a]	120	3.2	4.9	SWNT (0.2 vol.-%)
Laser ablation SWNT/TOR-NC	94	3.2	3.5	SWNT (0.1 vol.-%)
Polycarbonate 600™	88	0.002751	24	3-5% wt.-%
HiPCO SWNT/TOR-NC	0.06136	2.6	4.0	SWNT (0.2 vol.-%)
HiPCO SWNT/TOR-NC	99	2.7	4.2	SWNT (0.1 vol.-%
Poly(ether ether ketone)	101	5.6 ± 0.2	–	15% VGCF
MWNT/polyestrene	120	~2.2	–	0.05 vol.-% MWNT
LaRC™CP2/SWNT	~22	3.72	–	0.05 vol.-% SWNT
CFRP Q-I IM&/8552	138.9	58	1.58	None
Inconel 718	1300	190	14	None

With the development of nano-structured components, the properties of composites can be tailored and optimized for particular applications without affecting the main properties required of such advanced composites.

In the aerospace industry, polymer composites are widely used, in both structural and secondary aircraft parts, where high performance materials, durable over long operational periods in extreme climatic conditions where traditional composite materials cannot be used, are necessary. However, the development of nano-composites for an extended range of fields of application would have been both costly and potentially risky and therefore their initial development was confined to specific applications, such as high-performance sport and military applications, before the technology was later extended to a wider range of fields of application.

Some of the key advantages in aerospace in producing light-weight structures are:

1. Saving fuel, with significant cost reduction;
2. Ecologically, protecting the climate and nature (reducing NOx emissions according to climate agreements).
3. Satisfying increasing aircraft market requirements.

Thus, in this thesis we focus upon the study of composite nanostructured materials for aeronautics, and resins suitable for aeronautics applications were selected and the use of

different graphene-based materials tested to enhance multi-functionally different properties including:

1. Mechanical reinforcement: not to replace carbon fiber, but to improve inter-laminar strength
2. Electrical properties: lightning strike, electrostatic discharge
3. Gas barrier properties: water uptake.

5. Benchmarking of commercial GRM materials for applications in composites

In recent years, 2D materials (such as graphene, boron nitride and transition metal di-chalcogenides) have attracted increasing attention for a wide range of industrial applications, in particular for composite materials.

Bulk composites are currently the only commercially available GRM (graphene-related material) used in various applications. The number of products containing these composites is increasing continuously, from tennis rackets to bicycles, to skis. However, the lack of a clear metrology and quality control is creating confusion among industrial end-users, with many websites and companies advertising as graphene, graphite powders, platelets or other carbon materials. To improve the metrology of GRMs, a nomenclature [13] and a classification framework[29] have been recently proposed for 2D graphene-based materials.

A large number of graphene producers worldwide provide GRMs of very different qualities and it is thus difficult to evaluate correctly whether new materials developed and described in research papers or on company websites are truly competitive with commercially available ones, either in performance or in production costs.

In order to have a realistic evaluation of the state-of-the-art of existing commercialized products, which is of fundamental importance, we developed a procedure to compare and analyze GRMs of different origins.

The chapter is divided as follows:

1) The first section describes the various techniques for analyzing GRM flakes for industrial applications, typically on the kilogram scale. The materials are analyzed with a combination of techniques, as described below, to compare their exfoliation grade, average thickness, and statistical distribution of their lateral dimensions.
2) The second section reports some exploratory work on the analysis of complete GRM-based products, already commercially available, to evaluate if and how they truly contain graphene.

Our analysis involves only a few of the many GRM-based products on the market, only producers which can readily supply more than 1 kg of graphene nano-platelets powder, and some suppliers who are partners of European research projects together with larger companies which are no longer in their start-up phase.

The size and exfoliation grade of 2D materials are fundamental parameters to be assessed because they have an impact on final materials performance, influencing mechanical and electrical properties in polymer composites, charge transport and gas permeation in thin

films.

Most published articles and technical datasheets available report just the average lateral size of the GRMs, quantified using two common statistical parameters: arithmetical mean and standard deviation (SD), assuming implicitly that the nano-sheet length follows a Gaussian distribution. However, all published experimental data show that, for any given 2D material [30], the size distribution is non-Gaussian and highly asymmetric.

Recently, we analyzed in detail the size distribution of monoatomic GO nano-sheets during sonication, using scanning probe microscopy and image processing to measure, one by one, sheet size and shape of thousands of sheets, then defining their size distribution and the fragmentation mechanism with standard mathematical models [31]. However, this approach is not suitable for commercial GRM materials, where a significant fraction of the material usually shows high levels of thickness, which is problematic for Scanning Probe Microscopy (SPM) analysis. Thus, the morphology of these materials was studied using Laser Granulometry, Surface Area Measurements and Scanning Electron Microscopy (SEM), as detailed here below.

5.1. Characterization powder Techniques

The physicochemical properties of two-dimensional fillers which can influence the behavior of GRM-polymer composites were studied; in Figure 5.1 it is possible to see what GRMs look like:

Figure 5.1: Photographic picture of graphene powder

The GRMs were characterized morphologically with SEM and BET (Brunauer–Emmett–Teller) surface area measurements and laser granulometry were used for rapid estimation of the exfoliation grade and lateral dimensions of the GRMs. In summary, we used:

- SEM to analyze the morphology
- Laser granulometry to determine the average particle size
- BET surface area to determine the thickness of the platelets

5.2. Laser Granulometry

Laser granulometry allows one to evaluate the lateral dimensions of a powder in liquid suspensions. In the granulometer, a liquid suspension flows through the path of a laser, while a CCD camera measures the intensity of the scattered light. The present analysis was carried out with a Saturn II instrument (Micromeritics, USA). The output signal is the scattered intensity vs. the scattering angle. By using numerical models following Fraunhofer or Mie diffraction theory it is possible to calculate the size distribution of the particles in the suspension. In such models, the particles are assumed to be spherical; small particles scatter low amounts of light in all directions, while big ones scatter a significant amount of light mainly in the forward direction (small angle scattering). The accessible range of lateral sizes is between a few µm to fractions of a mm. This type of characterization is extensively used as a routine standard characterization in many industrial sectors (e.g., food and pharmaceutical).

Figure 5.2 shows an example of the measured size distribution of a graphene-based powder (XGNP-M25). The abscissa axis reports the lateral dimensions, while the ordinate gives the incremental percentage of the volume occupied by the particles.

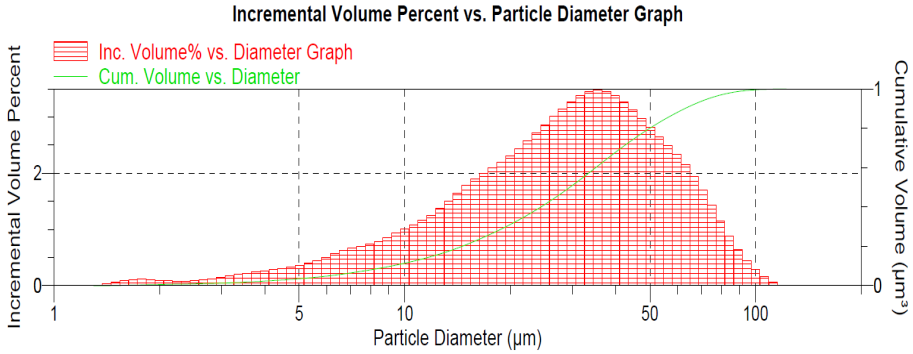

Figure 5.2: Incremental Volume Percent distribution. Sample XGNP-M25 measured using Saturn II

For practical reasons, different characteristic parameters of the distribution are always reported; the most useful and intuitive is the D50 (the length number larger than the diameter of 50% of the sample particles, also known as the "mass median diameter" as it divides the sample equally by mass). Similarly, D10 and D90 are given, i.e., the diameters larger than the 10% and 90%, respectively, of total particles.

The liquid suspension was obtained by dispersing a few mg of the powder in a 20-ml vial of isopropanol followed by 2-minute sonication. The dispersion procedure should be carefully tuned to avoid aggregation of particles on the one hand, but also to avoid further exfoliation or fragmentation of the particles, by prolonged sonication, on the other. Two samples were

prepared and measured for each powder, the mean value was chosen as the main value and the semi-dispersion as error.

5.3. Surface Area measurement

The specific surface area [m^2/g] is a key parameter in understanding the morphology of a powder. The numerical quantification of the area of high surface powders is performed by measuring the quantity of molecules physisorbed on the sample powder under controlled temperature and pressure conditions. The fundamental theory used in most commercial and scientific instruments is the BET model (Brunauer–Emmett–Teller), and for carbon-based powders the standard ASTM D6556-10 method is used. This allows measurement of specific surface areas from thousands of m^2/g (i.e., single sheets of graphene with 2700 m^2/g) down to the much lower values of commercial graphite. This value gives a rapid estimate of how much of the GRM has been exfoliated, whether they are more similar to "ideal", perfectly exfoliated graphene (surface area >2600 m^2/g) or to powder graphite (≈ 0.1 m^2/g).
Before performing the measurements following the ASTM D6556-10 [32,33] standard method, all the samples were degassed at 300 °C for 3 h. The surface area measurements were then made using an ASAP 2020 (Micromeritics, USA).

5.4. Scanning Electron Microscopy (SEM) to visualize the structure of GRM

The Scanning Electron Microscope (SEM) is a powerful tool to probe matter from the mm scale down to a few nm. It is possible to obtain SEM images with a spatial resolution of less than 5 nm. The samples were prepared by depositing a small amount of powder on conductive adhesive tape and the SEM images obtained with a ZEISS 1530 instrument under high-vacuum conditions (10^{-6} mBar).

This SEM characterization, was obtained at the CNR-IMM institute where different types of filler were examined. The following images show the typical differences observed between GRM fillers with low or high thicknesses.

Following the criteria mentioned above, the different qualities of commercial graphene nano-platelets were examined from a number of suppliers, including AVANZARE, NANESA, XG Science and GRAPHENEA characterized with SEM.

All the samples of Graphene nano-platelets (GNPs) were supplied as black powders, with high surface area and low apparent density.

SEM measurements were performed at 5kV directly on the powders attached to a sample holder by conductive carbon tape. Morphology, lateral size and sheet thickness were analyzed for each sample.

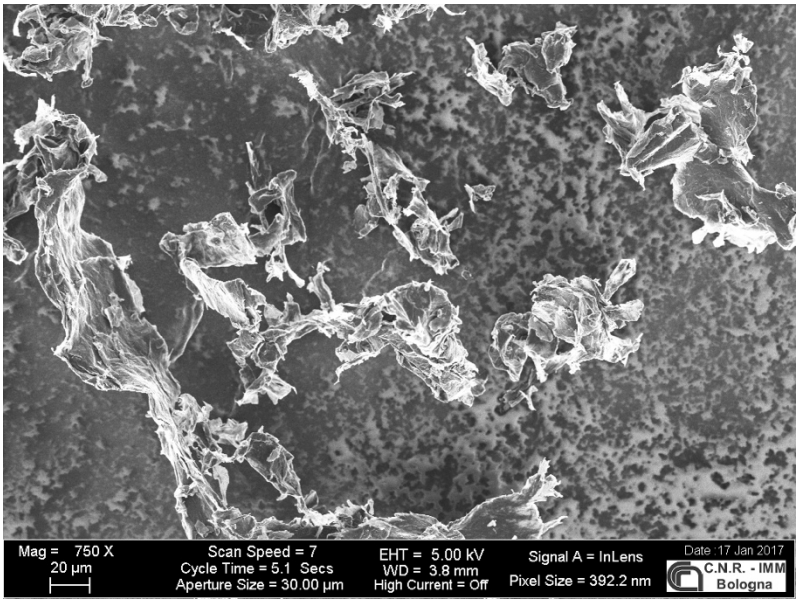

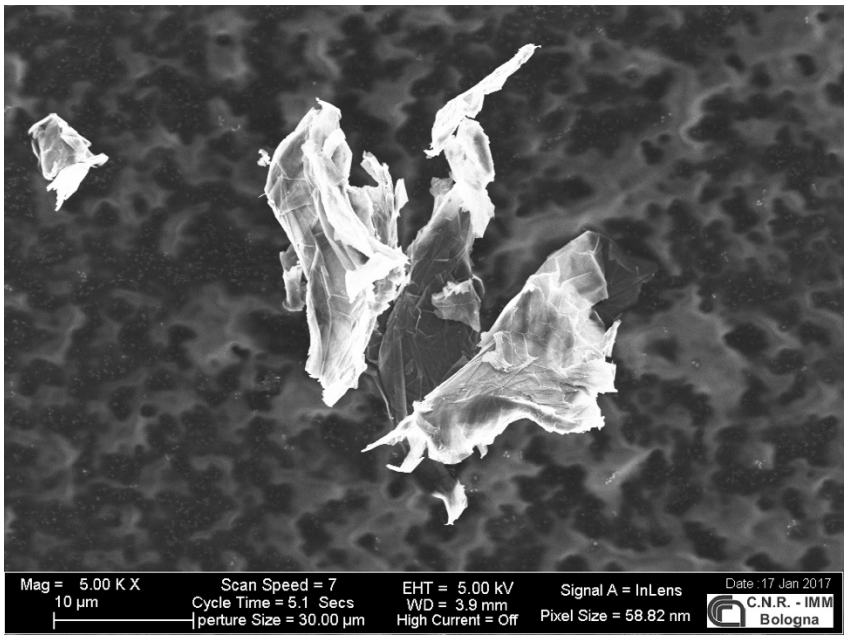

Figure 5.3: SEM microscopies of the typical commercial product (AVA FLG 19) at different magnification. See following section for more information

In Figure 5.3 shows typical GRM morphology, where the flakes are often flocculated and aggregated.

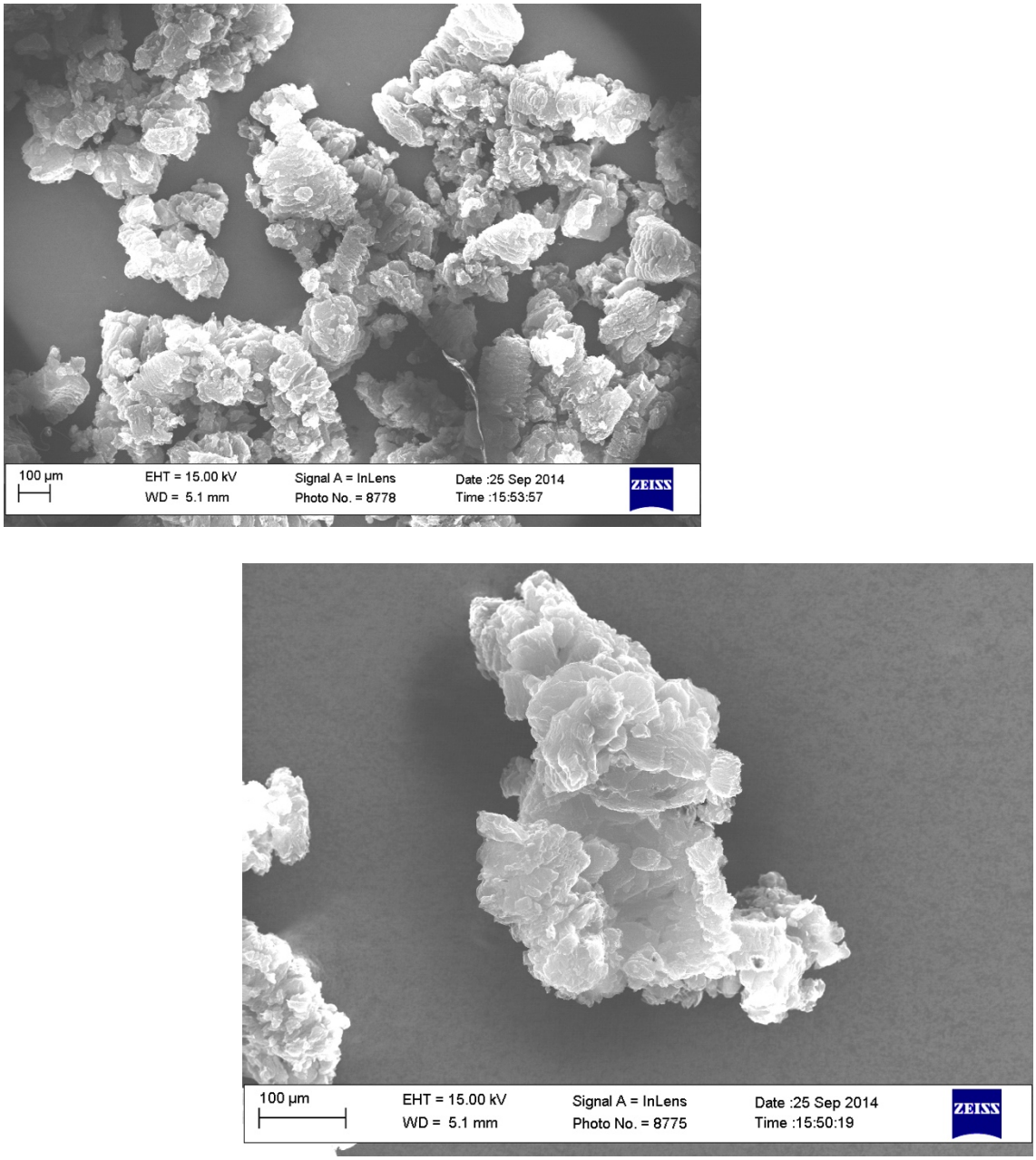

Figure 5.4: SEM microscopies of different product (AVA FLG 21) at different magnifications

In Figure 5.4 shows graphene nano-platelet morphology at different magnifications. In this example, the flakes have a typical, worm-like shape, and high surface area.

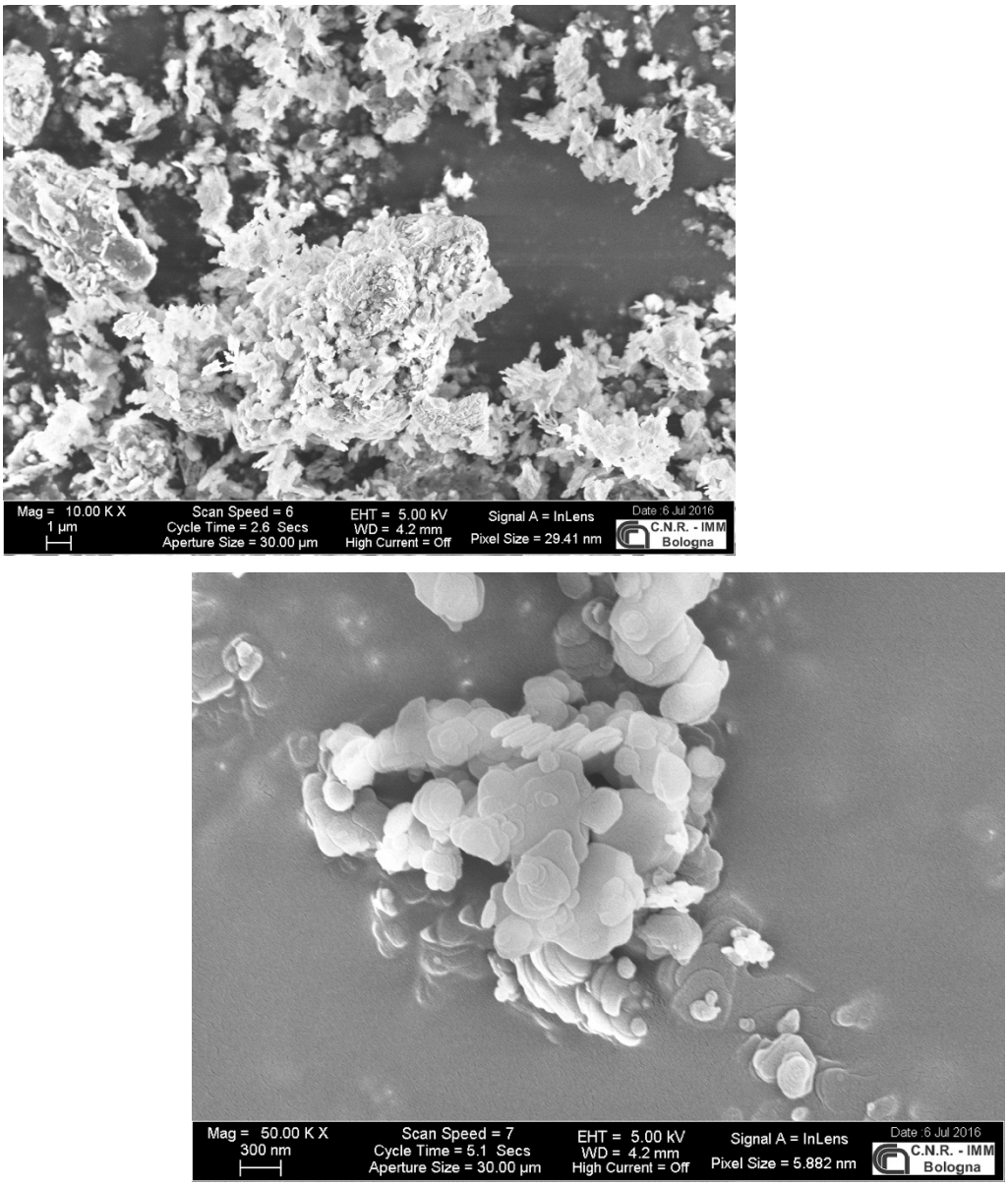

Figure 5.5: SEM microscopies of a different boron nitride flakes from Henze, Boron Nitride 410

Figure 5.5 shows commercial boron nitride platelet morphology, the flakes also showing a high level of aggregation.

5.5. List of graphene related materials analyzed

The tables below summarize the results of GRM product characterization. A short description is reported for each company whose products were tested, with some representative SEM images together with all the BET and granulometry values measured. The "expected values" are the values reported on technical datasheets or web pages. Measured values are those measured experimentally. All comparative analyses of the materials from the various producers were carried out at the CNR.

- Avanzare Innovacion Tecnologica (based in Spain) provides high-performance nanomaterials and nanotechnology-based solutions. They are specialized in the development, production and commercialization of specialty additives for different materials, mainly plastics and rubber, across many different industries. Avanzare has more than 10 years' extensive expertise in 2D materials research and production. They product various bulk graphenes and graphene/graphite nano-platelets and are partners in the European project Graphene Flagship. www.avanzare.es

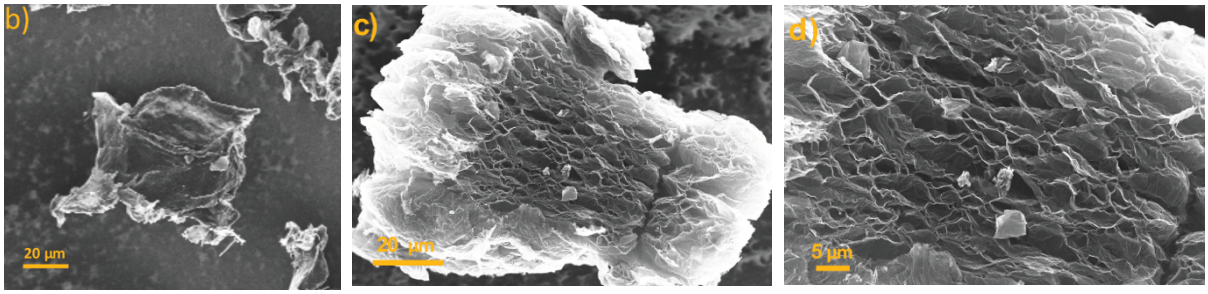

Figure 5.6: SEM images of b) AVA 18, and c, d) of AVA 24 a different magnification.

Table 5.1: Measured and reported characterization of Avanzare graphene derivatives

AVANZARE	Surface area (BET) [m²/g]	Thickness [nm]	Particle sizes [µm]			expected
	Measured	Given	D10 Measured	D50 Measured	D90 Measured	
AVA 18	22 ±4	10	14 ± 2	49 ± 4	100 ± 9	>50
AVA 19	22 ±3	10	15 ± 2	53 ± 5	110 ± 10	>40
AVA 20	225 ±5	<3	16 ± 2	40 ± 4	190 ± 15	20
AVA 21	225 ±5	<1	16 ± 2	39 ± 4	230 ± 20	20
AVA 23	190 ±4	3	17 ± 2	104 ± 10	240 ± 15	20
AVA 24	210 ±12	<1	17 ± 2	39 ± 4	205 ± 15	20
AVA 135	208 ± 2	-	12 ± 1	29 ± 2	55 ± 4	-
AVA 240	37 ±12	-	15 ± 1	50 ± 4	120 ± 10	-

- Graphenea, a Spanish technology company set up in 2010, is one of the leading main producers of CVD graphene. Now it produces CVD graphene on different substrates, Graphene Oxide and reduced Graphene Oxide. The company supplies its products to global operations for Universities, Research Centers and Industries. Further, it is part of a growing cluster of nanotechnology companies based at the nanotechnology research centre, CIC nanoGune. It is partner of the European project Graphene Flagship. www.graphenea.com

Table 5.2: Measured and reported characterization of Graphenea graphene derivative

Sample	producer	Surface area BET [g/cm^2]		Particle sizes D10 / D50 / D90 [µm]			
		measured	expected	D10	D50	D90	expected
GA1	Graphenea	486 ± 35	-	28	70	230	-

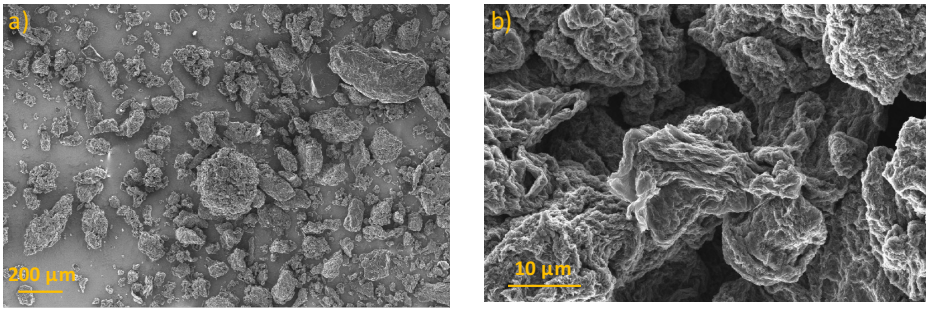

Figure 5.7: a, b) SEM images of RGO from Graphenea.

- Nanesa is an Italian-based start-up company which aims to produce and market conductive silver-based inks, pastes and graphene-based materials. The company currently offers graphene flakes, GO and graphene-based thermal foils. In 2014 Nanesa joined the Graphene Flagship. www.nanesa.com

Table 5.3: Measured and reported characterization of Nanesa graphene derivative

Sample	producer	Surface area BET [g/cm^2]		Particle sizes D10 / D50 / D90 [µm]			
		measured	expected	D10	D50	D90	expected
G2NAN	NANESA	30 ± 3	-	16	40	59	30

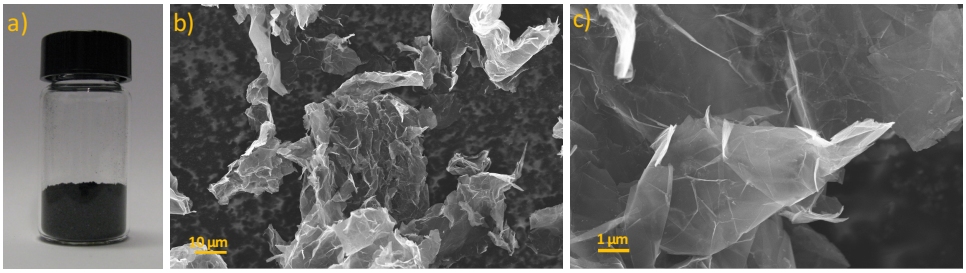

Figure 5.8: (a) Optical image of 0,25 grams of G2NAN. (b, c) SEM images of G2NAN

- XG Sciences is a world-leading American graphene manufacturer. They manufacture and sell graphene nanoplatelets and develop advanced engineering materials based on them. They work with end-users, compounders, universities and research groups to customize materials for specific applications. In particular, they have a partnership with Samsung, POSCO, and Cabot Corporation. www.xgsciences.com

Table 5.4: Measured and reported characterization of XG Sciences graphene derivatives

Sample	producer	Surface area BET [g/cm²]		Particle sizes D10 / D50 / D90 [µm]				note
		measured	expected	D10	D50	D90	expected	
XGnP M5	XG science	96 ± 10	120 - 150	4,5 ± 0,4	14 ± 1	35 ± 3	5	Fine powder
XGnP M15	XG science	113 ± 10	120 - 150	8,4 ± 1	26 ± 2	56 ± 5	15	Fine powder
XGnP M25	XG science	115 ± 10	120 - 150	9 ± 1	30 ± 3	65 ± 5	25	Fine powder
XGnP C750	XG science	745 ± 50	750	1,1 ± 0,2	3 ± 0,4	14 ± 1	<2	Fine powder
XGnP H25	XG science	75 ± 15	50 - 80	10 ± 1	28 ± 3	53 ± 4	25	Fine powder

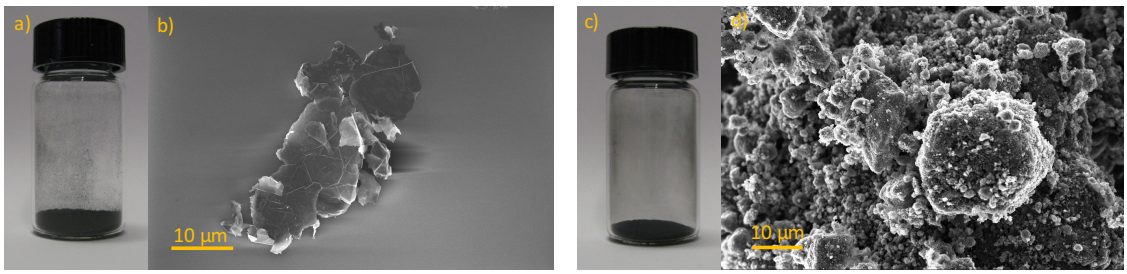

Figure 5.9: Optical images of 0,25 grams of a) XGnP M25 and c) XGnP C750. SEM images of b) XGnP M25, d) XGnP C750

- HENZE is a German company founded in 1993, allowing us to build on the cornerstones of quality, innovation and know-how in the application of hexagonal boron nitride. www.henze-bnp.com

Table 5.5: Measured and reported characterization of HENZE boron nitride.

HeBoFill #	Surface area BET [g/cm²]		Particle sizes D10 / D50 / D90 [µm]			
	measured	expected	**D10**	**D50**	**D90**	expected
110	10.7 ± 0.9	15	0.85	2.5	4.2	3
205	17 ± 1	20	1.0	3.1	8.9	3
230	14 ± 3	15-20	1.3	4.1	14.3	3
400	14 ± 1	16	1.0	4.2	13.5	5
410	19 ± 2	20	0.64	1.9	3.7	2
490	2.6 ± 0.6	2-4	7.2	26	37	27
501	0.44 ± 0.1	1	15	45	76	45
511	11 ± 1	14	1.6	9.6	26	10
630	26 ± 3	30	3.5	12	23	9
641	20 ± 2	7	0.71	2.8	16	12

6. Nano structured polymeric composites

The fabrication of polymer nano-composites is one of the most important branches of current nanotechnology and composite science as the reinforcement of a polymer with nano-fillers can profoundly change the properties of polymers, including their density, flexibility, transparency, and electrical and thermal conductivity.

Nanocomposites require small amounts of filler in polymeric composites to achieve significant property enhancements, as opposed to macroscopically-filled polymer systems, making them a key candidate, for example, in aerospace applications.

This is why, in collaboration with major aeronautics company (Airbus) we studied how the inclusion of GRMs in standard aeronautic polymeric materials (in particular, epoxy resin) can enhance the properties of the composites.

Some of these enhancements include increased modulus [34], improved gas barrier properties to water and oxygen molecules [35], and better thermal and electrical performance[36].

A main problem in the production of graphene/2D-based composites is the dispersion of the material in the polymeric matrix: nano-flakes can create large macroscopic aggregates, which create defects and compromises the final material properties.

The optimal procedure to produce a composite depends strongly on the properties of the GNP (graphene nano-platelets) and of the polymer matrix. For this reason, systematic studies were carried out to find the optimal parameters to avoid aggregates, inhomogeneity and other issues in the production of nano-composites.

6.1. Graphene based composite fabrication

Various kinds of materials were prepared and characterized as starting components for composites, especially low-cost graphene nano-platelets (GNPs), produced with a combination of mechano-chemical and thermochemical reduction processes, and boron nitride nano-platelets. Some of these materials are currently produced industrially on the gram or kilogram scale.

GNPs were used as a 2D nanoscopic filler to create thin layers or bulk composites with functional properties suitable for applications in various fields such as aeronautics and the automotive industry.

Epoxy resins for industrial applications supplied by Airbus were mixed with tailored GNPs. Tests were carried out following different standard specifications to improve mechanical properties, electrical and thermal conductivity and gas barrier properties

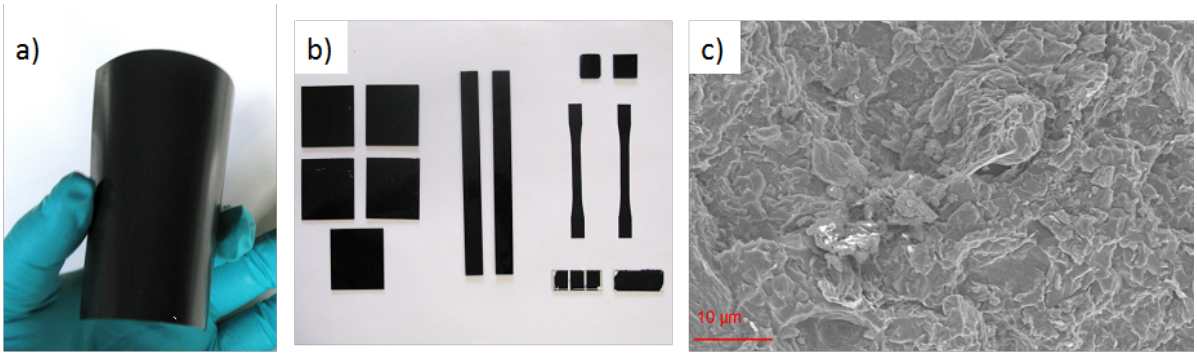

Figure 6.1: a) Photograph of a Graphene/epoxy composites prepared using Airbus and Avanzare materials. b) Samples prepared for different standard tests. c) Representative SEM image of one of the composites obtained

The key for reaching an improvement in the global properties of the composites was to achieve a correct percolation and mixing of the filler within the epoxy resin, so one of the most common problems is the agglomeration and poor dispersion of graphene in the polymer matrix. To avoid such problems, various methods for obtaining the composites were studied as a function of the polymer.

The main activities carried out with epoxy resin used a combination of an epoxy resin provided by Huntsmann (epoxy resin ARALDITE LY 5052 with respective hardener ARADUR 5052 CH) with commercial bulk graphene nano-platelets (GNPs), using two different techniques to obtain bulk graphene-based composites.

The composites were made by manual casting in a mould to obtain the shaped samples required for the various tests. Different types of commercial graphene were used at different concentrations, nine types of graphene-based composites with different fillers (**XG Sciences, Avanzare, Graphenea**) and loading, following different standard specifications for water absorption, mechanical and electrical properties and heat transport tests.

The GNPs were supplied as a black powder with high specific surface area and low apparent density as showed in Figure 6.2

Figure 6.2: graphene related material, black volatile powder

6.1.1. Graphene-based Composite bulk fabrication

The fabrication method for a bulk epoxy composite involves mixing the filler with the polymer matrix using a DISPERMAT VL-01 (VMA-gentzmann GMBH Verfahrestechnik, Reichshof, Germany) (Figure 6.5) for 15 minutes at 5500 rpm to generate large shear forces to improve mixing.

This operation is useful because nano fillers are prone to form agglomerates due to their high specific surface area (SSA) and such aggregates are difficult to break down during processing.

Then, a lab-scale three-roll mill (3RM) (Torrey Hills®, USA) [37] was used to disperse the nano fillers throughout the epoxy matrix. The gap between the feed roll and the apron roll was maintained at 20µm and the whole suspension was milled five times, to achieve uniform dispersion.

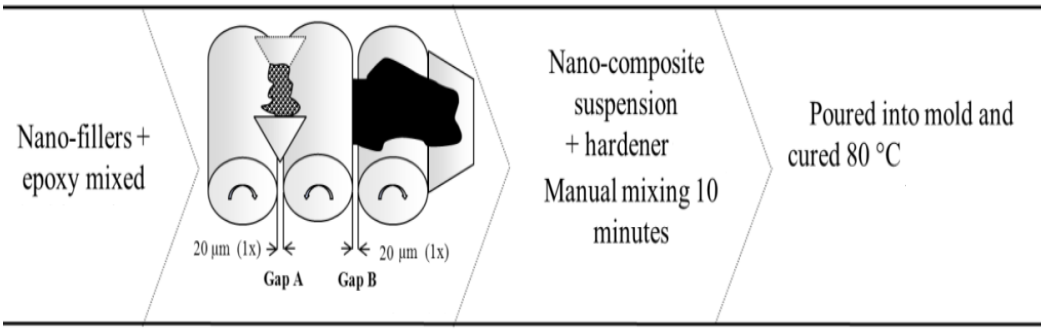

Figure 6.3: A flow chart of the dispersion methods used for preparation of the nano-composite

Varying amounts of hardener were added to this epoxy-resin/GNP slurry [38], then the slurry was manually mixed for 10 minutes, degassed at 50 °C and then oven-cured for 2 hours at 80 °C. A detailed flow chart explaining the composite preparation is presented in Figure 6.3

The percentage of additive ranged from 0.5 to 7 % (the percentage is calculated with respect to the total amount of composite: epoxy resin + hardener + filler). After several steps in the 3RM (see Figure 6.5 b) the compound showed good uniformity, with no aggregation

Figure 6.4: graphene based compound before the casting and curing

List of used instrumentation

- DISPERMAT, a mechanical mixer working at 6000 rpm.
- THREE ROLL MILLING (Torrey Hills), having three counter-rotating rolls it homogenizes the compound of resin and graphene (high shear force),

Figure 6.5: (A) Dispermat VL-01, (B) three roll milling

Once the homogenization of the composite mixture was complete, it was cast in an iron frame to give the composite a first shape (see Figure 6.6), then the curing process was performed in an oven at 80°C for two hours, the data being reported in Table 6.1.

Table 6.1: Manufacturing parameters for the graphene sample (Araldite LY 5052 + Aradur 5052 CH)

Pressure (PSIG)	No
Vacuum (mm Hg)	No
Heat-up Time (min)	Pre-heated oven: 10
Stabilised T^a (°C)	80
Stabilised Time (min)	120
Cool-down Time (min)	2
Demoulding T^a (°C)	RT

Figure 6.6: Picture of (A) metallic frame (200 x 270 mm) and (B) GNP-resin composite cast in the metallic frame

6.1.2. Fabrication steps for thin film Graphene Based Composite

Besides the thick, bulk pieces cast with the metallic frame, thin coatings were also prepared using a blade technique (ERICHSEN GmbH & Co. KG, Am Iserbach 14, 58675 Hemer, Germany). This instrument uses a blade to spread the viscous slurry over a substrate, and is used for film depositions of materials with high viscosity as had the resin with 7% of filler, as represented in Figure 6.7 [39].

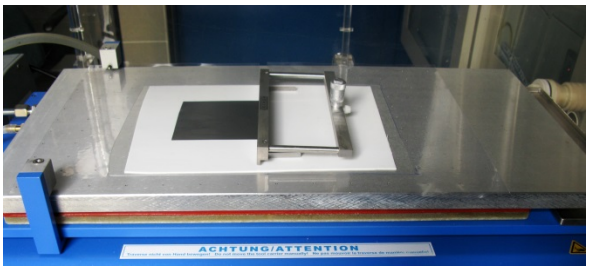

Figure 6.7: Image of the blade used for a fabrication of a thin film

Two parameters are important for the uniformity of the final thin film:

1. the micro-meter spacing defining the thickness of the thin film made,
2. the operating speed of the cutter,

We prepared different thin sheets with commercial graphene concentrations from 0 to 7%, and sheet thickness ranging from 90 to 160 µm.

6.2. Hybrid composites of Glass fiber, graphene and epoxy resin

The resin infusion process is used widely in the automotive, aerospace, and marine industries. The use of nano-materials as secondary reinforcements is new to large-scale industrial activities and thus requires a more complete scientific understanding of their interactions with the dry glass- or carbon-fiber fabric.

Here, the resin infusion process used was based on vacuum-assisted resin transfer molding (VARTM). The mold is single-sided and was utilized to manufacture medium-sized composite panel structures (≈ 30 cm^2).

A polytetrafluoroethylene (PTFE) panel was used as rigid substrate with a sealed flexible polymeric film (for temperatures up to 200 °C) on the other side to seal the vacuum bag.

The vacuum provides the compaction and driving force for resin flow through the pre-form.

Multilayer preparation for a glass fiber fabric process consists of three basic phases:

1. pre-filling,
2. vacuum,
3. curing.

In the pre-filling phase, the pre-form is impregnated with the reinforced resin to obtain a good spreading of the resin in the glass fiber tissue layer. This vacuum method, contrary to the conventional method, provides an initial consolidation and removal of the reinforced resin excess, saturating the multilayer of hybrid composite. Once the glass fiber is completely saturated with resin the panel can cure during the vacuum phase.

Resin infusion is a low-cost process to achieve a smooth and excellent surface, the technique giving high homogeneity, low porosity and higher fiber volume fraction.

The steps in the process are as follows:

1. graphene was mixed with epoxy resin, such that the weight fraction of graphene was 7% of the weight of the total amount of the slurry (resin + curing agent + filler);
2. the mixture was placed in the mold alternating layers of reinforced resin and layer of dry glass fabric. A conventional scheme of the vacuum-assisted resin transfer molding (VARTM) [40] setup is shown in Figure 6.8.

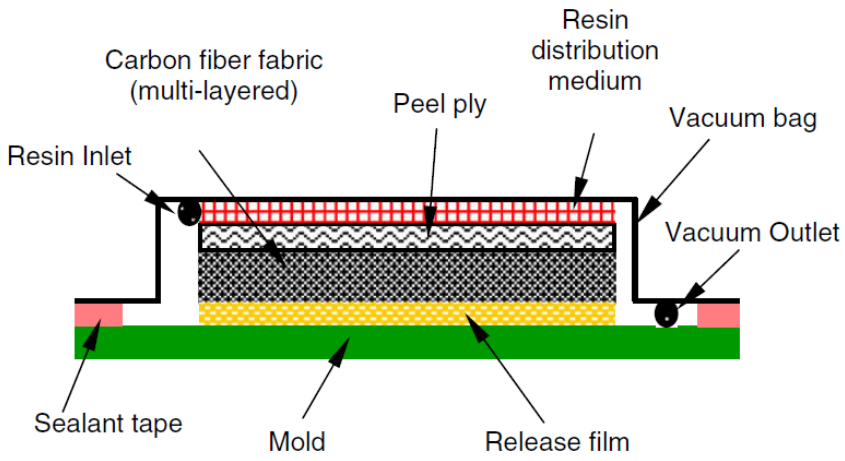

Figure 6.8: Schematic of VARTM setup

3. Six layers of glass fiber fabric, each measuring approximately 300 mm by 300 mm, were stacked in alternating warp-fill directions and closed in a vacuum bag with sealant tape to ensure the vacuum [41] action to consolidate the samples of glass-fiber resin and graphene,
4. to cure the sample the entire system was placed in an oven at 80 °C for 2 h, keeping the samples under vacuum pumping during the curing.

Figure 6.9 shows the VARTM modified to help the infiltration of the nano-reinforcement in all area of the glass fiber dry fabric.

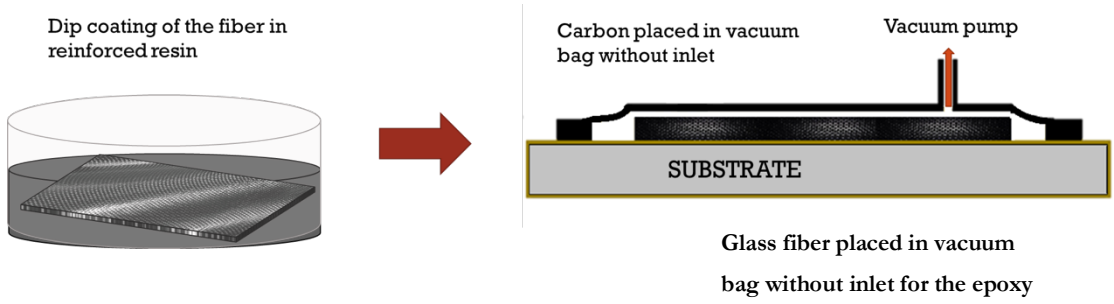

Figure 6.9: modified VARTM process without inlet

6.3. Graphene Oxide/Epoxy Composites

Most composites are obtained by mixing the polymer matrix with the (nano) additive, in this way obtaining a bulk material where the additive (in our case GRM) is dispersed uniformly in the composite. This approach has some disadvantages: it may be difficult to mix the GRM with the polymer, the GRM may show non-uniform distribution in the polymer such as aggregating; most importantly, the GRM might modify not only the property we want to improve, but also other important properties of the polymer, such as increasing the viscosity. This can be a problem for the further processing of the composite. An interesting approach to increase the barrier effect against humidity absorption would be to deposit the GRM only on the surface of the sample, before curing, to achieve a coating of the cured resin samples with a high content of graphene on the surface, as schematized in Figure 6.10 with no change in the bulk mechanical properties and in the fabrication procedure of the sample.

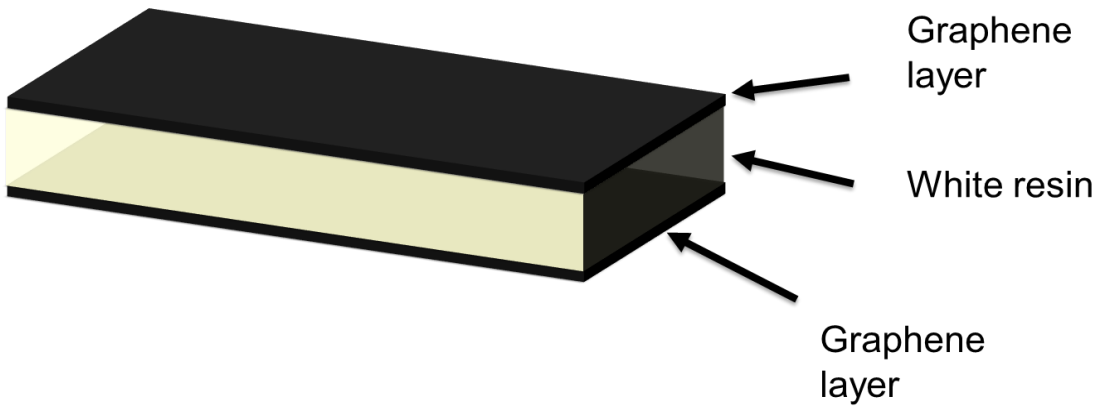

Figure 6.10: Schematization of the white epoxy resin covered with high content graphene layer

Thus, a graphene oxide (GO)[43] aqueous solution was prepared to coat uniformly the resin sample, and the GO reduced to RGO by heating at 180°C.

The main advantages of this fabrication method are:

1. Small amount of graphene used
2. No alteration in the final composite properties and fabrication procedure

The resin used for this test (HexFlow® RTM 6, HEXCEL, Piazza De Gasperi, 32 Saronno 21047, Italy) can use high curing temperatures, which are ideal for reducing the GO (≈ 180 °C). The advantages of this mono-component resin are manifold:

- It is a mono-component system
- It has a high glass transition temperature
- It has excellent hot/wet properties
- It is easy to process (low injection pressure)

- It has a long injection window ≥150 min at recommended injection temperature.
- It has low moisture absorption properties
- It needs short, simple curing cycles

Graphene oxide, synthesized by the oxidation of graphite using a modified Hummer method, is soluble in water due to the polar groups (i.e., hydroxyl and carboxyl) present on its surface and can be deposited as single sheets (see Figure 6.11 a) or continuous film (see Figure 6.11 b) on different substrates.

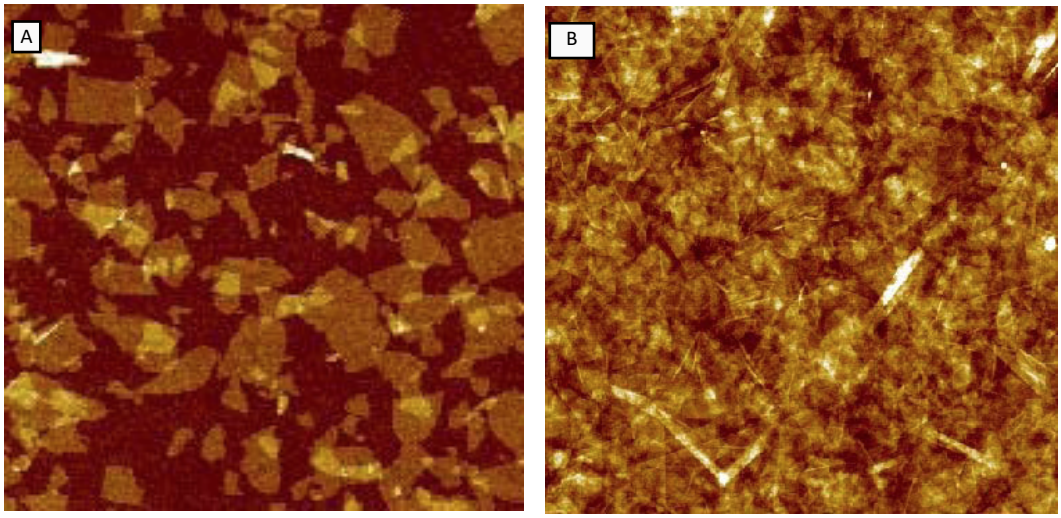

Figure 6.11: AFM images of graphene oxide (a) flakes, (b) thin film on silicon substrate [2]

Thermal reduction can partially restore the graphitic network of the material lost during the oxidation process.

For this work, graphene oxide supplied by GRAPHENEA was used. Nominally, it presents the following characteristics:

- Color: Yellow-brown
- Solvent: Water
- Concentration: 4 mg/ml
- pH: 2,2-2,5
- Monolayer content: (measured in 0.5mg/ml): >95%
- Carbon content: 49-56%
- Hydrogen content: 0-1%
- Nitrogen content: 0-1%
- Sulfur content: 2-4%
- Oxygen content: 41-50%

The fabrication process started with the preparation of a mono-component resin composite cured at 180 °C for 2 hours. After that, the sample was shaped with the engraver to obtain a 75x75x2 mm panel, uniform in thickness and roughness (**Errore. L'origine riferimento non è stata trovata.**).

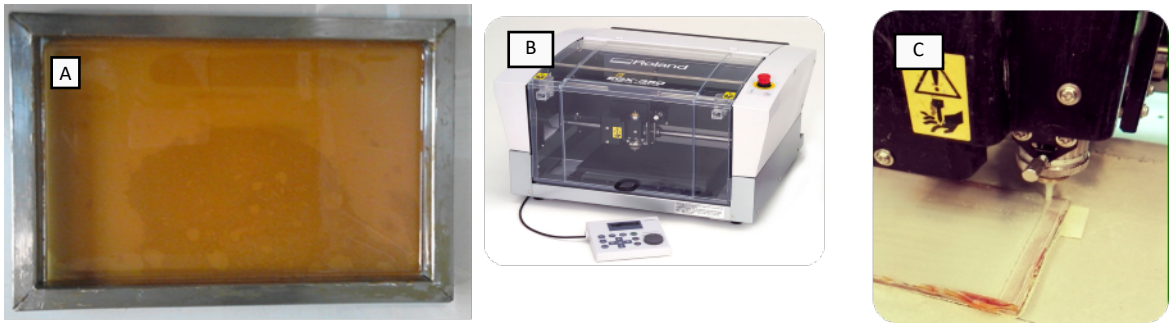

Figure 6.12: Picture of: (a) the mono-component epoxy resin after curing, (b) the Roland EGX 350 engraver, (c) the engraver during the refining of the cured resin face

The coupon was immersed in a water solution of GO (2 mg/ml), as schematized in Figure 6.13, to obtain a uniform covering of the surface. After the dip-coating, the coupon was dried in oven for 1 hour at 200 °C. The coupons (a) without and (b) with the reduced graphene oxide layer on the surface are shown in Figure 6.14.

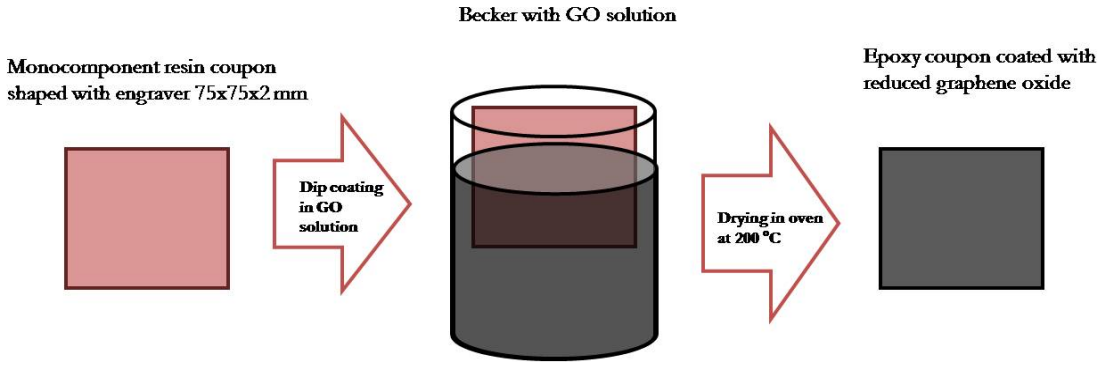

Figure 6.13: Sketch of the fabrication steps for the mono-component epoxy coupon coated with GO and reduced at 200°C for 1h

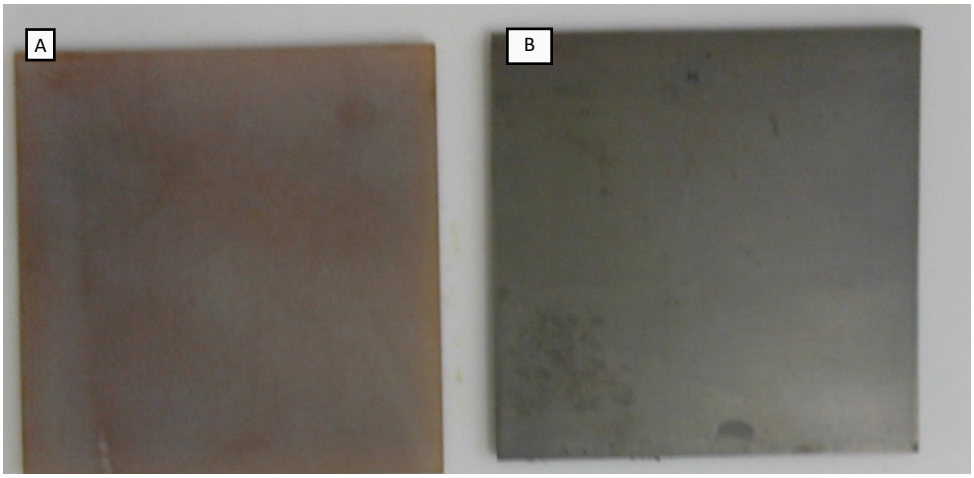

Figure 6.14: (A) reference resin coupon, (B) coupon coated with reduced graphene oxide

The wettability of the two samples prepared, the reference one and the coated one, were tested by placing water drops on the surface. As presented in Figure 6.15 a), b) the sample coated with reduced graphene oxide clearly shows increased hydrophobicity compared to the reference. This preliminary result looks promising for improving the water absorption barrier in epoxy resin composites for aeronautics, because it is possible to reduce the surface adsorption of water which at high altitudes can freeze and increase aircraft weight with a series of disadvantages (fuel consumption, decreasing aerodynamic performance).

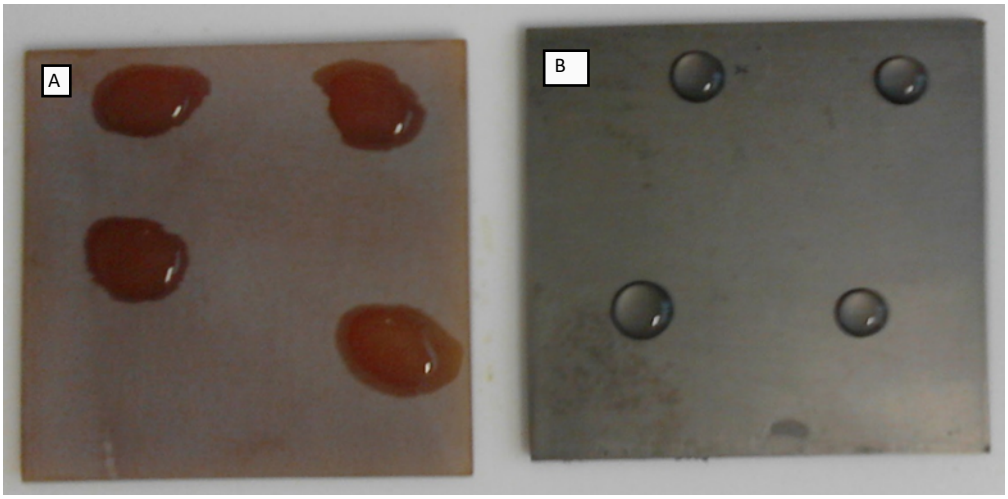

Figure 6.15: Water drops (A) on the reference resin coupon and (B) on the coupon coated with reduced graphene oxide

Besides graphene-based composites, we also prepared other composites, based on boron nitride, for a particular application. The composites were produced to be tested for applications where electrical field grading or electrical stress control is important to be evaluated in high voltage cable and device accessories to mitigate and dissipate high electrical stresses which may cause breakdowns of the entire electrical system.

6.1. Boron nitride/graphene based composites

Due to the unique properties of boron nitride (BN), this thesis investigates the influence of BN and graphene in polymeric composites [42].

Dielectric polymer nanocomposites can exhibit significant improvements in strength, endurance and dielectric breakdown strength compared to the unfilled polymer.

Ceramic particles are widely used to increase the dielectric constant of polymer composites because of their high dielectric constant and low dielectric loss.

Composites with high aspect ratio (AR) fillers are predicted to exhibit higher dielectric constants at lower loading. In this thesis, higher volume fractions bring increases in dielectric constant which can improve the electrical breakdown strength and mechanical resistance due to the two-dimensional nature of boron nitride flake (see Hillborg et al. [43]).

The dielectric properties of a polymer composite containing boron nitride flakes were investigated for an innovative approach in combination with conductive particles at low volume fractions such as graphene nano-platelets (GnP) which are a good candidate for studying the effects of high-aspect-ratio conductive fillers.

A commercial polydimethylsiloxane (PDMS), Sylgard 184 supplied by Dow Chemical was used as the polymer matrix.

PDMS has a volume resistivity of 2.9E+14 Ω·cm, viscosity of 5100 cP, tensile strength of 980 PSI.

The BN powder (Henze BNP AG, Grundweg 1, D-87493 Lauben (Germany) was used as a dielectric conductive filler, having a melting point above 2000 °C, density of 2.27 g/cm^3, and average particle size of 0.5 μm.

Viscous PDMS and BN + graphene nano-platelets were mixed initially by manual stirring at different mass ratios at room temperature, until the BN/GnP particles were wetted with the PDMS. The mixture was then transferred to a three-roll milling (3RM) with a fixed gap between the rollers of 20 μm, as shown in Figure 6.16.

Figure 6.16: A) BN-PDMS compound milled with three roll milling; (B) different bottle of not cured PDMS with different concentration of boron nitride and graphene nano-platelets

Composites with BN and GNP (graphene nano-platelets) powder concentrations ranging between 0 and 23% by weight were prepared with 5 mixing cycles in the 3RM at 85 rpm.

7. Characterization of the produced composites

Graphene nanoplatelets (GNP) supplied by European Flagship partners and external private companies were compared in order to choose an appropriate candidate for use in composites for specific applications in the automotive and aeronautics fields. The GRMs were supplied as black powders with high specific surface area and low apparent density.

Morphology, lateral dimensions and sheet thicknesses were analysed for all GRM samples, and SEM measurements were performed on the powders to analyse the morphology and the structure of each powder.

Bulk epoxy composites were then synthesised with the GNP powders as filler, to analyse the behaviour of the powders when incorporated into epoxy resins.

Various techniques were then used to characterize the composites obtained, as detailed in the following sections.

7.1. Scanning electron microscopy Characterization

The properties of nanocomposites are mainly determined by the quality of the dispersion of the particles in the matrix, and the morphological characterization of the cured nano-composites was performed using scanning electron microscopy (SEM) at the CNR-IMM institute using a 5kV acceleration voltage with a sputtering of gold to create a conductive nano-metric film.

The SEM measurements were carried out with a Zeiss LEO 1530 instrument on composites with different types of filler at different percentages.

The morphology obtained from the SEM images show significant differences between the composites charged with, respectively, no filler, graphene nanoplatelets (AVA FLG 12) a filler with low specific surface area and high lateral dimension flakes, few layer graphene (AVA FLG 18) with low specific surface area and high lateral dimensions and graphene nano-platelets (AVA FLG 23) with high specific surface area and low lateral dimension flakes.

As mentioned above, the nano-fillers have different aspect ratios which gives them greater possibilities for interactions in the matrix.
Figure 7.1 shows different SEM images of the nature fabricated composites.

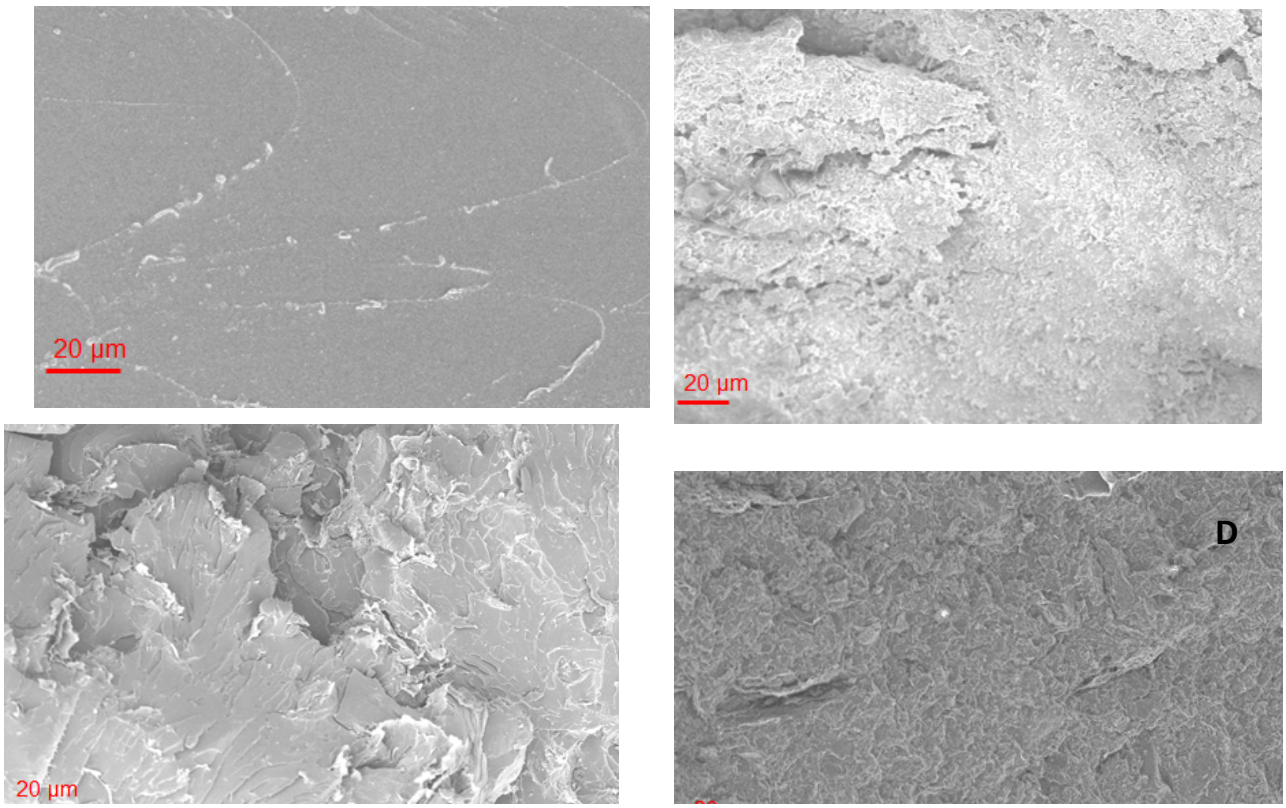

Figure 7.1: SEM microscopy of (A) resin, (B) graphene flake AVA 12-resin composite; (C) graphene flake AVA 18-resin composite and (D) graphene flake AVA 23-resin composite

7.2. Electrical percolation in graphene based composites

Polymers are generally good insulators due to the lack of free charge carriers, but when reinforced with conducting particles such as carbon nano-fillers, there is a transition from insulating to conductive behavior in polymer nano-composites. To explain this conduction mechanism, percolation theory is usually applied to nano-composites, being a standard model for disordered systems. According to this theory, at low filler concentrations, as there are no overall conducting paths, the conducting particles are either separated or they are present in the form of small clusters, and hence the electrical properties are characterized by those of the matrix. As the concentration increases, at a certain point percolation through the matrix with clusters begins but below this concentration the composite remains an insulator. This concentration is called the percolation threshold[4].

To study of the electrical properties of the composites, graphene sheets with different average thicknesses (ranging from 1 to 50 layers of graphene) and lateral dimensions were used. The different GRMs were mixed with epoxy resins to form the composite. Then, the electrical conductivity of these nano-composites was determined by electrochemical impedance spectroscopy (EIS).

The polymer used was Araldite resin (AIRBUS), and significant differences were observed depending on the graphene type used. The lowest percolation threshold (0,5%) was obtained using few layer graphene nano-platelets with lateral dimensions of 40 μm obtaining impedances of 10^{-6} S/m. A multi-layer sample with graphene nano-platelets (composed of >50 sheets) with lateral dimensions of 40 μm requires a 4% loading to reach the percolation threshold.

7.2.1. Electrical Characterization

Bulk electrical properties were characterized using the ASTM D4496 standard procedure "DC Resistance of Conductance of Moderately Conductive Materials".

The electrical contacts are aligned in a row in silver paste of 3 mm length and placed at constant distances of 22 mm. Four contacts were made by application of common silver enamel (silver nanoparticles in acetone): before application of the enamel surface of the sample was roughened with sandpaper, in order to obtain a good contact between resin and silver nanoparticles. After application, the contacts were dried for several hours.

A typical 4-point probe setup was used to minimize artifacts due to high contact resistance on the final measurements. A fixed current was injected into the 2 outer contacts, reading the current on the 2 inner contacts.

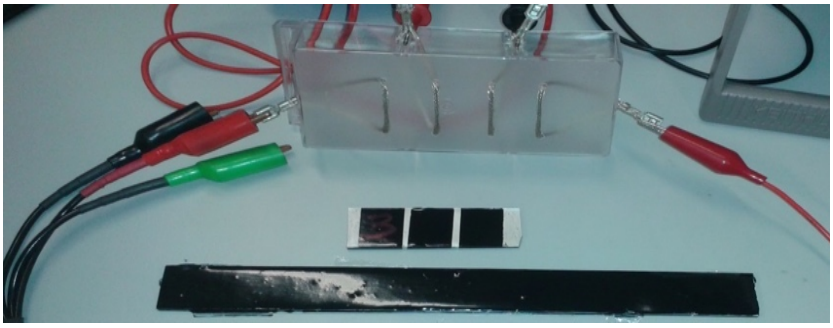

Figure 7.2: Experimental set-up for electrical characterization Bulk sample

Current scan (0.1 nA-100 uA) was performed in order to check the ohmic behavior of the filled resin, which was confirmed in all the conductive samples. The current generator was a Keithley 6517A, while the voltage reader a Keithley 2002. The 4-probe electrical characterization allows one to estimate the resistance of the sample without the contact resistance, which is not a negligible factor in this kind of conductive composites: in some cases, the contact resistance could be up to 3-4 times the bulk resistance. Contact resistance usually follows a non-ohmic behavior, as confirmed by 2-probe measurements.

The conductivity is measured as:

Equation 1: conductivity equation

$$\sigma = \frac{L}{R \cdot t \cdot W} \left[\frac{S}{m}\right]$$

Where R = measured resistance (slope of V/I curve); t= thickness of sample, W=24 mm, L=22 mm.

Table 7.1 reports the electrical behavior of the composites with the same amounts of reinforcement.

insulating composites

Table 7.1: Electrical resistance and resistivity of different samples at the same % of filler. Errors is around 20% of the main value

Graphene	Sample name	% of filler	Resistance BULK [Ω]	Conductivity [S/m] BULK
XG 25	N129	2	>10 10^6	<3E-8
AVA-FLG 21	N130	2	280 10^3	1.0E-3
AVA-FLG 24	N132	2	70 10^3	2.5E-3
AVA-FLG 12	N133	2	>10 10^9	<3E-8
AVA-FLG 20	N134	2	407 10^3	7.0E-4
AVA-FLG 11	N135	2	>10 10^9	<3E-8
AVA-FLG 18	N136	2	>10 10^9	<3E-8
AVA-FLG 19	N137	2	>10 10^9	<3E-8
AVA-FLG 23	N138	2	2.3 10^6	1.3E-4

Bulk samples N130, N132, N134, N138 are conductive, with a reasonable ohmic behavior. All the electrical tests were performed with 2% filler for technical reasons, but it would be possible to increase the concentration and observe the higher percolative thresholds of

7.2.2. Electrical Tests On Graphene Nanocomposites With Different % of Filler

Two different powders were tested in order to ascertain the electrical properties of the final composites: AVA FLG 21 (high specific surface area), the most interesting from the electrical point of view and AVA FLG 18 (low specific surface area).

Figure 7.3: Sample sizes, 70×24×3.2 mm^3

Table 7.2: Electrical resistance and resistivity of different samples at different % of filler. Errors is around 20% of the main value

Graphene	Sample name	% of filler	Resistance BULK [Ω]	Conductivity [S/m] BULK
AVA-FLG 18	N180	0,5	1 E12	3 E-10
AVA-FLG 18	N179	1	1 E12	3 E-10
AVA-FLG 18	N178	2	1 E10	3 E-10
AVA-FLG 18	N176	5	4 E7	4 E-6
AVA-FLG 18	N172	7	1,8 E7	1,7 E-5
AVA-FLG 21	N150	0,5	3,4 10^7	1,27 E-5
AVA-FLG 21	N151	0,75	7,71 10^7	5,7 E-4
AVA-FLG 21	N152	1	6,49 10^5	5,04 E-4
AVA-FLG 21	N153	1,5	2,7 10^5	1,1 E-3
AVA-FLG 21	N154	2	4,8 10^5	0,9 E-3

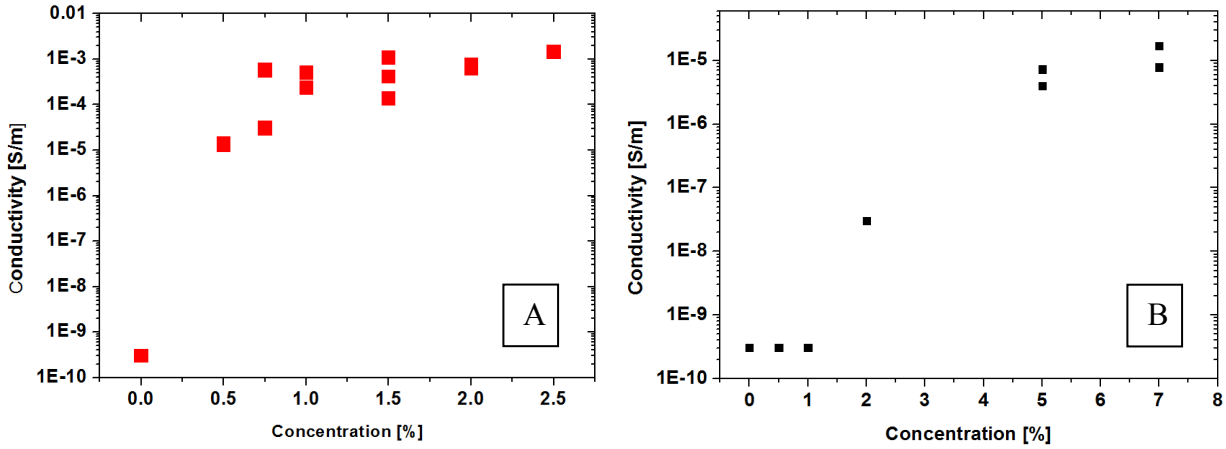

Figure 7.4: (A) Percolative behaviour of AVA-FLG 021; (B) Percolative behaviour of AVA-FLG 018

Figure 7.4 abowe shows the percolative behavior of the two composites fabricated at different percentage loadings.

The main results can be summarised as follows:

1. Percolative threshold in AVA FLG 21 is below 0,5 %, and in AVA-FLG 18 below 4%. The AVA-FLG 21 is two orders of magnitude more conductive with respect to AVA-FLG 18.
2. Two batches were produced for each filler concentration. Repeatability for different batches was within one order of magnitude.
3. The percolative nature of AVA 21 was confirmed by log-log plot and linear fit (see (see Figure 7.5) with a critical exponent of 1.4 ± 0.1.

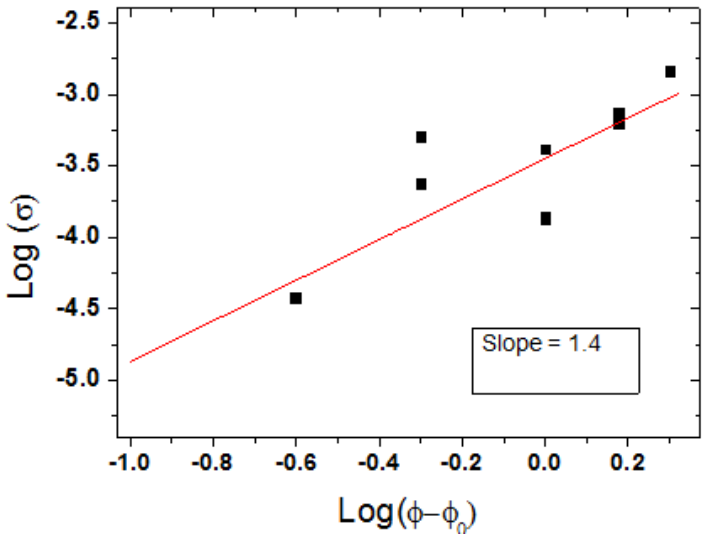

Figure 7.5: Log-Log plot of AVA 21 percolation, linear fit R^2=0.85, slope 1.4±0.1

7.2.3. Comparison Electrical Tests And Morphological Characterization

The electrical properties of the composites can be correlated with the morphological properties, and all the conductive samples were produced by high-surface-area powder (200 m^2/g), but specific surface area is not the only important parameter as lateral dimensions also seem to be critical for achieving electrical conductivity at 2% loading. As shown in Figure 7.6 only the region with high specific surface area and large lateral dimensions are effectively conductive.

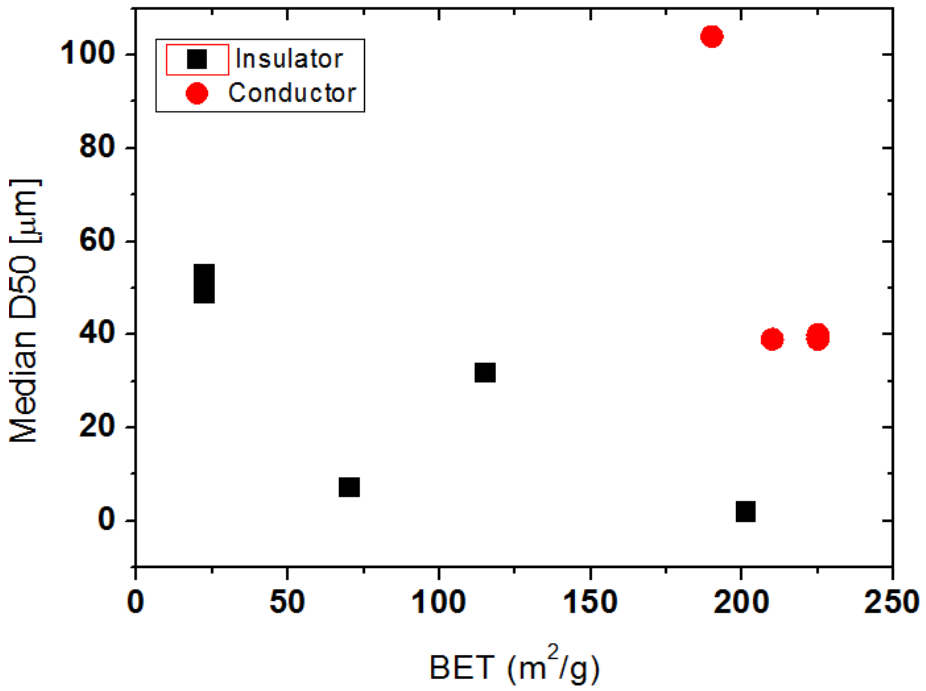

Figure 7.6: Lateral Size (D50) vs BET. Red values are the conductive composites, black values are the insulators

Table 7.3 shows the electrical conductivity of the different composites fabricated with different graphene powder at 2% loading. The conductivity can be estimated from the double green circle, whereas if one of the parameters (lateral dimensions or the BET specific surface area) is not achieved, the final composites will not conduct.

Table 7.3: Morphological characterization VS Conductivity

Graphene	% filler	Given Thickness [nm]	BET surface [m^2/g]	Conductivity [S/m]	Given lateral Size [µm]	Laser Granulometry D50 [µm]
XG 25	**2**	**6-8**	**115**	**Ins.**	**30**	**32**
AVA-FLG 11	**2**	**10**	**70**	**Ins.**	**5**	**7,4**
AVA-FLG 12	**2**	**10**	**201**	**Ins.**	**2**	**2,2**
AVA-FLG 18	**2**	**10**	**22**	**Ins.**	**50**	**49**
AVA-FLG 19	**2**	**10**	**22**	**Ins.**	**40**	**53**
AVA-FLG 20	**2**	**3**	**225**	**7E-4**	**20**	**40**
AVA-FLG 21	**2**	**1**	**225**	**1E-3**	**20**	**39**
AVA-FLG 23	**2**	**3**	**190**	**1,3E-4**	**20**	**104**
AVA-FLG 24	**2**	**1**	**210**	**2,5E-3**	**20**	**39**

7.3. Electrical percolation in graphene hybrid panel composites

7.3.1. Electrical conductivity

As discussed in the previous chapter, besides standard GRM polymer composites, composites where a glass fiber tissue was impregnated with a reinforced resin at different filler loadings were also prepared and tested.

Figure 7.7 shows the difference in color of the various percentage filler loadings in the glass fiber samples.

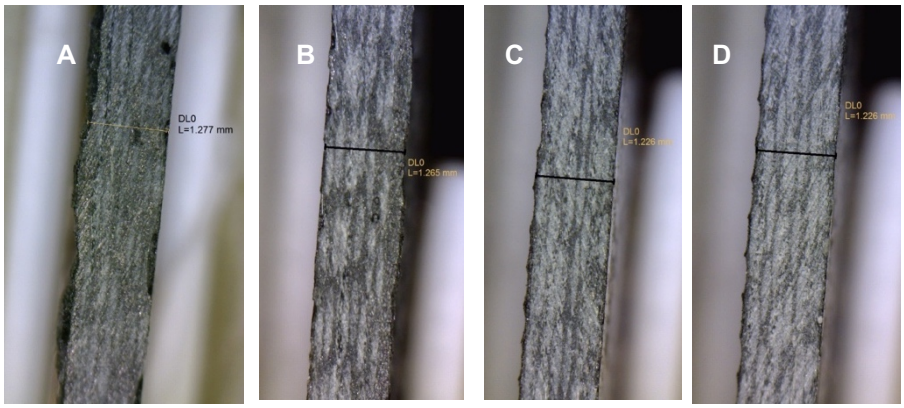

Figure 7.7: Optical microscopies of hybrid composites panel cross section: (A) 8%, (B) 4 %, (C) 2%, (D) 1%

SEM measurements confirm high abundance of graphene flakes in glass fiber cured composites, see Figure 7.8:

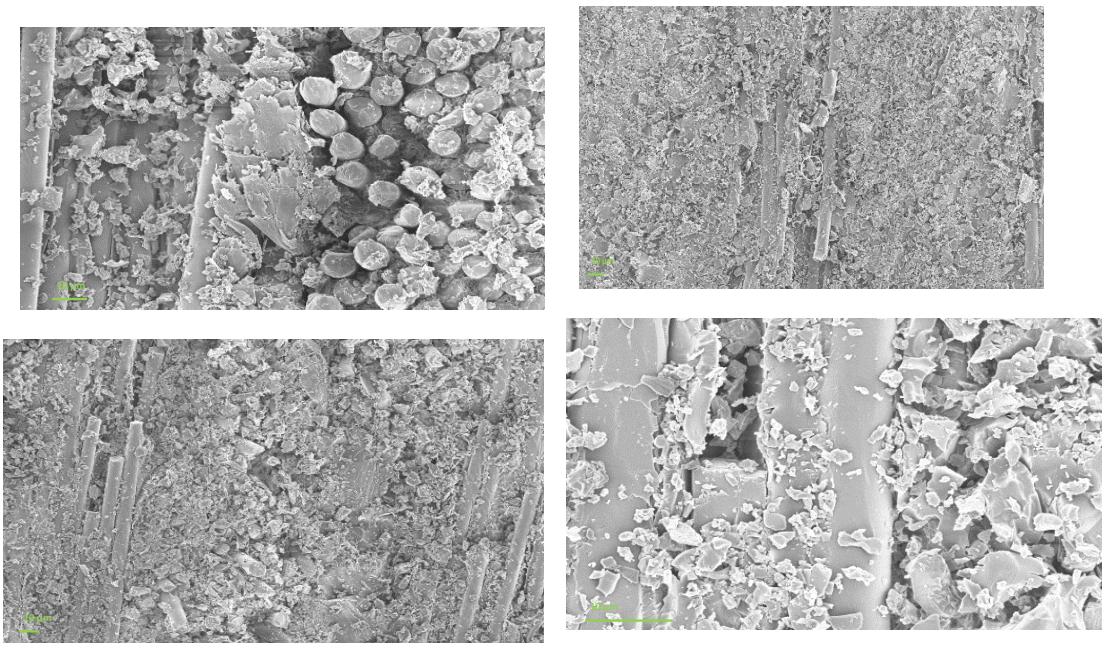

Figure 7.8: SEM microscopies of hybrid composites at different magnification, it is possible to observe GnP over the glass fiber

Once again, the ASTM D4496 standard procedure "DC Resistance of Conductance of Moderately Conductive Materials" was used to measure the electrical conductivity of this type of composite.

The electrical contacts were made at constant distances of 22 mm, with a length of about 3 mm. The contacts were made by application of common silver enamel (silver nanoparticles in acetone) and before application of the enamel, the sample surface was roughened with sandpaper, in order to obtain a good contact between resin and silver nanoparticles. After application, the contacts were dried for several hours.

Table 7.4 shows the resistivity of all samples, measured with the a Keithley 6517A current generator. The voltage drop was measured with a Keithley 2002 and a 2-probe voltmeter, and the data analyzed using Current scan (0.1 nA-100 uA) was performed in order to check the ohmic behavior of the filled resin, which was confirmed in all the conductive samples. The current generator was a Keithley 6517A, while the voltage reader a Keithley 2002. The 4-probe electrical characterization allows one to estimate the resistance of the sample without the contact resistance, which is not a negligible factor in this kind of conductive composites: in some cases, the contact resistance could be up to 3-4 times the bulk resistance. Contact resistance usually follows a non-ohmic behavior, as confirmed by 2-probe measurements.

The conductivity is measured as:

Equation 1Current scan (0.1 nA-100 uA) was performed in order to check the ohmic behavior of the filled resin, which was confirmed in all the conductive samples. The current generator was a Keithley 6517A, while the voltage reader a Keithley 2002. The 4-probe electrical characterization allows one to estimate the resistance of the sample without the contact resistance, which is not a negligible factor in this kind of conductive composites: in some cases, the contact resistance could be up to 3-4 times the bulk resistance. Contact resistance usually follows a non-ohmic behavior, as confirmed by 2-probe measurements.

The conductivity is measured as:

Equation 1: conductivity equation.

Table 7.4: Electrical conductivity and resistivity of hybrid glass fiber panel at different percentage of filler.

Concentration	R_s 2p [Ω/sq]	R_s 4p [Ω/sq]	σ 4p [S/m]
8	80 ± 15	31 ± 15	25 ± 12
4	2000 ± 400	1000 ± 400	0.76 ± 0.3
3.5	1000 ± 300	500 ± 300	1.57 ± 0.9
2.5	2300 ± 200	2300 ± 200	0.34 ± 0.2
2	insulating	insulating	1 E-11
1	insulating	insulating	1 E-11

Errore. L'origine riferimento non è stata trovata. shows the difference in conductivity b etween the composites with different GRM loadings, with and without glass fiber. Note the different scales of the Y axes.

In the presence of glass fiber (Figure 7.9 b), we measured a conductivity 6 orders of magnitude higher than in the standard composite (Figure 7.9 a).

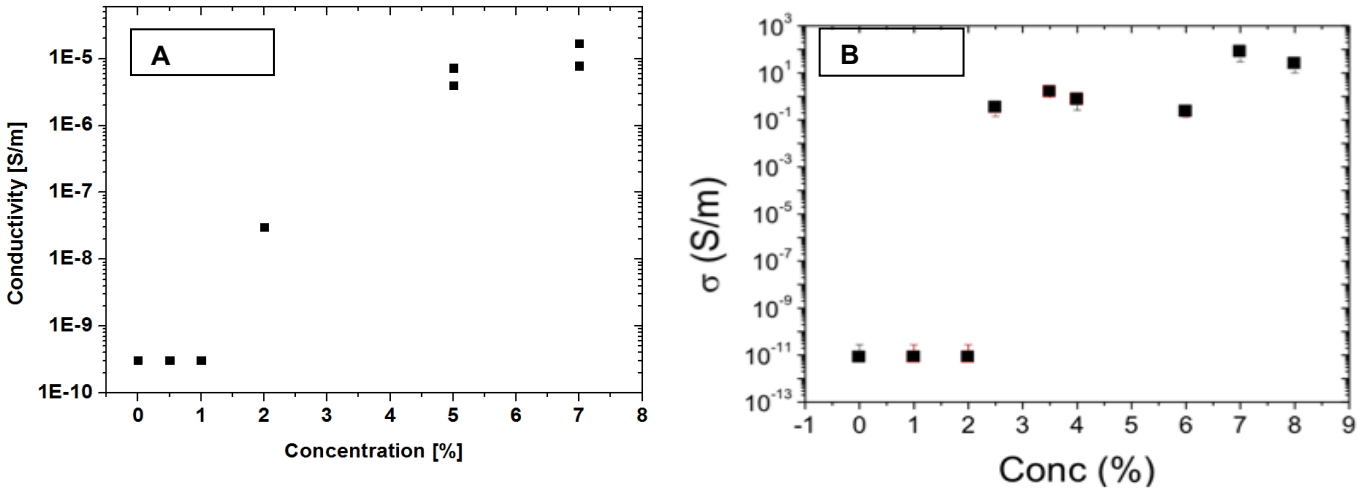

Figure 7.9: (A) Percolative behaviour of AVA FLG 18 graphene bulk composites with 10-5 S/m without glass fiber; (B) Percolative behaviour of hybrid graphene bulk composites with 10 S/m

The composites prepared show very high electrical conductivity. This good performance is not just due to the addition of the GRMs, but also to the presence of the fibers which, even though insulating, enhance the conductivity probably by aligning the GRM flakes.

7.3.2. Piezo-resistive behavior

In collaboration with Centro Ricerche Fiat (FIAT Research Centre), experimental measurements were carried out in order to analyze the electromechanical behavior of the GF-graphene-epoxy composites described in the previous section. For these measurements, we used a standard dynamometer for mechanical tests equipped with a dedicated electronic interface able to acquire both deformation and electrical resistance data simultaneously. deformation and electrical resistance simultaneously.

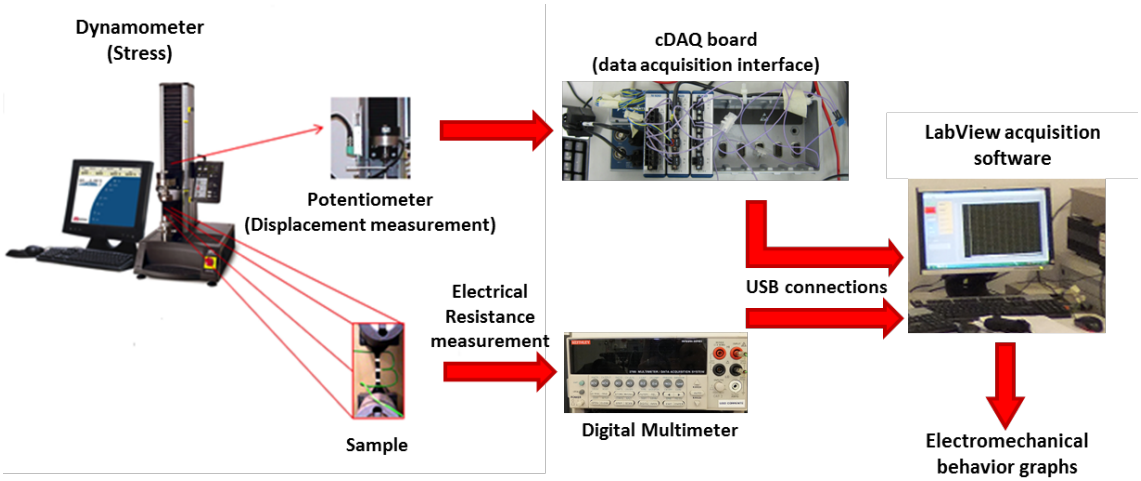

Figure 7.10: Experimental software set up with electrical and mechanical instruments.

The tested specimens were cut from a composite material sheet using a water-jet cutter. Subsequently, two metal electrodes were painted (with silver paint) onto the rod specimens for the flexural tests (all around the specimens as in Figure 7.11. Finally, a wire was positioned and bound with the silver epoxy paste onto each electrode.

The samples were subjected to cyclic bending (3-point bending mode) tests with an Instron dynamometer while an acquisition card NI-cDAQ acquired the value of the resistance and the applied displacement.

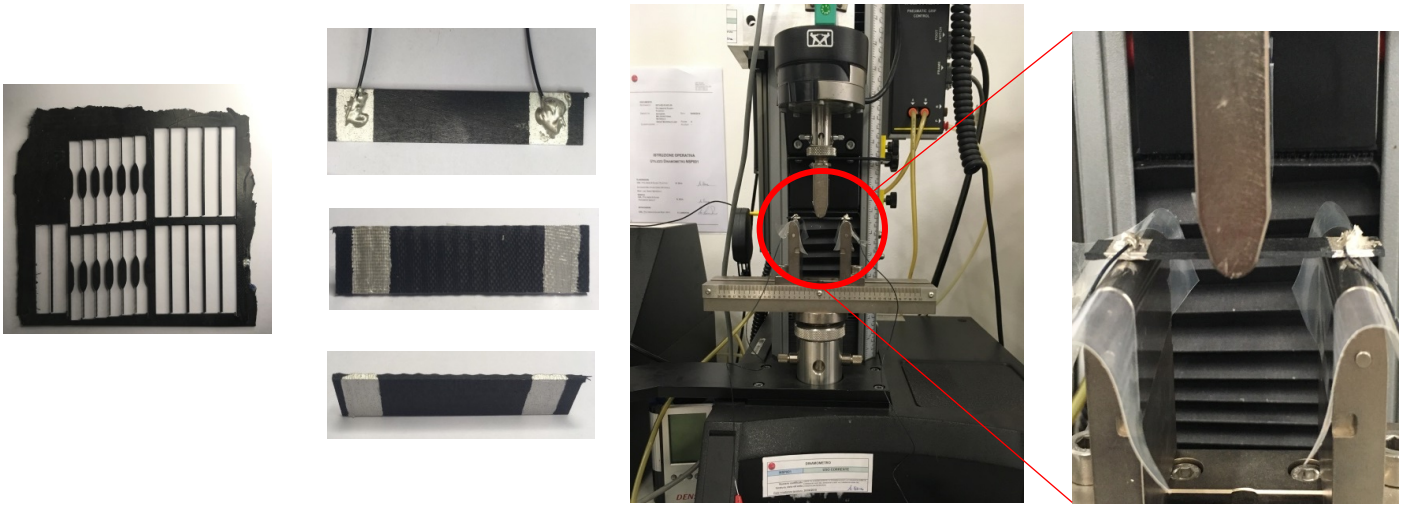

Figure 7.11: Specimen and experimental set-up

The graphs in Figure 7.12 cycles of the fatigue test of specimen 8. We observed a very good piezo resistive behavior, with changes in electrical resistance following the deformation of the specimen with very low noise on the signals.

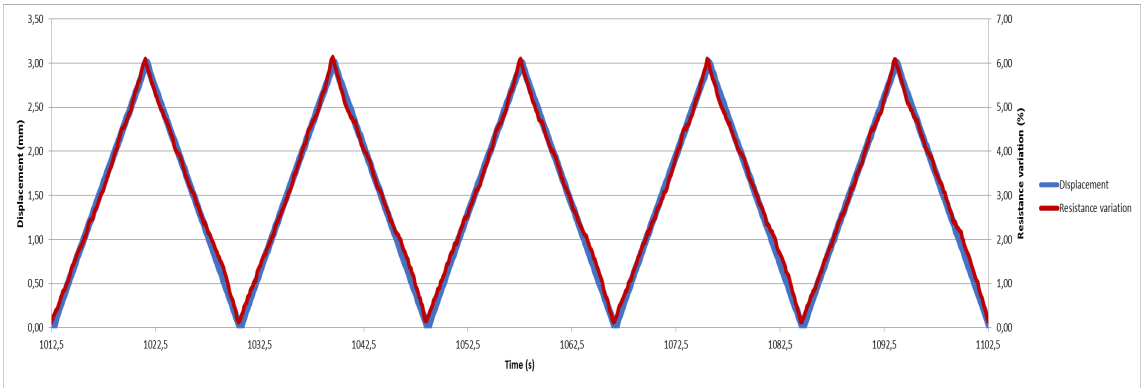

Figure 7.12: Piezo resistive behaviour of electro mechanical tests

7.4. Thermal Characterization

Thermal measurements of the prepared composites were also carried out in collaboration with Turin Polytechnic (dr. Alberto Fina). A TPS 2500S (HotDisk AB, Sweden) was used according to the UNI EN ISO 22007-2 method: "determinazione della conduttività termica e della diffusività termica".

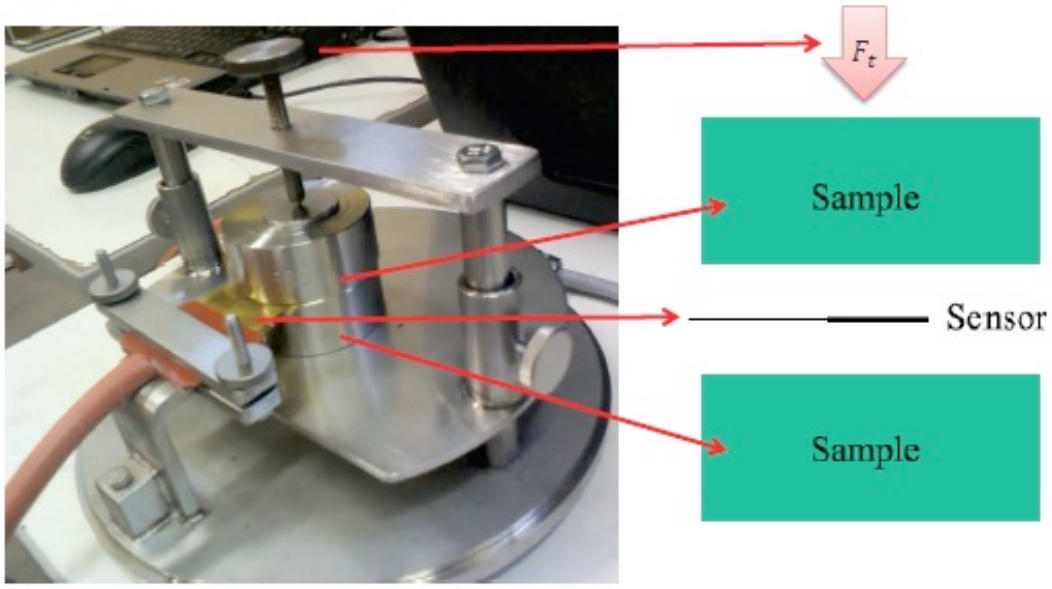

Figure 7.13: Photo image of instrument set up

A schematic of the instrumentation is given in Figure 7.14

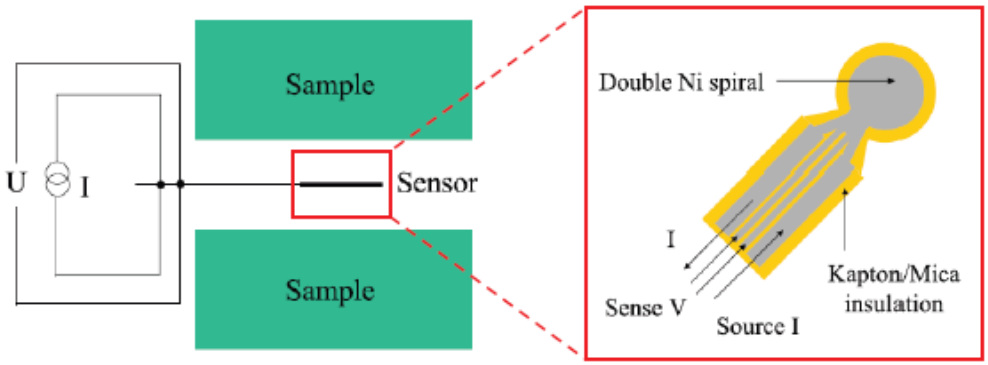

- Sensor electrically **heated up** by feeding constant current (I)
- **Voltage drop** (V) across Ni spiral is **measured**
- **Electrical resistance** is calculated: $R = V/I$
- **Sensor temperature** (T) is **known**: $R(T) = R_0(1 + \alpha\Delta T)$

Figure 7.14: Schematize image of the instrumental set up

7.4.1. Thermal Conductivity on composite with different filler

Specimens for this test are shown in the image below, where the rectangular portion is 3×4 cm, followed by Figure 7.15 where it is possible to see the "bottom" of the composites reinforced with the GRM used

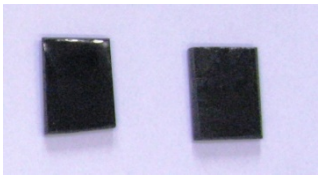

Figure 7.15: Photographic image of the composite "bottom"

A Kapton covered nickel probe with a radius of 6.4 mm was used and all specimens tested for 40 seconds with each different output power.

Table 7.5: Thermal stability value for composite made with different filler

Sample	Graphene	Contenuto [%]	k1	k2	k3	kmedia	Dev. St.
			[W/(m·K)]				
Reference			0.235	0.235	0.230	0.233	0.003
N130	AVA 21	2	0346	0.348	0.351	0.348	0.002
N132	AVA 24	2	0.339	0.341	0.339	0.340	0.001
N133	AVA 12	2	0.312	0.308	0.316	0.314	0.004
N134	AVA 20	2	0.324	0.326	0.321	0.324	0.003
N135	AVA 11	2	0.283	0.282	0.277	0.281	0.003
N136	AVA 18	2	0.479	0.479	0.480	0.479	0.001
N137	AVA 19	2	0.483	0.482	0.485	0.483	0.002
N138	AVA 23	2	0.321	0.323	0.324	0.323	0.002

The testing temperature was set to 50.00 ± 0.01 °C controlled with a silicon oil bath. The test apparatus with the specimens were kept for about an hour at the selected temperature to reach thermal stability.

Three measurements for each specimen were performed with a 15-minute delay between each test.

Best results were obtained using the GRM with large lateral dimensions and low specific surface area, because they are thicker than the GRM with high specific surface area, as they can transport the heat more efficiently.

7.4.2. Thermal conductivity on composite at different %

After testing a range of different GRMs, a promising powder was selected to observe the difference at various filler loadings. AVA FLG 18 was chosen because it showed significant improvements in thermal conductivity with respect to the native non-reinforced epoxy resin. AVA FLG 18 and AVA FLG 19 have the same morphological data.

Table 7.6: thermal stability value for composite made AVA FLG 18 at different percentage

Sample	Graphene	filler [%]	k1	k2	K3	kmedia	Dev. St.	Improvment %
			[W/(m·K)]					
Reference	-	-	0.247	0.247	0.247	0.247	0.001	0
N178	AVA 18	0.5	0.287	0.289	0.288	0.288	0.001	17
N177	AVA 18	1	0.342	0.342	0.343	0.342	0.001	39
N175	AVA 18	2	0.406	0.404	0.405	0.405	0.001	64
N176	AVA 18	5	0.780	0.781	0.782	0.781	0.001	216
N172	AVA 18	7	0.898	0.898	0901	0.899	0.002	264

The improvement as can be seen in Table 7.6 is around 250 %.

7.5. Mechanical Characterization

Mono-atomic graphene layers (with defects) has a Young's modulus twice that of steel [1], and this thesis investigates the possibility of exploiting this property in order to produce polymer composites with enhanced mechanical properties.

Literature data report an improvement in the modulus of these composites as compared to the pure polymer, and the percentage enhancements vary with filler content, filler modification, host polymer matrix and interfacial bonding strength [3].

The mechanical properties strongly depend upon the lateral flake size of the filler [37].

Studies on graphene dispersed in epoxies showed improvements not only in tensile properties but also in compression after impact, strength fatigue life, compression strength, flexure strength and also in fracture toughness [34].

7.5.1. Tensile test on graphene based nano-composites

The mechanical properties of GRM nanocomposites with different graphene nano-platelet powder (AVA-GLG xx) samples were tested through tensile tests, carried out with a dynamometer Instron 5966 (load cell of 10 kN) at a speed of 10 mm/s.

The specimen samples were chosen according to normative ASTM D638-14 with the dog-bone shape as shown in Figure 7.16

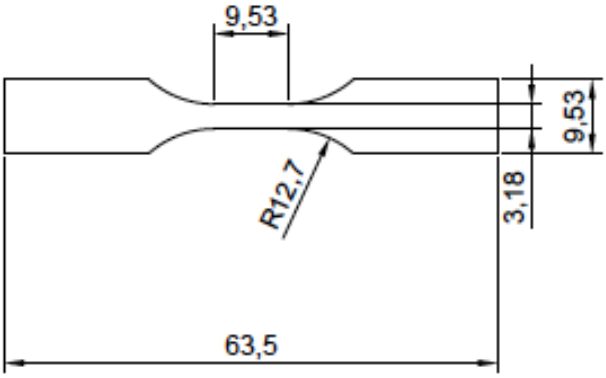

Figure 7.16: dog bone shape specimen in according with ASTM D638-14

In order to avoid slip between the sample and the loading frame, paper strips were glued to the opposite sample ends and, as expected, fracture initiated in the sample region with the smallest width (Figure 7.16).

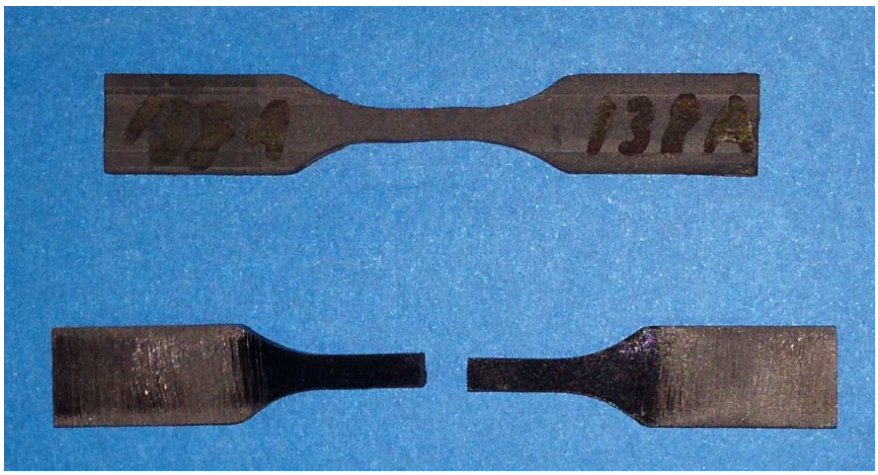

Figure 7.17: Picture of a dog-bone shaped sample before and after tensile testing

The addition of graphene nano-platelets (GnP) improved the stiffness of the nanocomposites, in agreement with previous results reported in the literature.

Mechanical properties, such as Young's modulus and tensile strength, are increased with the addition of GnP. For example, the addition of 0,5% weight of GnP increases the Young's modulus by around 10%. However, the addition of GnP also leads to a reduction in the strain at break, which could be associated with an embrittlement effect of rigid particles in a soft matrix.

In particular, we tested the following composites reported in a Table 7.7

Table 7.7: Mechanical properties resulting from tensile testing of bulk nanocomposite samples

Samples		Filler %	Tensile strength [MPa]	Young Modulus [MPa]	Tensile strength standard deviation	Young modulus standard deviation
Blank resin		0	64	1574	5,93	31,22
N172	AVA18	7	38	1864	1,13	38,03
N176	AVA18	5	44	1920	0,83	21,79
N177	AVA18	1	48	1709	3,3	38,56
N178	AVA18	0,5	57	1543	3,41	5,21
N148	AVA21	2,5	19	1681	4,04	31,73
N180	AVA21	2	34	1664	1,53	47,86
N181	AVA21	1,5	40	1685	1,66	20,56
N182	AVA21	1	38	1486	4,11	62,27
N183	AVA21	0,5	46	1737	0,74	21,72

Figure 7.18 shows that GMR-based composites have comparable maximum stress at low percentages (dark grey bar) of graphene nano-platelet filler, whereas the Young's modulus increases in composites with high filler loadings (yellow and light grey bar); the improvement in Young's modulus is around 20% with respect to the native epoxy matrix.

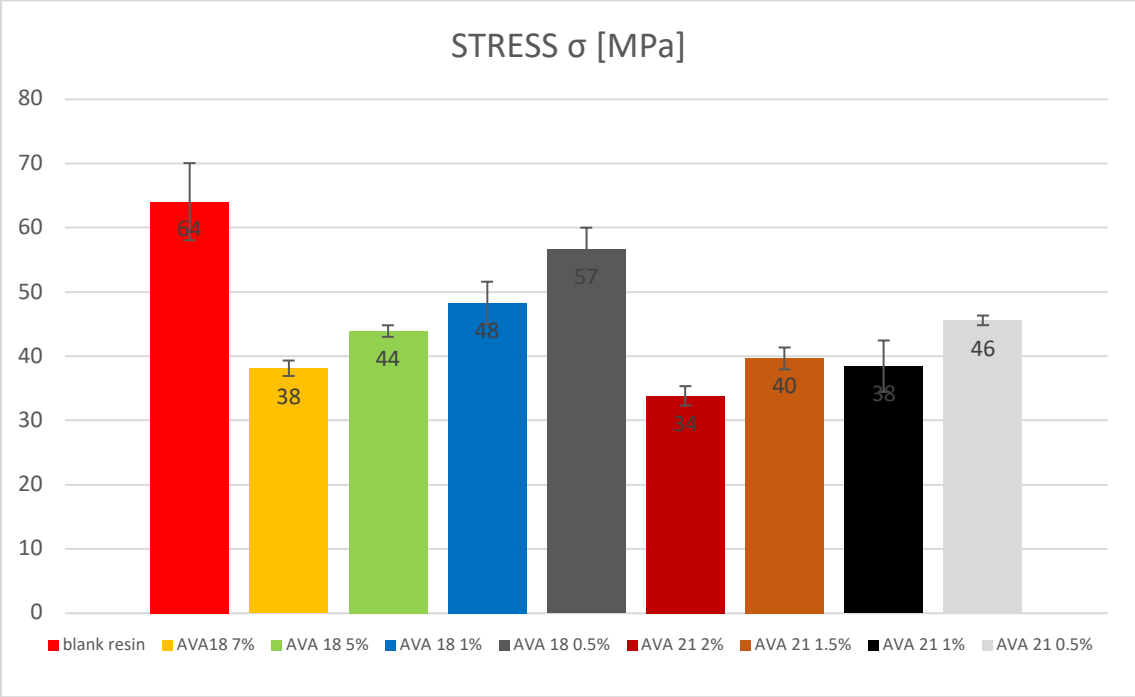

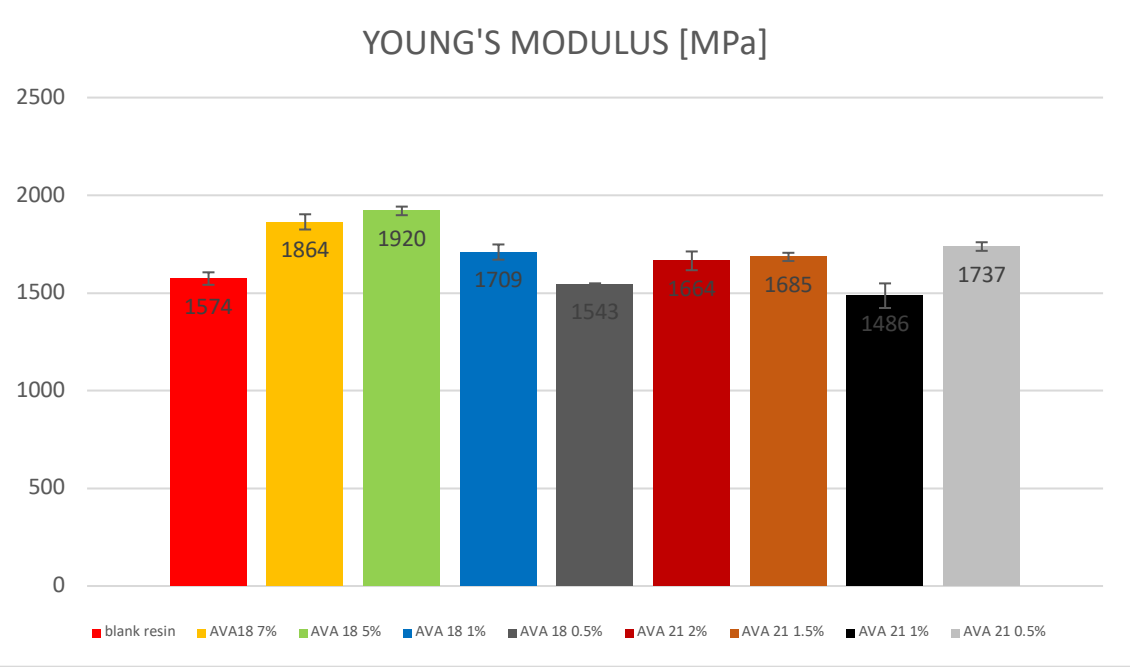

Figure 7.18: Stress and Young modulus of tested reinforced composites

7.5.2. Fracture toughness

Fracture toughness measurements using three-point bending (3PB) test set-ups for single-edge notch bending (SENB) tests were carried out. For the insertion of notches, a standard procedure used in ASTM standard D5045 was implemented. A raw notch was cut using a diamond saw blade down to half the sample height, and this notch was then further tapered by sliding a razor blade across the raw notch as shown in the schematic presented in Figure 7.19

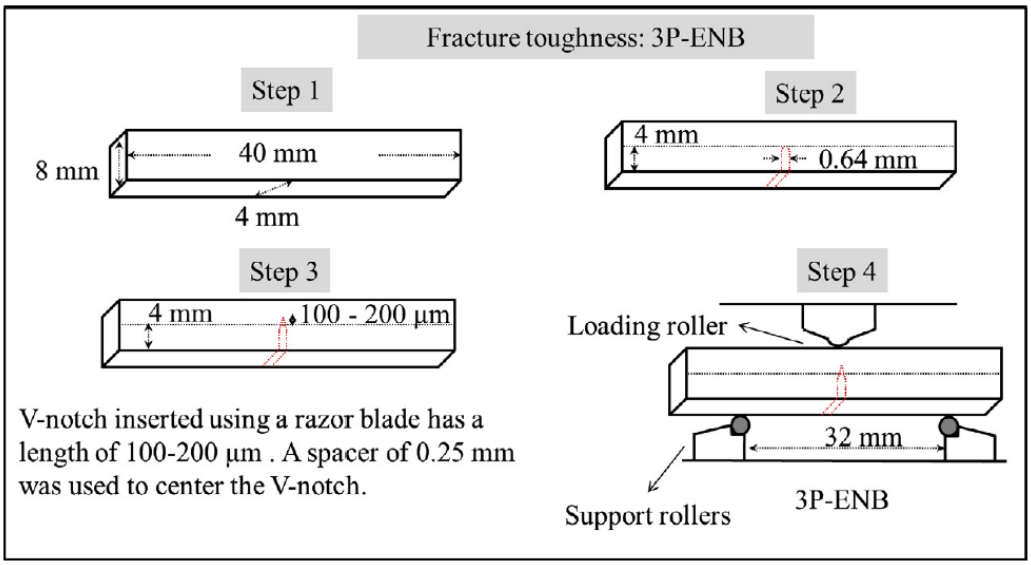

Figure 7.19: Specimen geometry and notch preparation for fracture toughness tests[11].

An example of the SEN-3PB testing of samples, is shown in the image.

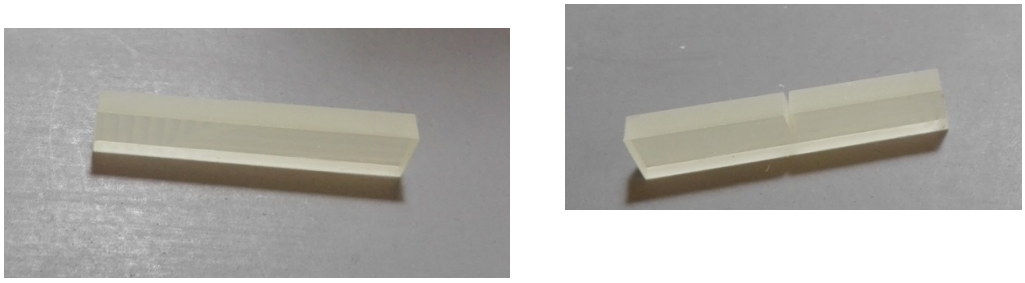

Figure 7.20: Photographic picture of the specimen sample for toughness fracture test

The raw notch was cut using a 0.64 mm thick diamond cutting wheel. The V-notch insertion procedure was carried out by a Proxxon FET (Proxxon, Via Moreo 13 22010 Laglio CO, Italy) showed in **Errore. L'origine riferimento non è stata trovata.**.

Figure 7.21: Proxxon FET used to create the V-notch in fracture toughness sample

The data were analyzed using the equation of Shulte et al. (Equation 2) [11],

Equation 2: fracture toughness equation

$$K_{IC} = \frac{FL}{B\,w^{\frac{3}{2}}} \cdot f\left(\frac{a}{w}\right) \qquad with\ 0 < \frac{a}{w} < 1$$

$$f(x) = 3\left(\frac{a}{w}\right)^{\frac{1}{2}} \left\{ \frac{\left[1.99 - \frac{a}{w}\left(1 - \frac{a}{w}\right)\left(2.15 - 3.93\frac{a}{w} + 2.7\left(\frac{a}{w}\right)^2\right)\right]}{2\left(1 + 2\,\frac{a}{w}\right)\left(1 - \frac{a}{w}\right)^{\frac{3}{2}}} \right\}$$

where F is the maximum force; L, span length; B, specimen width; a, crack length; w, specimen height.

The results are presented in Table 7.8

Table 7.8: Data of fracture toughness

GnP type	Filler %	K_{IC} (MPa √m)	Deviazione standard K_{IC} (MPa √m)
AVA 12	0,5	0,96	0,07
AVA 19	0,5	0,90	0,04
AVA 23	0,5	0,64	0,03
White	0	0,8	0,05

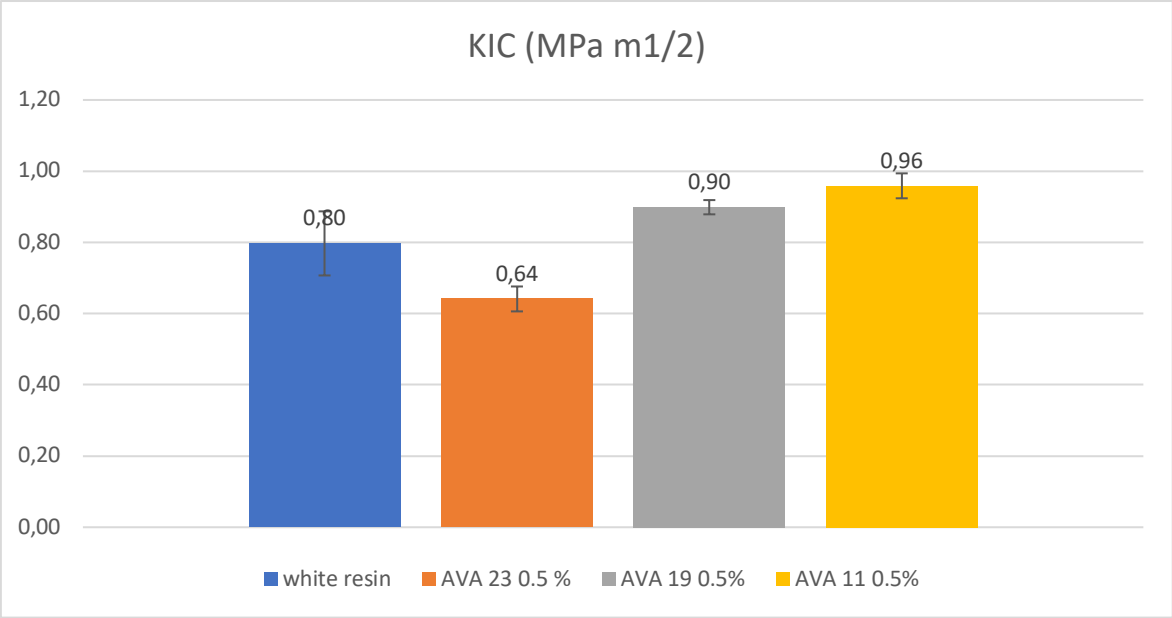

Figure 7.22: Fracture toughness of GRM based composites at the same %

Figure 7.22 shows the fracture toughness of the GRM-based composites, it is possible to observe an improvement in the fracture resistance for composites with low loadings (yellow and light grey bar) and in composites with low-surface-area graphene nano-platelets.

1.1. Humidity adsorption tests

In aeronautic applications, fiber-reinforced epoxy resins are currently used for structural applications in considerable amounts. Such material indeed can provide a considerable improvement in aircraft performance due to the lower weight and higher corrosion resistance compared to metals.

A problem related to this kind of material, however, is its moisture absorption resistance. Moisture, indeed, can be very damaging for composites because it can degrade the physical properties of the material. In particular, the adsorbed moisture can decrease the glass transition temperature by plasticizing the polymer, it can compromise adhesion between the matrix and the carbon fibers used.

Materials with high surface-to-thickness ratios, such as graphene, should create a physical barrier against molecular diffusion of water in epoxy resin. Furthermore, graphene also shows high hydrophobicity at its surface. Therefore, the diffusion coefficient, as well as the final moisture absorption, could be reduced by the introduction of graphene into the composite materials. To this end, graphene-epoxy composites were prepared and characterized using two different approaches (see Figure 7.23):

- Bulk approach: graphene nano-platelets in epoxy resin can create a tortuous path that decrease the moisture absorption inside the composite

- Surface approach: The graphene coating applied on the surface should create physical barrier against H_2O molecule diffusion in epoxy resin.

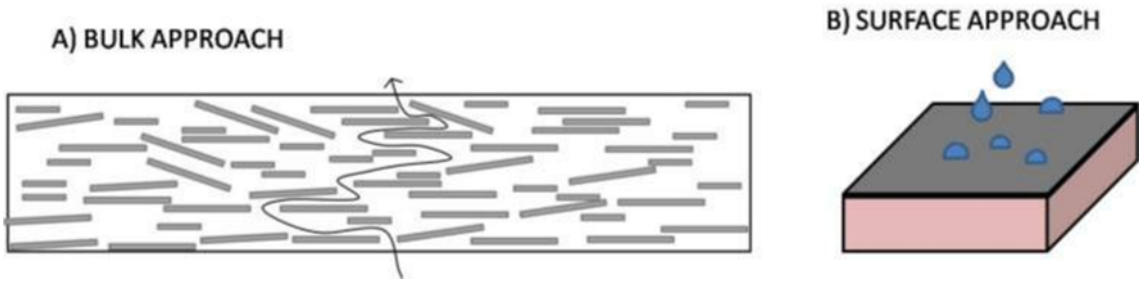

Figure 7.23: A) Bulk approach: schematization of the graphene nano-platelets in the epoxy resin, and the moisture tortuous path through the composite, B) Surface approach: The graphene coating applied on the surface should create physical barrier against H_2O molecules

The main objective of this chapter is the study of moisture absorption for the reference, cured epoxy resin and the graphene-modified epoxy composites.

For the design of, and calculations on, aeronautical composite structures, the wet conditioning during in-service life has to be considered. Thus, with the aim of fulfilling the requirements for the certification of structural components, controlled accelerated ageing is carried out (70ºC /85 % R.H until reaching equilibrium), in order to simulate the ageing during aircraft life (average of worst climate conditions: 20ºC /85 % R.H.) in accelerated conditions.

In composite materials, the main effect of epoxy resin moisture absorption/uptake is the decrease in resin-dependent mechanical properties. The drop from Hot/AR (As-Received) to Hot/wet properties selects the material allowable, and is used to calculate the specification for aeronautical structural components. This drop thus results in heavier structures. A potential decrease in resin moisture absorption by means of graphene nanoparticle dispersion should lead to a decrease in weight of the final composite/carbon-fiber reinforced component.

the decrease in mechanical properties due to wet ageing can be up to 20% in the worst case. In a first approach of this study the target was to reduce this drop to around a 10% by using graphene materials (Figure 7.24).

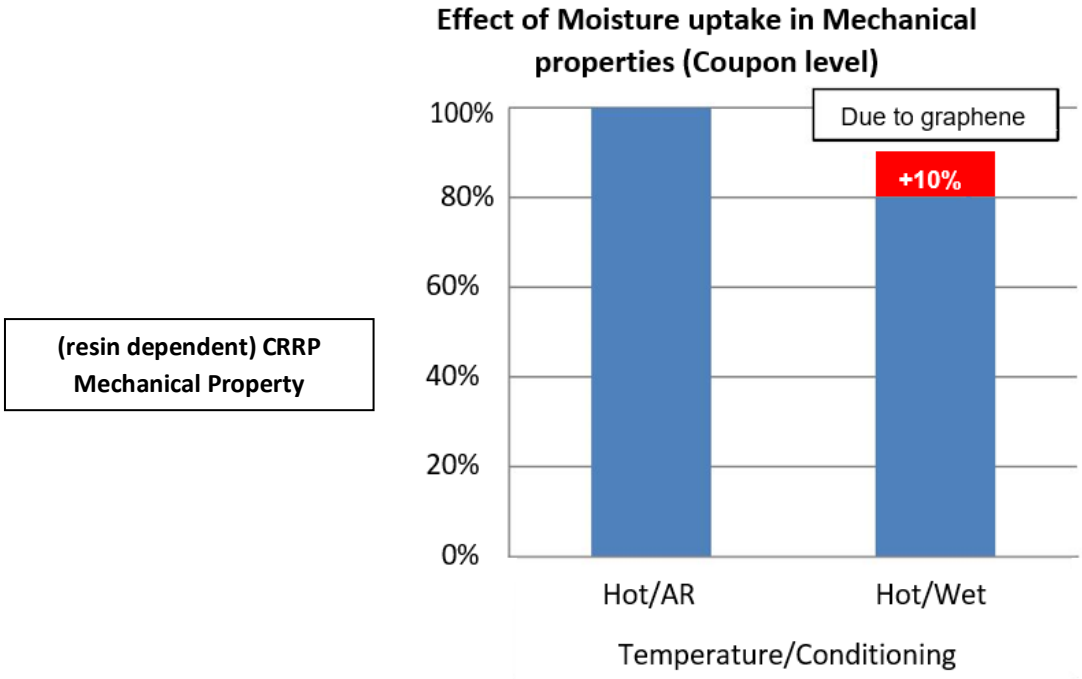

Figure 7.24: Effect of moisture uptake in mechanical properties at coupon level

The experience of Airbus shows, for a typical structural thickness of 10 mm, around 5 mm thickness is wet conditioned after the in-service life of the structure. Using graphene as a

moisture absorption barrier, the target could be a 20% increase in the unconditioned thickness. In this case, the structural thickness conditioned would be only 4 mm instead of the initial 5 mm without graphene (Figure 7.25)

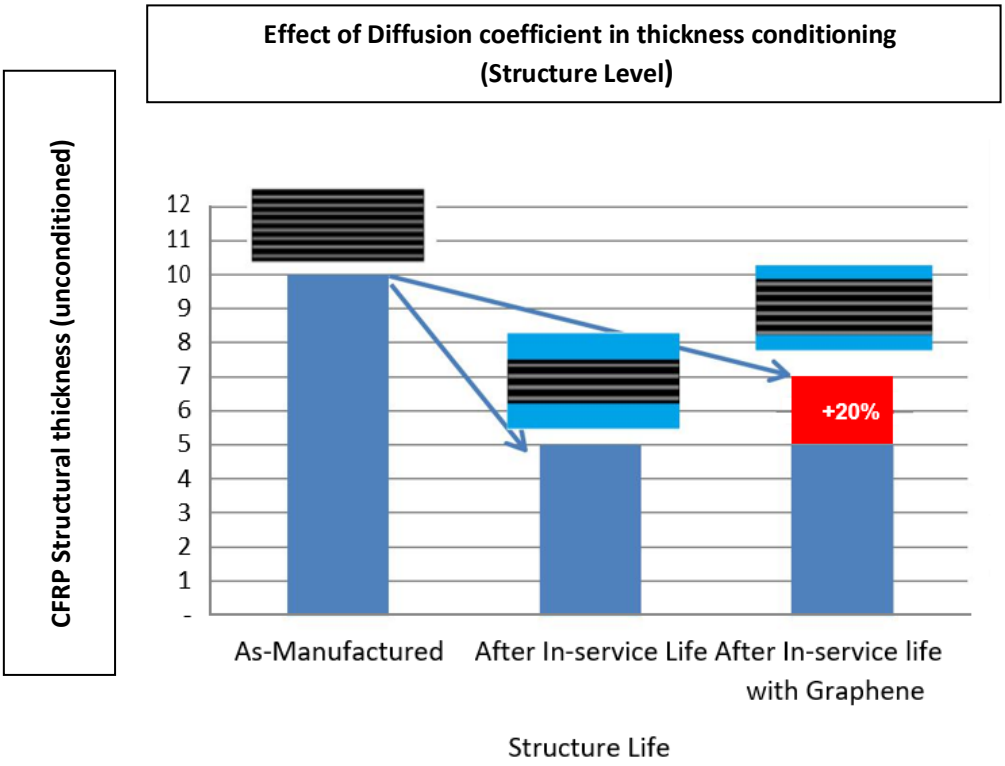

Figure 7.25: Effect of diffusion coefficient in thickness conditioning at structure level. Typical values for a 10mm thick structure

7.5.3. Humidity adsorption results

The preparation of the advanced bulk epoxy composite samples in this research involves two basic components, an epoxy resin (Huntsman Performance Products, Huntsman Surface Sciences Italia Srl Via Cavour 50 46043 Castiglione delle Stiviere) and various graphene powders supplied by Graphene Flagship partners (AVANZARE and GRAPHENEA) or commercial partner XG Science.

The epoxy resin (Araldite LY 5052) and the hardener (Aradur 5052 CH), supplied by Huntsman have properties which are particularly useful in aircraft construction and, in particular, this resin is already used internally in Airbus planes, mainly for cosmetic repair operations. Some important properties of this resin are:

1. Low viscosity, easy impregnation of reinforcement materials
2. Long pot life (2 hours for 100 ml at Room Temperature (RT))

Moisture absorption has been evaluated by Airbus. The main scope was to assess the moisture absorption behavior of the cured epoxy resin Araldite LY5052/Aradur 5052 CH as reference in comparison with the resin doped with the dispersed graphene nano-platelets.

All specimens of each graphene type and concentration were pre-dried (see Table 7.9) and conditioned. The thickness and weight of each specimen were measured prior to ageing/conditioning. The moisture absorption test was carried out on bulk materials, following the reference standard EN3615: “Fiber reinforced plastics-Determination of the conditions of exposure to humid atmosphere and of moisture absorption”

The climatic chamber used to perform the sample conditioning must be calibrated and regularly controlled to check proper operation at the required temperature and humidity. The climatic chambers have to guarantee the appropriate conditions of temperature and humidity over long periods of time.

Due to the low cure cycle temperature (T_c = 80ºC) the test conditioning was selected as follows:

1) Pre-drying: Samples introduced in an oven to be dried, 50 °C up to reaching equilibrium
2) Hot/Wet: Samples introduced in an oven at 60 °C/85%R.H. up to reaching equilibrium

The weights of each specimen were recorded as shown in Table 6 during testing in order to obtain the sample moisture pick-up curves. All samples for each kind of graphene type and concentration, introduced into the chamber were identified with letters.

.

Table 7.9: Pre-drying and conditioning planning time

Pre-drying (1)	Conditioning (2)
t=0	t=0
Every week up to equilibrium	Day: 1,2,3,4,5,8,10,14 and then every week up to equilibrium
t=tend	t=tend

The percentage of moisture absorbed by each specimen and the corresponding absorption curves were reported by the testing lab, besides the temperature and any incident likely to have affected the results.

The first phase of the analysis focused on the doping of the bulk resin with different types of graphene from **Avanzare** (different BET & Diameter) with the same filler loading (2%). Only one specimen from a different supplier (**XG Science**) and with different content was evaluated. Table 7.10 shows the characteristics of all the specimens tested whereas **Errore. L'origine riferimento non è stata trovata.** shows the moisture absorption evolution for this first batch, Batch 1.

Table 7.10: Batch 1 - Specimen to test

Graphene type	Specimen ID	Diameter 50% (µm)	BET (m^2/g)	Amount Filler [%]
REFERENCE	N100	-	-	
AVA-FLG011	N135	7,4	70 ± 5	2
AVA-FLG012	N133	2,2	201 ± 3	2
AVA-FLG018	N136	49	22 ± 4	2
AVA-FLG019	N137	53	22 ± 3	2
AVA-FLG020	N134	40	225 ± 5	2
AVA-FLG021	N130	39	225 ± 5	2
AVA-FLG023	N138	104	190 ± 4	2
AVA-FLG024	N132	39	210 ± 12	2
XGNP-M25	N129	33	115	7

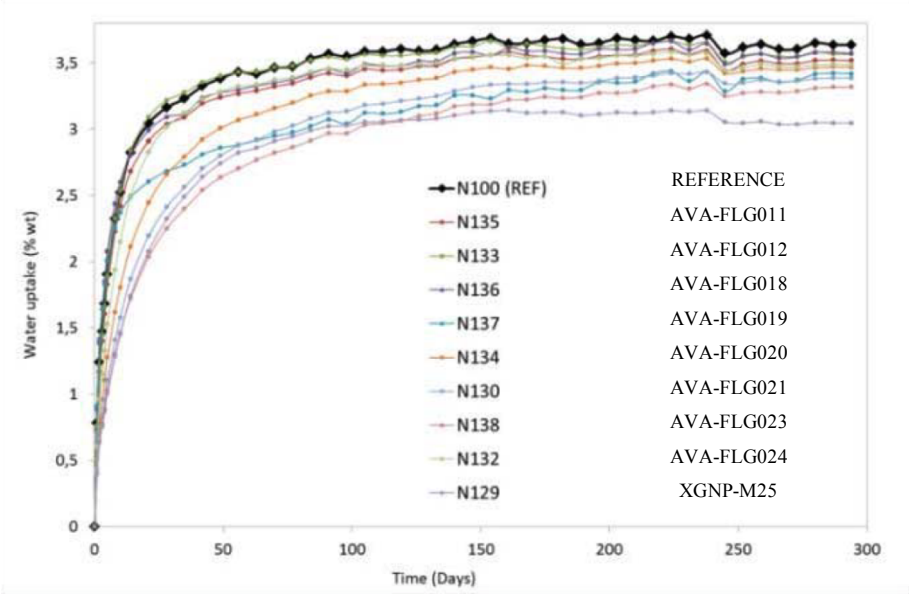

Figure 7.26: Results in moisture pick-up curves for Batch 1. Moisture uptake (% wt) vs time

The second phase of this study focused on a selection of two types of graphene, using different filler loadings. Two graphene types from Batch 1 with similar lateral dimensions but different BET values were selected Table 7.11 shows the characteristics of all specimens tested whereas Figure 7.26 shows the moisture absorption evolution for Batch 2.

Table 7.11: Batch 2 - Specimen to test

Graphene type	Specimen ID	Diameter 50% (μm)	BET (m^2/g)	Amount Filler [%]
REFERENCE	N100	-	-	
AVA-FLG018	N172	49	22 ± 4	7
	N176			5
	N177			1
	N178			0,5
AVA-FLG021	N180	39	225 ± 5	2
	N181			1,5
	N182			1
	N183			0,5

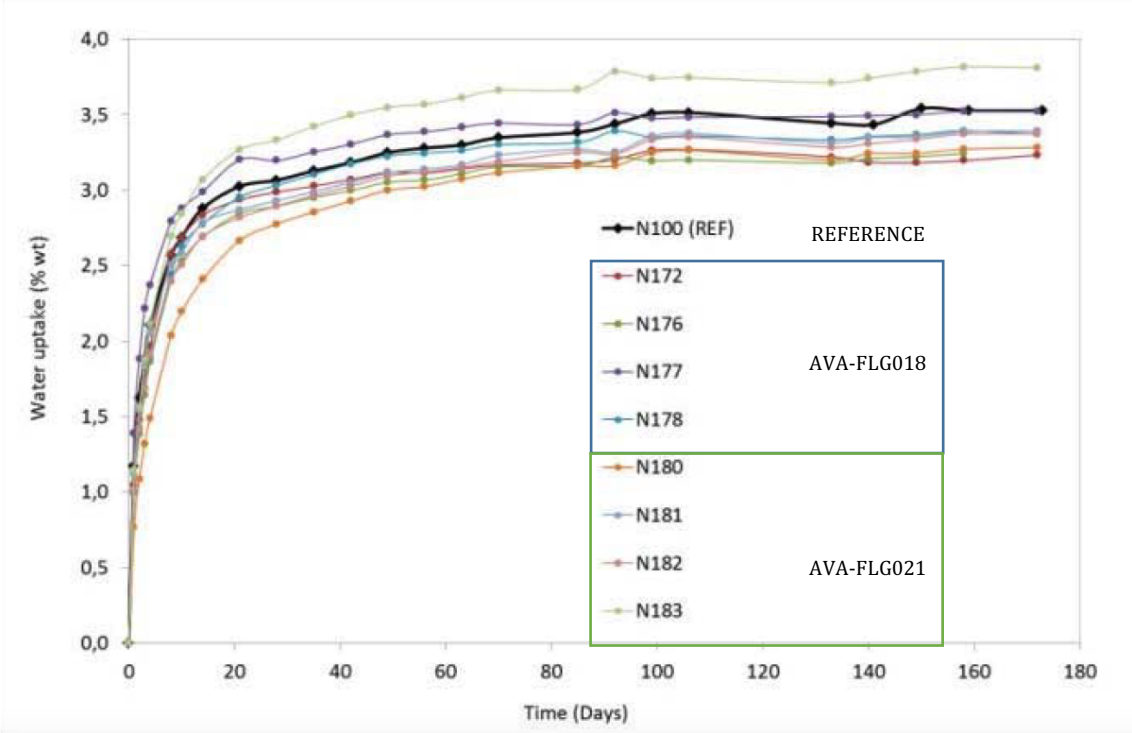

Figure 7.27: Results in moisture pick-up curves for Batch 2. Moisture uptake (% wt) vs time

Moisture absorption in equilibrium is the maximum quantity of moisture absorbed by the resin under the defined conditions, whereas the diffusion coefficient measures the resin moisture absorption rate: in other words, how much and how fast the resin takes up the moisture. In general terms, a reduction in both parameters was observed when adding graphene nano-platelets, thus improving the moisture absorption behavior.

In Figure 7.26 (results obtained for Batch1) a fluctuation starting from day 231 was noticed as a signal that equilibrium had been reached. Thus, it was decided to consider only the values obtained up to that point in time. The equilibrium condition was reached in both cases. The results for Batch 1 are summarized in Table 10 with the percentage reduction in both final moisture absorption and diffusion coefficient. It was decided to remove the specimen with 7% loading as the influence of this parameter was to be studied in Batch 2.

Table 7.12: Batch 1 - Results Summary

BATCH 1 RESULTS SUMMARY								
Specimen	Graphene type	Diameter 50% Φ (μm)	BET (m2/g)	Filler content	M(∞) (equilibrium) [%]	Reduction Percentage In final weight	D (Diffusion Coefficient) [mm^2/s]	Reduction Percentage in D
N100	Reference	-	-	0%	3,68	0%	9,87E-07	0%
N136	AVA-FLG018	49	22	2%	3,6	2%	7,92E-07	20%
N137	AVA-FLG019	53	22	2%	3,36	9%	7,21E-07	27%
N135	AVA-FLG011	7,4	70	2%	3,56	3%	8,19E-07	17%
N138	AVA-FLG023	104	190	2%	3,3	10%	6,78E-07	31%
N133	AVA-FLG012	2,2	201	2%	3,63	1%	4,93E-07	50%
N132	AVA-FLG024	39	210	2%	3,56	3%	5,71E-07	42%
N130	AVA-FLG021	39	225	2%	3,41	7%	6,49E-07	34%
N134	AVA-FLG020	40	225	2%	3,51	5%	5,64E-07	43%

According to the results, the first behavior observed was the small effect of graphene nano-platelets in the final moisture uptake compared with its effect on diffusion coefficients. The highest reduction in moisture uptake (10%) was found with the highest lateral size (104 μm) and a BET value of 190 m^2/g. The highest diffusion-coefficient reduction reached (50 %) was for the lowest lateral dimensions (2.2 μm) with a BET value of 201 m^2/g.

For Batch 2, the same analyses were performed and, also here, two types of graphene nano-platelets were selected with different filler loadings. The scope was to understand the filler content effect on moisture uptake properties. Table 7.13 summarizes the results obtained for Batch 2.

Table 7.13: Batch 2 - Results Summary

BATCH 2 RESULTS SUMMARY								
Specimen	Graphene type	Filler content in resin	Diameter 50% (μm)	BET (m2/g)	M(∞) (equilibrium) [%]	Reduction Percentage In final weight	D (Diffusion Coefficient) [mm^2/s]	Reduction Percentage in D
N100	REFERENCE	0%	--	--	3,53	0%	9,59E-07	0%
N172	AVA-FLG018	7%	49	22 ± 4	3,18	10%	7,51E-07	22%
N176		5%			3,25	8%	8,88E-07	7%
N177		1%			3,51	1%	1,03E-06	-7%
N178		0,5%			3,39	4%	1,07E-06	-12%
N180	AVA-FLG021	2%	39	225 ± 5	3,26	8%	8,75E-07	9%
N181		1,5%			3,35	5,1%	1,03E-06	-7%
N182		1%			3,36	5%	8,42E-07	12%
N183		0,5%			3,79	-7,4%	1,07E-06	-12%

The first behavior observed was that by increasing filler content above 2% the moisture absorption properties improved with reductions in both final moisture absorption uptake and diffusion coefficient. Again, the effect was higher for the diffusion coefficient (up to 20% for 7% loading). It was also observed that loading percentages below 2% could deteriorate

the moisture absorption behavior.

7.6. High field grading results

Semiconducting materials based on SiC or mixing of BN and GnP with insulating or low conducting materials, are used for over-voltage protection in high voltage systems. The current-voltage curve for the protective material resembles that of a Schottky diode: at low electric fields the material is electrically insulating and above a specific threshold electric field the material conducts. This is commonly used in surge arresters, motors, as well as in joints and terminations in cable systems, and could also be useful for other HV components. The stress grading properties of electric field grading materials (FGMs) for pure HVDC (high voltage direct current) applications can be described by three important parameters:

- The conductivity under normal operation, called the low field conductivity (σ_0);
- The threshold electric field (E_{th}), above which the conductivity starts to increase rapidly;
- The non-linearity coefficient (α) which describes how quickly this increase takes place.

Different degrees of semiconductor filling can be found in different components.
Polymer composites with lower filler loadings (up to 30 v%) are used in cable systems and motors; lowering the loading of the semiconducting material further could result in several advantages, the most important one being the enhanced mechanical properties. On the other hand, the system needs to be percolated but robust, otherwise the material may not have the field grading property or the conductivity variation may be too high at the same electric field. The material studied in this thesis consists of a network of around 16%wt. of boron nitride flake and 0.5%wt. of graphene nano-platelets (GnPs) in an insulating silicone rubber matrix of Sylgard 184. Initially, various loadings of boron nitride (Henze BN 205) alone were tested:

- 16 %wt.
- 23 %wt.

The boron nitride and graphene nano-platelets were selected for this application based on the conceptual idea that a high local electric field is created at the high aspect ratio of the flakes and this electric field would be high enough to initiate non-linear conductivity within the composite.

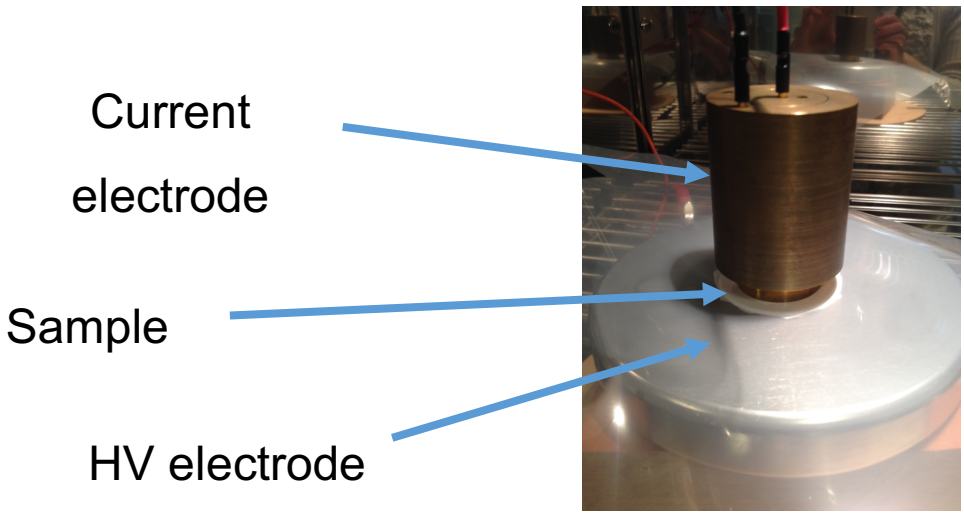

Figure 7.28:Experimental set up for high field grading tests

Maintaining the gap between the three-roll milling fixed at 20 µm, the final material exhibited insulating properties (2^{-14} S/m) at electrical fields between 0.5–12 kV/mm, except for the composite where graphene nano-platelets were added.

Table 7.14: conductivity measurement data

Sample	Content	Conductivity [S/m]	Electric field range [V/m]	note
reference	-	8×10^{-15}	2×10^{6} to 30×10^{6}	σ: relatively constant
Sample 5	16 % wt.	1×10^{-15}	2×10^{5} to 1×10^{7}	Low E-field: lower σ
Sample 6	23 % wt.	1×10^{-15} to 1×10^{-14}	1×10^{6} to 35×10^{6}	Low E-field: lower σ, V. high E-field: higher σ
Sample 7	16 % wt. of BN + 0.5 % wt of GnP	1×10^{-15} to 3×10^{-14}	1×10^{6} to 29×10^{6}	Low E-field: lower σ, high E-field: higher σ and increasing

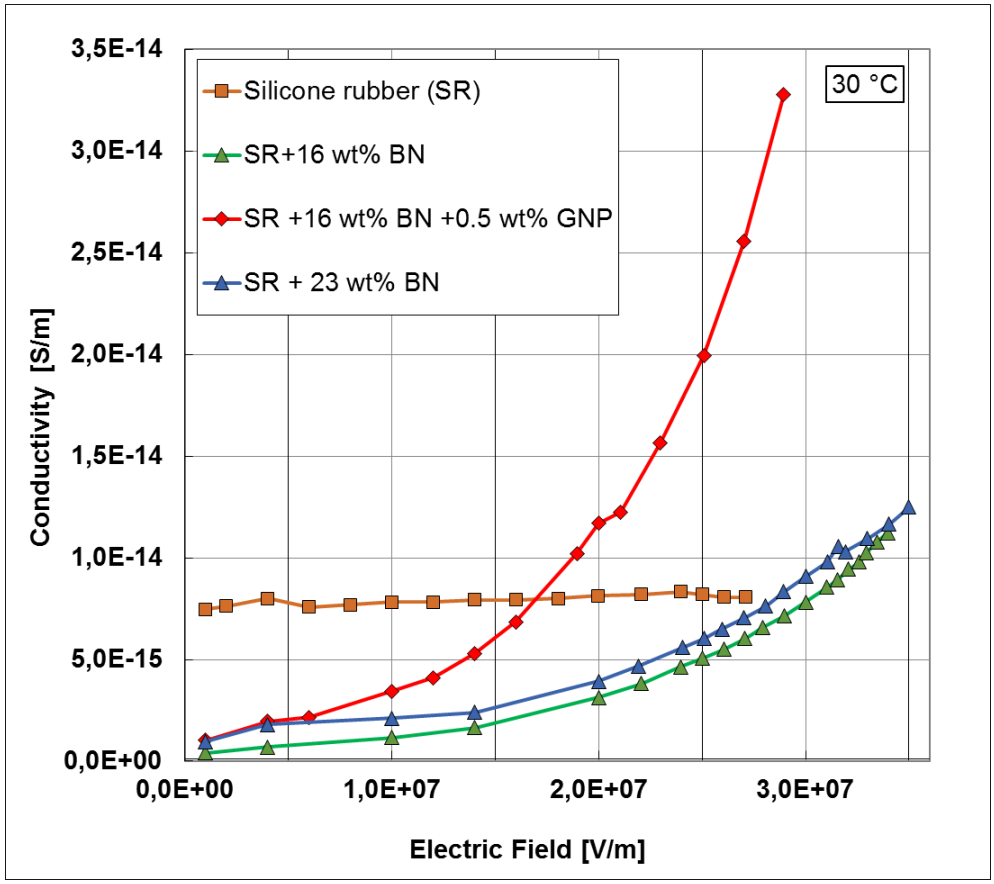

Figure 7.29: Conductivity measurement plot for each concentration and type of composites

It was noted that there was a significant difference in resistivity, which depended upon the addition of graphene nano-platelets to the silicone resin (Figure 7.29), where the maximum conductivity reached 3^{-14} S/m at electrical fields between 10–20 MV/mm.

7.7. Conclusion and Outlook

This thesis reports the general characteristics and the optimization of a number of parameters used in the preparation of nano-structured two-dimensional-filler composites to change in a multifunctional way various aspect of composite properties useful in technological fields such as aeronautics and the automotive industry.

In conclusion, 2-D nano-filler materials embedded into thermosetting polymers are excellent candidates to create a uniform and homogeneous macro structure of composite materials.

Several commercial graphene powders were characterized and used to prepare graphene-epoxy composites.

This work shows that the most interesting effects and changes in properties of composites by GnP loading in epoxy matrices are produced by loadings from around 0,5% to 7% by weight. It has been demonstrated that increases in filler concentrations lead to changes in macroscopic properties such as electrical, mechanical, thermal and water barrier characteristics.

The materials prepared and tested gave significant improvements in their electrical and thermal conductivity.

From the electrical and thermal point of view, the more exfoliated nano-platelets (surface area 220 m^2/g) give greater improvements in electrical conductivity of the final composites (≈ 6 orders of magnitude improvement).

Less exfoliated, thicker nano-platelets (surface area 22 m^2/g) lead to greater improvements in the thermal conductivity of the composite (≈ 50% improvement).

However, from the mechanical point of view certain types of GnPs, used in polymer matrices in aeronautical systems provides no evidence of improvements in composite characteristics and may sometimes even degrade them.

From the point of view of the humidity barrier, addition of nano-fillers to the composite matrix lead to maximum reductions in epoxy moisture absorption at equilibrium of around 10% and around 50% for the diffusion coefficient (specimens from Batch 1, with 2% filler loading), but a good compromise between both values led to a smaller reduction (between 5–10% in moisture uptake and 31-43% in diffusion coefficient). Thus, to check the effects of such reductions obtained with graphene, it is recommended that the resin samples be tested after wet ageing (in tensile, compression etc..) to see the real, overall effects in material mechanical behavior.

7.8. Conference and workshop

1st year

November 2014: Talk, Eu Graphene Flagship Task 10.12 Of Wp10 - Bergamo

February 2015: school, Sinchem Winter School - Bologna

March 2015: talk, Graphene for Airframe, AIRBUS, 24-25/03/2015, Tolouse

May 2015: talk, Composites materials, Coffe talk - CNR ISOF

September 2015: poster, GraphITA 2015 - CNR Bologna

September 2015: poster, X-ray diffraction: A tool for solid state investigation

October 2015: seminar**,** tecniche di analisi termiche nello sviluppo e nel controllo di materiali e processi nel settore automotive - Venezia

November 2015: seminars, VVT Passion and Deployment Challenges - Bologna

2nd year

April 2016: seminars, Us-ltaly JCM Advanced Materials - Bologna

April 2016: seminars, Low-energy ion implantation on graphene: towards nano-functionalization of 2D materials – Bologna IMM

April 2016: seminar, multifunctional adaptive insulation elements enabled by - Bologna

April 2016: seminar, Low-energy ion implantation on graphene: towards nano-functionalization of 2D materials.

April 2016: seminar, Growth of Mono- and Bi-layer Graphene Single Crystals - Bologna

April 2016: seminar, From fire ants to graphene: some considerations on water-hydrophobic interfaces - Bologna

April 2016: Poster, GRAPHENE 2016 - Genova

May 2016: seminar, Aerosols, air quality, and climate - Bologna

May 2016: seminar, Workshop in honour of Carlo Taliani (May 22-24)

September 2016: talk, IC AUTO C 2016 - Lisbon

September 2016: seminar, Xray scattering techniques: strategic tools for material science - Bologna

September 2016: talk, Nanoscience and Nanotecnology - FRASCATI

October 2016: seminar, Giornata di incontro su igiene industriale e tecnologie correlate – Firenze

3rd year

November 2016: seminar, **"**From Distorted Aromatics to 2D Materials" - Bologna

November 2016: seminar, Hybrid Polymer Nanocomposites: Enhanced Properties &Applications - Bologna

December 2016: seminar, The honeymoon of supramolecular chemistry and graphene: hybrid materials with tunable properties - Bologna

December 2016: seminar, GLOBAL CITIZENSHIP EDUCATION: the role of Education in a Globalized World - Bologna

March 2017: seminar, Phosphorene and 2D companions - Rome

March 2017: talk, Graphene Market Place, Airbus Getafe – Madrid

May 2017: lecture, inorganic chemistry course at university of Bologna - Bologna

July 2017: seminar, Scanning probe microscopy and spectroscopy for mineral biological and material sciences - Bologna

September 2017: poster, Nano innovation - Rome

7.9. Attended PhD Course

- Laboratory of material characterization, May 2015
- Scientific Writing, May 2015
- From IP management to technology transfer for business, May 2015
- Corso Chimica fisica, May - June 2016
- Complementi Chimica Inorganica, May - June 2016
- Corsi di formazione per i dottorandi per l'acquisizione e lo sviluppo di competenze trasversali, May - June 2017

7.10. Patent

1. *Multifunctional diffusion barrier,* ***submitted****; in collaboration with airbus*
2. *nanocomposite material for over-voltage protection in high voltage components;* ***invention disclosure****; in collaboration with ABB*

Bibliography

1. Ferrari, A. C.; Bonaccorso, F.; Fal'ko, V.; Novoselov, K. S.; Roche, S.; Boggild, P.; Borini, S.; Koppens, F. H. L.; Palermo, V.; Pugno, N.; Garrido, J. A.; Sordan, R.; Bianco, A.; Ballerini, L.; Prato, M.; Lidorikis, E.; Kivioja, J.; Marinelli, C.; Ryhanen, T.; Morpurgo, A.; Coleman, J. N.; Nicolosi, V.; Colombo, L.; Fert, A.; Garcia-Hernandez, M.; Bachtold, A.; Schneider, G. F.; Guinea, F.; Dekker, C.; Barbone, M.; Sun, Z.; Galiotis, C.; Grigorenko, A. N.; Konstantatos, G.; Kis, A.; Katsnelson, M.; Vandersypen, L.; Loiseau, A.; Morandi, V.; Neumaier, D.; Treossi, E.; Pellegrini, V.; Polini, M.; Tredicucci, A.; Williams, G. M.; Hee Hong, B.; Ahn, J.-H.; Min Kim, J.; Zirath, H.; van Wees, B. J.; van der Zant, H.; Occhipinti, L.; Di Matteo, A.; Kinloch, I. A.; Seyller, T.; Quesnel, E.; Feng, X.; Teo, K.; Rupesinghe, N.; Hakonen, P.; Neil, S. R. T.; Tannock, Q.; Lofwander, T.; Kinaret, J., Science and technology roadmap for graphene, related two-dimensional crystals, and hybrid systems. *Nanoscale* **2015,** *7*, 4598-4810.
2. Treossi, E., Chemical Production and Microelectronic Applications of Graphene and Nano-Graphene Derivatives. **2012**.
3. Chandrasekaran, S.; Schulte, K., *Development of Nano-particle Modified Polymer Matrices for Improved Fibre Reinforced Composites*. TuTech Innovation2014.
4. Pakdel, A.; Bando, Y.; Golberg, D., Nano boron nitride flatland. *Chemical Society Reviews* **2014,** *43*, 934-959.
5. Papageorgiou, D. G.; Kinloch, I. A.; Young, R. J., Graphene/elastomer nanocomposites. *Carbon* **2015,** *95*, 460-484.
6. Young, R. J.; Liu, M., The microstructure of a graphene-reinforced tennis racquet. *Journal of Materials Science* **2016,** *51*, 3861-3867.
7. Debelak, B.; Lafdi, K., Use of exfoliated graphite filler to enhance polymer physical properties. *Carbon* **2007,** *45*, 1727-1734.
8. Stankovich, S.; Dikin, D. A.; Dommett, G. H. B.; Kohlhaas, K. M.; Zimney, E. J.; Stach, E. A.; Piner, R. D.; Nguyen, S. T.; Ruoff, R. S., Graphene-based composite materials. *Nature* **2006,** *442*, 282-286.
9. Wang, Z.; Nelson, J. K.; Hillborg, H.; Zhao, S.; Schadler, L. S., Graphene Oxide Filled Nanocomposite with Novel Electrical and Dielectric Properties. *Advanced Materials* **2012,** *24*, 3134-3137.
10. Prolongo, S. G.; Moriche, R.; Jiménez-Suárez, A.; Sánchez, M.; Ureña, A., Advantages and disadvantages of the addition of graphene nanoplatelets to epoxy resins. *European Polymer Journal* **2014,** *61*, 206-214.
11. Chandrasekaran, S.; Sato, N.; Tölle, F.; Mülhaupt, R.; Fiedler, B.; Schulte, K., Fracture toughness and failure mechanism of graphene based epoxy composites. *Composites Science and Technology* **2014,** *97*, 90-99.
12. Young, R. J.; Kinloch, I. A.; Gong, L.; Novoselov, K. S., The mechanics of graphene nanocomposites: A review. *Composites Science and Technology* **2012,** *72*, 1459-1476.
13. Bianco, A.; Cheng, H.-M.; Enoki, T.; Gogotsi, Y.; Hurt, R. H.; Koratkar, N.; Kyotani, T.; Monthioux, M.; Park, C. R.; Tascon, J. M. D.; Zhang, J., All in the graphene family – A recommended nomenclature for two-dimensional carbon materials. *Carbon* **2013,** *65*, 1-6.
14. Geim, A. K.; Novoselov, K. S., The rise of graphene. *Nat Mater* **2007,** *6*, 183-191.
15. Novoselov, K. S.; Falko, V. I.; Colombo, L.; Gellert, P. R.; Schwab, M. G.; Kim, K., A roadmap for graphene. *Nature* **2012,** *490*, 192-200.
16. Avouris, P.; Dimitrakopoulos, C., Graphene: synthesis and applications. *Materials Today* **2012,** *15*, 86-97.
17. Lee, J.-H.; Loya, P. E.; Lou, J.; Thomas, E. L., Dynamic mechanical behavior of multilayer graphene via supersonic projectile penetration. *Science* **2014,** *346*, 1092-1096.

18. Kim, H.; Abdala, A. A.; Macosko, C. W., Graphene/Polymer Nanocomposites. *Macromolecules* **2010,** *43*, 6515-6530.
19. Terzi, F.; Zanfrognini, B.; Dossi, N.; Ruggeri, S.; Maccaferri, G., Voltammetric determination of hydrogen peroxide at high concentration level using a copper electrode. *Electrochimica Acta* **2016,** *188*, 327-335.
20. Graphenea, Graphene Applications & Uses. **2016**.
21. Paine, R. T.; Narula, C. K., Synthetic routes to boron nitride. *Chemical Reviews* **1990,** *90*, 73-91.
22. 3M, Global Boron Nitride and Boron Carbide Market. **2012**.
23. Wetzel, B.; Rosso, P.; Haupert, F.; Friedrich, K., Epoxy nanocomposites - fracture and toughening mechanisms. *Engineering Fracture Mechanics* **2006,** *73*, 2375-2398.
24. Sellam, C., Graphene based Nanocomposites for Mechanical Reinforcement. **2015**.
25. Vallés, C.; Abdelkader, A. M.; Young, R. J.; Kinloch, I. A., The effect of flake diameter on the reinforcement of few-layer graphene–PMMA composites. *Composites Science and Technology* **2015,** *111*, 17-22.
26. Du, J.; Cheng, H.-M., The Fabrication, Properties, and Uses of Graphene/Polymer Composites. *Macromolecular Chemistry and Physics* **2012,** *213*, 1060-1077.
27. Smith, F., The Use of composites in aerospace: Past, present and future challanges. **2015**.
28. Njuguna, J.; Pielichowski, K., Polymer Nanocomposites for Aerospace Applications: Properties. *Advanced Engineering Materials* **2003,** *5*, 769-778.
29. Wick, P.; Louw-Gaume, A. E.; Kucki, M.; Krug, H. F.; Kostarelos, K.; Fadeel, B.; Dawson, K. A.; Salvati, A.; Vázquez, E.; Ballerini, L.; Tretiach, M.; Benfenati, F.; Flahaut, E.; Gauthier, L.; Prato, M.; Bianco, A., Classification Framework for Graphene-Based Materials. *Angewandte Chemie International Edition* **2014,** *53*, 7714-7718.
30. Kouroupis-Agalou, K.; Liscio, A.; Treossi, E.; Ortolani, L.; Morandi, V.; Pugno, N. M.; Palermo, V., Fragmentation and exfoliation of 2-dimensional materials: a statistical approach. *Nanoscale* **2014,** *6*, 5926-5933.
31. Andrea, L.; Konstantinos, K.-A.; Xavier Diez, B.; Alessandro, K.; Emanuele, T.; Nicola Maria, P.; Giovanna De, L.; Loris, G.; Vincenzo, P., Evolution of the size and shape of 2D nanosheets during ultrasonic fragmentation. *2D Materials* **2017,** *4*, 025017.
32. Knerelman, E. I.; Zvereva, G. I.; Kislov, M. B.; Davydova, G. I.; Krestinin, A. V., Characterization of products on the base of single-walled carbon nanotubes by the method of nitrogen adsorption. *Nanotechnologies in Russia* **2010,** *5*, 786-794.
33. Hou, C.-H.; Liu, N.-L.; Hsi, H.-C., Highly porous activated carbons from resource-recovered Leucaena leucocephala wood as capacitive deionization electrodes. *Chemosphere* **2015,** *141*, 71-79.
34. Wang, F.; Drzal, L. T.; Qin, Y.; Huang, Z., Size effect of graphene nanoplatelets on the morphology and mechanical behavior of glass fiber/epoxy composites. *Journal of Materials Science* **2016,** *51*, 3337-3348.
35. Pierleoni, D.; Xia, Z. Y.; Christian, M.; Ligi, S.; Minelli, M.; Morandi, V.; Doghieri, F.; Palermo, V., Graphene-based coatings on polymer films for gas barrier applications. *Carbon* **2016,** *96*, 503-512.
36. Wang, F.; Drzal, L. T.; Qin, Y.; Huang, Z., Mechanical properties and thermal conductivity of graphene nanoplatelet/epoxy composites. *Journal of Materials Science* **2015,** *50*, 1082-1093.
37. Prolongo, S. G.; Jiménez-Suárez, A.; Moriche, R.; Ureña, A., Graphene nanoplatelets thickness and lateral size influence on the morphology and behavior of epoxy composites. *European Polymer Journal* **2014,** *53*, 292-301.
38. Prolongo, S. G.; Moriche, R.; Sánchez, M.; Ureña, A., Self-stratifying and orientation of exfoliated few-layer graphene nanoplatelets in epoxy composites. *Composites Science and Technology* **2013,** *85*, 136-141.

39. Gojny, F. H.; Wichmann, M. H. G.; Köpke, U.; Fiedler, B.; Schulte, K., Carbon nanotube-reinforced epoxy-composites: enhanced stiffness and fracture toughness at low nanotube content. *Composites Science and Technology* **2004,** *64*, 2363-2371.
40. Avila, A. F.; Soares, M. I.; Neto, A. S., A study on nanostructured laminated plates behavior under low-velocity impact loadings. *International Journal of Impact Engineering* **2007,** *34*, 28-41.
41. Movva, S.; Zhou, G.; Guerra, D.; Lee, L. J., Effect of Carbon Nanofibers on Mold Filling in a Vacuum Assisted Resin Transfer Molding System. *Journal of Composite Materials* **2009,** *43*, 611-620.
42. Jan, R.; May, P.; Bell, A. P.; Habib, A.; Khan, U.; Coleman, J. N., Enhancing the mechanical properties of BN nanosheet-polymer composites by uniaxial drawing. *Nanoscale* **2014,** *6*, 4889-4895.
43. Wang, Z.; Nelson, J. K.; Miao, J.; Linhardt, R. J.; Schadler, L. S.; Hillborg, H.; Zhao, S., Effect of high aspect ratio filler on dielectric properties of polymer composites: a study on barium titanate fibers and graphene platelets. *IEEE Transactions on Dielectrics and Electrical Insulation* **2012,** *19*, 960-967.